Aus dem Institut für Humanernährung und Lebensmittelkunde
der Christian-Albrechts-Universität zu Kiel

The *C. elegans* potassium leak channel TWK-7 and the canonical $G\alpha_s$-Protein Kinase A pathway act epistatically in GABAergic motor neurons to affect locomotion behavior

Dissertation
zur Erlangung des Doktorgrades
der Agrar- und Ernährungswissenschaftlichen Fakultät
der Christian-Albrechts-Universität zu Kiel

vorgelegt von

M.Sc. Dieter-Christian Gottschling

aus Iaşi

Kiel, 19.05.2016

Dekan: Prof. Dr. Eberhard Hartung
1. Berichterstatter: Prof. Dr. Frank Döring
2. Berichterstatter: Prof. Dr. Gerald Rimbach
Tag der mündlichen Prüfung: 13.07.2016

Contents

Summary

The change of locomotion activity in response to external cues is a considerable achievement of animals and is required for escape responses, foraging, and other complex behaviors. Less is known about the molecular regulators of such an adaptive locomotion. The conserved eukaryotic two-pore domain potassium (K_2P) channels are recognized as regulatory background K^+ channels that modify the membrane potential of cells. By using the *Caenorhabditis elegans* system combined with cell-type specific approaches and locomotion analyses in-depth, here, we found that the K_2P channel TWK-7 affects the activity of two locomotory gaits, swimming and crawling, in a coordinated mode. TWK-7 is expressed in cholinergic excitatory B-type and GABAergic inhibitory D-type motor neurons to affect fundamental aspects of adaptive locomotion behavior which may be characteristic for a stimulus induced fast targeted movement. In order to unravel signaling pathways that might act through TWK-7, we identified a loss-of-function allele *cau-1* of KIN-2 in a forward genetic screen. The gene *kin-2* encodes the negative regulatory subunit of the *C. elegans* protein kinase A (PKA-1/KIN-1) which is part of the canonical $G\alpha_s$ pathway. An activated $G\alpha_s$-PKA pathway and/or the absence of TWK-7 pores in GABAergic D-type motor neurons epistatically induce a persistent fast straightforward crawling behavior. Whereby, the five central aspects of stimulated locomotion - velocity, direction, wave parameters, duration and straightness - were synchronically affected by both the $G\alpha_s$-PKA pathway and TWK-7. In conclusion, we found that TWK-7 acts in cholinergic B-type and GABAergic D-type motor neurons as a prime candidate for the modulation of locomotor activity and locomotion behavior that enables persistent fast and straightforward locomotion. We presented convincing evidence for an epistatic interaction between the $G\alpha_s$-PKA pathway and TWK-7 which most probably share a common pathway being involved in the modulation of both locomotor activity and locomotion behavior during forward crawling that may mimic an adaptive response to specific environmental cues. Thus, we uncover a simple mechanism where a complex locomotion behavior might be modulated at the level of certain types of motor neurons by the activity of the $G\alpha_s$-PKA pathway acting epistatically through the leak K^+ channel TWK-7.

Zusammenfassung

Die Änderung des Bewegungsverhaltens in Anpassung an sich verändernde Umwelteinflüsse ist eine zentrale Eigenschaft vieler Lebewesen und ist lebensnotwendig für die Flucht, die Futtersuche und anderen komplexen Verhaltensweisen. Über die molekularen Regulatoren dieses adaptiven Bewegungsverhaltens ist bislang wenig bekannt. Die evolutionär konservierten eukaryotischen Kalium-Kanäle mit zwei Poren-Domänen (K_2P) wurden als regulatorische Hintergrund K^+ Kanäle identifiziert und charakterisiert. Sie verändern das Membranpotential und damit die Erregbarkeit von Zellen. Mit Hilfe genetischer Ansätze Zelltyp-spezifischen Funktionsanalysen und detaillierten Untersuchungen zum Bewegungsverhalten im Modellorganismus *Caenorhabditis elegans,* konnten wir zeigen, dass der K_2P Kanal TWK-7 die Aktivität zweier Bewegungsarten, nämlich Schwimmen und Kriechen, in einer koordinierten Art und Weise modulieren kann. Die in exzitatorischen cholinergen Typ-B und inhibitorischen GABAergen Typ-D Motorneuronen exprimierten TWK-7 Poren beeinflussen diejenigen Aspekte des adaptiven Bewegungsverhaltens, die für eine extern induzierte, schnelle und gerichtete Bewegung charakteristisch sind. Zur Identifizierung von Signalwegen, die dieses Bewegungsverhalten über TWK-7 regulieren, haben wir einen Screen basierend auf der Vorwärtsgenetik durchgeführt. Hierbei gelang die Identifizierung eines neuen Funktionsverlustallels *cau-1* des Gens *kin-2*. Dieses Gen kodiert für die inhibitorische Untereinheit der Proteinkinase A (PKA-1/KIN-1), die im kanonischen Signalweg $G\alpha_s$ ihre Funktion erfüllt. Wir konnten zeigen, dass ein aktiver $G\alpha_s$-PKA Signalweg und/oder ein TWK-7-Nullallel schnelle, nachhaltige Kriechbewegungen in Vorwärtsrichtung auslösen. Dabei beeinflussen $G\alpha_s$-PKA und TWK-7 epistatisch fünf zentrale Charakteristika einer stimulierten Vorwärtsbewegung - Geschwindigkeit, Richtung, Wellenparameter, Nachhaltigkeit und Geradlinigkeit - in GABAergen D-Typ Motorneuronen. In dieser Arbeit etablieren wir TWK-7 als einen Hauptkandidaten, der für die Modulation einer nachhaltigen, schnellen und gerichteten Vorwärtsbewegung auf der Ebene der cholinergen B-Typ und GABAergen D-Typ Motorneuronen in Frage kommt. Weiterhin zeigen die genetischen Experimente, dass dieses adaptive Bewegungsverhalten durch den $G\alpha_s$-PKA Signalweg, der über TWK-7 seine Wirkung in GABAergen D-Typ Motorneuronen entfaltet, gesteuert wird. Somit haben wir einen sehr einfachen Mechanismus identifiziert, der komplexes Bewegungsverhalten auf neuronaler Ebene unter Beteiligung von $G\alpha_s$-PKA und TWK-7 erklären könnte.

1. Introduction

Locomotion is a fundamental aspect of life, because it is required for escape responses, foraging, and other behaviors. In both invertebrates and vertebrates, rhythmic and patterned locomotion is usually controlled by specific motor circuits with autonomous rhythmic activities called central pattern generators (MARDER and CALABRESE 1996). The overall output of the motor network depends on the interplay of premotor interneurons, motor neurons, muscle cells, and the intrinsic membrane properties of the involved cells. For example, in insects, motor activity appears to increase during walking by tonic depolarization of interneurons and/or motor neurons (LUDWAR *et al.* 2005). In response to environmental cues, animals often adjust their locomotion activity, which, in principle, can be regulated at the level of central pattern generators, interneurons, motor neurons, or muscle cells.

Two-pore domain potassium (K_2P) channels are evolutionarily conserved eukaryotic membrane proteins (ENYEDI and CZIRJAK 2010). They contain two pore domains per subunit and function as dimers building one conductance pore. K_2P channels operate as voltage-independent background K^+ channels to stabilize the negative resting membrane potential and to counterbalance membrane depolarization. They are specifically regulated by a variety of factors including temperature, pH, membrane stretch, fatty acids, and signaling pathway dependent phosphorylation. The physiological function of most K_2P channels remains to be elucidated. They have been implicated in the regulation of several processes, such as chemoreception, mechanical nociception, and excitation of motor neurons. Experiments on slice preparations of anaesthetized adult turtles revealed that the neurotransmitter serotonin increases the excitability of spinal motor neurons via inhibition of a K_2P-like K^+ current (PERRIER *et al.* 2003), for example.

In nature, the nematode *C. elegans* is mainly found on rotten fruits and vegetables (FELIX and BRAENDLE 2010; PETERSEN *et al.* 2015). These habitats are characterized by solid and liquid micro-niches suggesting that crawling and swimming are natural locomotory gaits of the nematode. In the laboratory, the kinematic and biophysical parameters (e.g. mechanic forces) of *C. elegans* crawling and swimming have been described in detail (BOYLE *et al.* 2012; FANG-YEN *et al.* 2010; MAJMUDAR *et al.* 2012; PIERCE-SHIMOMURA *et al.* 2008). The pattern of muscle activity were found to differ between the gaits, whereby the frequency of spontaneous alternating *C*-shape conformations (swimming) is considerably higher compared to undulating

S-shape conformations (crawling). In response to mechanical, gustatory, olfactory, and thermal stimuli or food deprivation (BEN AROUS *et al.* 2009; CLARK *et al.* 2007; LUERSEN *et al.* 2014; LUO *et al.* 2008; SAWIN *et al.* 2000; SHTONDA and AVERY 2006), *C. elegans* shows adaptive locomotion behaviors. Locomotion is controlled by excitatory cholinergic (A- and B-type) and inhibitory GABAergic (D-type) motor neurons that are localized in the ventral nerve cord of the worm. B-type motor neurons are responsible for forward, A-type motor neurons for backward locomotion (CHALFIE *et al.* 1985). A-, B- and D-type motor neurons are further divided into V and D subclasses that innervate the longitudinally aligned ventral and dorsal muscle cells, respectively. A- and B-type motor neurons synapse not only onto their respective muscle cells but also onto corresponding inhibitory D-type motor neurons (VD or DD) leading to contralateral muscle inhibition (GJORGJIEVA J 2014; WEN *et al.* 2012; WHITE *et al.* 1976). Recently, it has been shown that the B-type motor neurons (responsible for forward locomotion) are coupled by proprioception thereby transducing the rhythmic movement, which is probably initiated by a postulated central pattern generator near the head, into bending waves propagated along the body by a chain of reflexes (WEN *et al.* 2012).

C. elegans K_2P channels are designated as TWK channels (two-pore-forming) domain K^+ channels). More than 40 TWK-encoding genes representing six subfamilies have been identified in the worm (BUCKINGHAM *et al.* 2005; SALKOFF *et al.* 2001). In *Drosophila* and mammals, only eleven and fifteen K_2P channels have been annotated, respectively. Most *C. elegans* TWK channels are expressed in a few cell types including body-wall muscle cells, chemosensory neurons, interneurons, and motor neurons (KRATSIOS *et al.* 2012; SALKOFF *et al.* 2001). Up to now, only two TWK channels, both expressed in body-wall muscle, have been functionally characterized in *C. elegans* (DE LA CRUZ *et al.* 2003; DE LA CRUZ *et al.* 2014; KUNKEL *et al.* 2000). TWK-18 has been implicated in locomotion activity in response to higher temperature. TWK-23 (SUP-9) is activated by a putative iodotyrosine deiodinase (SUP-18) and might be involved in the excitability of muscle membranes. Overall, our knowledge regarding the physiological functions of two-pore domain potassium channels in *C. elegans* and other experimental systems such as fly, zebrafish, or mouse is rather limited. The modulator molecules, the pathways and their targets that are involved are widely unknown.

In *C. elegans* neurotransmitter release from synaptic vesicles of motor neurons is regulated by a network of three canonical heterotrimeric G protein signaling pathways, $G\alpha_q$, $G\alpha_0$ and $G\alpha_s$. The diacylglycerol (DAG) producing $G\alpha_q$ pathway represents the core pathway that promotes

the release of acetylcholine, the major excitatory neurotransmitter at neuromuscular junctions. The $G\alpha_q$ homologue EGL-30 exerts its stimulating function in acetylcholine release through EGL-8/PLCβ and PLC-3/PLCγ, two parallel acting phospholipase C (YU *et al.* 2013). DAG levels and hence acetylcholine release are negatively regulated by diacylglycerol kinase DGK-1 and the $G\alpha_0$ pathway with GOA-1/G protein alpha subunit G_0. Accordingly, gain of function mutants of *egl-30* or loss of function mutants of *goa-1* and *dgk-1* were found to move hyperactively on agar plates (NURRISH *et al.* 1999) showing increased bending amplitudes (BHATTACHARYA *et al.* 2014), whereas $G\alpha_q$ loss of function mutants are lethargic or move slowly (LACKNER *et al.* 1999; MILLER *et al.* 1999; REYNOLDS *et al.* 2005). In addition, the $G\alpha_s$ signaling pathway has been reported to control *C. elegans* crawling activity by interaction with the $G\alpha_q$ pathway, however, downstream of DAG production. Gain-of-function mutants that activate cAMP dependent protein kinase A (PKA-1/KIN-1) are hyperactive (REYNOLDS *et al.* 2005; SCHADE *et al.* 2005). Downstream targets of PKA-1/KIN-1 involved in this process have not been identified yet (REYNOLDS *et al.* 2005; ZHOU *et al.* 2007).

Consequently, we have performed a forward genetic screen to identify putative regulators of the *C. elegans* TWK-7 channel function. To this end, we identified mutants that showed enhanced and coordinated body bending swimming frequencies comparable to *twk-7(null)* mutants. We isolated the allele *cau-1* of the gene *kin-2* encoding the negative regulatory subunit of PKA-1/KIN-1. In agreement with a previous study on a *kin-2* reduction-of-function allele (SCHADE *et al.* 2005), our *kin-2(cau-1)* mutants also exhibit enhanced crawling activity. Detailed comparative locomotion analyses in-depth revealed that *kin-2(cau-1)* phenocopies *twk-7(null)* animals to a great extent. Our genetic interaction studies in combination with cell-type specific expression approaches indicate that the $G\alpha_s$ pathway may act as an upstream regulator of TWK-7. Moreover, detailed locomotor analyses suggest that in *C. elegans* PKA-1/KIN-1 dependent regulation of TWK-7 on the level of cholinergic B-type and GABAergic D-type motor neurons might contribute to adaptive locomotion in response to external stimulation. We found that TWK-7 acts as a prime candidate for the modulation of adaptive locomotion behavior that enables fast, persistent and directed forward crawling behavior.

2. Results

2.1 Deficiency of *C. elegans* leak K^+ channel TWK-7 in motor neurons causes a fast and persistent straightforward crawling behavior

2.1.1 TWK-7 deficiency led to an enhanced activity of both swimming and spontaneous crawling in a coordinated mode

The *C. elegans* genome contains more than 40 genes encoding TWK channels. Of these TWK-7, -30, -40, -43, and -46 have been previously shown to be expressed in motor neurons (KRATSIOS *et al.* 2012; SALKOFF *et al.* 2001). Because the evolutionary conserved K_2P/TWK channels are discussed to set the membrane potential and, hence, influence the excitability of cells, we investigated whether these channels have a physiological role in *C. elegans* locomotion. When tested for their locomotor activity, solely, the *twk-7* mutant allele *nf120* showed an altered spontaneous crawling activity than wild type worms, whereas mutant alleles of other TWK channels expressed in motor neurons did not induce a similar phenotype **(Fig. 1A)**. Consistent with the general structure of K_2P channels, *in silico* analyses predicted that the deduced TWK-7 protein contains four transmembrane domains (M1-M4) and the two pore domains P1 and P2 that specify ion selectivity **(Fig. 1B; Fig. S1)**. In the *nf120* allele the *twk-7* gene contains a deletion of 303 bp which leads to the disruption of the P1 and M2 domains causing a translational frameshift within the open reading frame.

On agar plates, the *twk-7(nf120)* worms moved with an elevated spontaneous crawling body bending frequency of 0.48 ± 0.11 Hz (wild-type: 0.16 ± 0.05 Hz) resulting in an increased crawling velocity of 0.15 ± 0.01 $mm*s^{-1}$ (wild-type: 0.10 ± 0.02 $mm*s^{-1}$) **(Fig. 2A, B; Mov. M1, M2)**. The *twk-7(nf120)* mutant worms also exhibited an enhanced swimming activity of 2.16 ± 0.05 Hz when compared to wild type animals with a body bending swimming frequency of 1.68 ± 0.09 Hz **(Fig. 2C; Mov. M3, M4)**. Hence, for further analysis, we focused on TWK-7. Genetic analysis revealed that *nf120* is a recessive *null* allele of *twk-7* **(Fig. 2D)**. Thus, *twk-7(nf120)* was specified as *twk-7(null).* Accordingly, similar higher crawling and swimming activities were determined for a second loss-of-function allele of *twk-7, gk760044* that is characterized by a premature stop at position W^{325} **(Fig. 1A, B; Fig. 2A-C; Fig. S1)**. Importantly, although the two *twk-7* mutants swam and crawled with higher frequencies than the wild-types, they maintained both normal C-shape conformations during swimming and

normal undulating S-shape conformations during crawling **(Fig. 3A, B)**. These results suggest that TWK-7 has an impact on the two locomotory gaits in a coordinated mode.

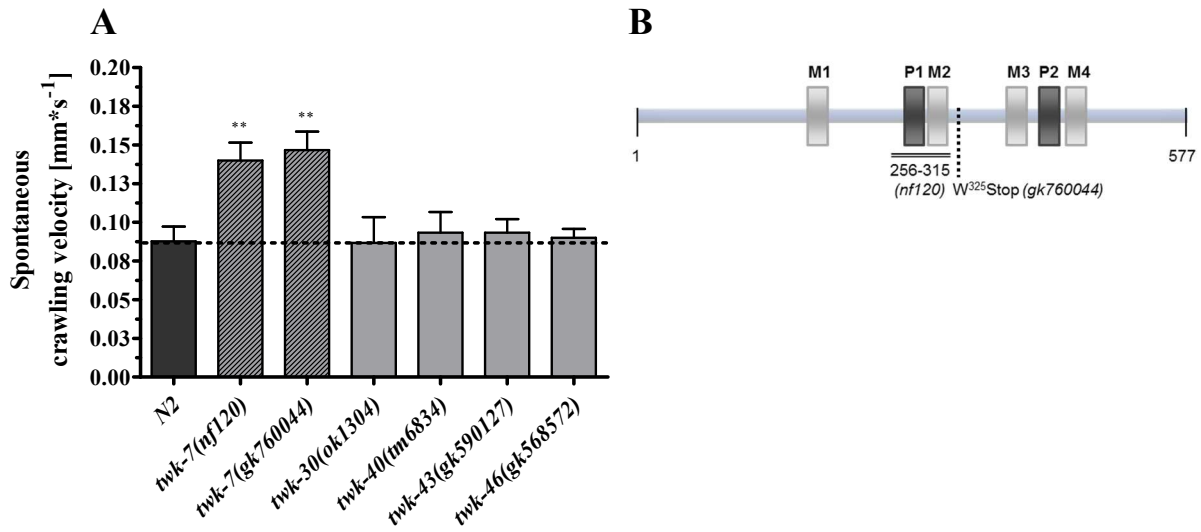

Figure 1: Locomotion screen of K_2P channels expressed in motor neurons and schematic visualization of TWK-7 deficiencies that enhance locomotion behavior.

(A) *twk-7(null)* animals exhibited notably enhanced velocities during spontaneous crawling under *ad libitum* feeding condition compared with wild-type and mutant strains of other TWK-family members expressed in motor neurons. **(B)** The schematic diagram of the TWK-7 protein indicates the predicted position of the pore domains P1 and P2 (dark grey) and the transmembrane domains M1-M4 (light grey). The polypeptide region that is not encoded by the deletion mutant allele *nf120* and the localization of the premature stop of the allele *gk760044* are depicted. Dotted lines in (A) indicate the respective wild-type level. The values represent the means (± SEM) of N ≥ 4 (A) independent experiments involving n ≥ 40 animals. *p < 0.05;**p < 0.01; ***p < 0.001 (Student's t-test).

An age-dependent decline of locomotor activity has been reported for wild-type *C. elegans* (SCHREIBER *et al.* 2010). Both *twk-7* loss-of-function mutants also showed a constant decrease of swimming activity over 12 days starting with L4 larvae **(Fig. S2)**. Nevertheless, during the whole aging period the *twk-7* mutants still had higher locomotor activities than age-matched control worms. Thus, TWK-7 is able to affect locomotion throughout *C. elegans* adulthood but does not influence the gradual reduction of activity caused by the aging process.

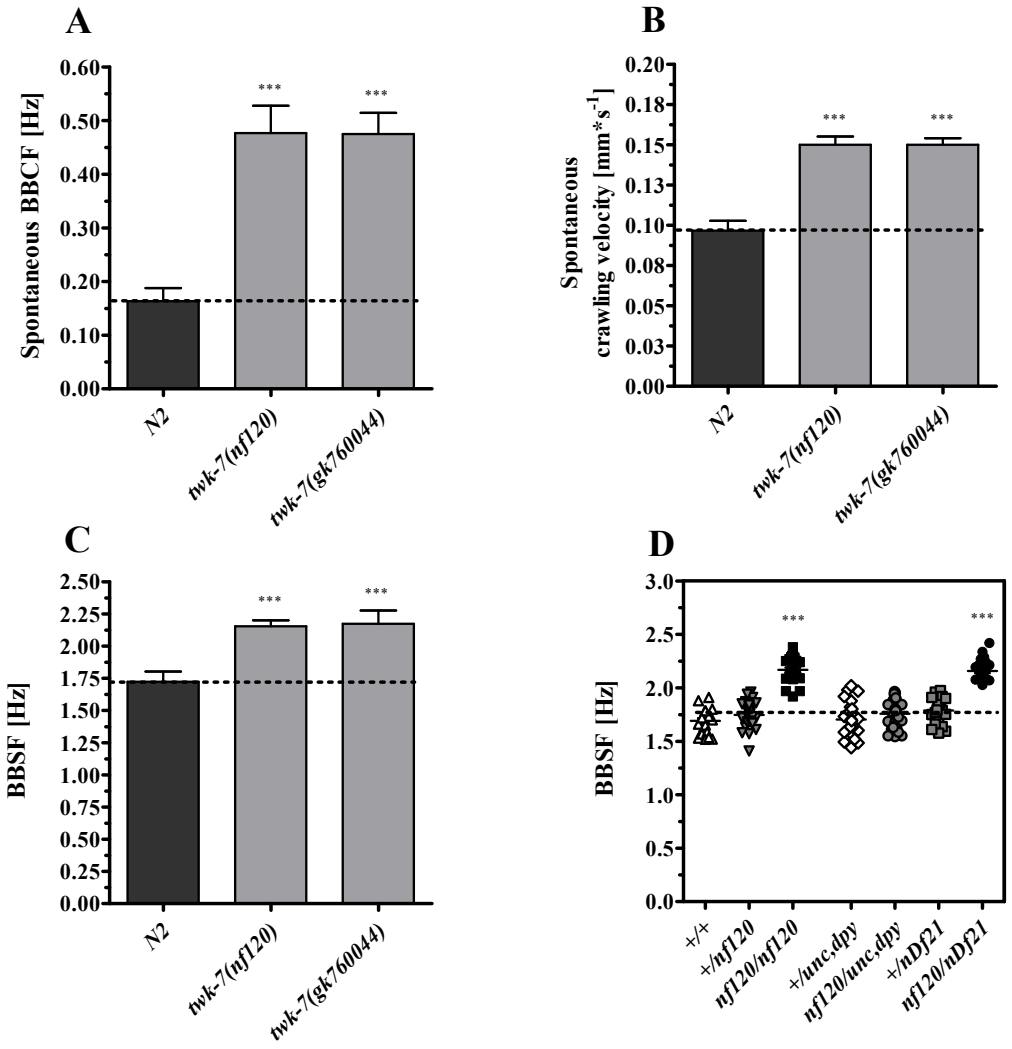

Figure 2: Locomotion assays of spontaneous locomotor activity and genetic complementation analyses of the *twk-7(nf120)* allele.

(A) The spontaneous body bending crawling frequencies (BBCF) and **(B)** the corresponding spontaneous crawling velocities of *twk-7(null)* alleles. **(C)** The body bending swimming frequencies (BBSF) of the *twk-7* mutant alleles are depicted. **(D)** Only worms homozygote for the *twk-7* deletion allele (*nf120/nf120*) exhibited increased BBSF. Heterozygote worms (+/*nf120*) swam like wild-type (+/+). Bringing the *nf120* allele *in trans* to the chromosomal deletion *nDf21* of the balanced deficiency mutant *nDf21/dpy-19(e1259),unc-32(e189)III* resulted in worms (*nf120/nDf21*) with elevated BBSF similar to *twk-7(nf120)* homozygotes. Symbols represent single worms. Genotypes of the tested worms were determined by PCR and/or phenotype analyses of progeny n ≥ 20 animals. Dotted lines indicate the respective wild-type level. The values represent the means (± SEM) of N ≥ 4 (A, B and C) and N =3 (D) independent experiments involving n ≥40 animals. *p < 0.05;**p < 0.01; ***p < 0.001 (Student's t-test).

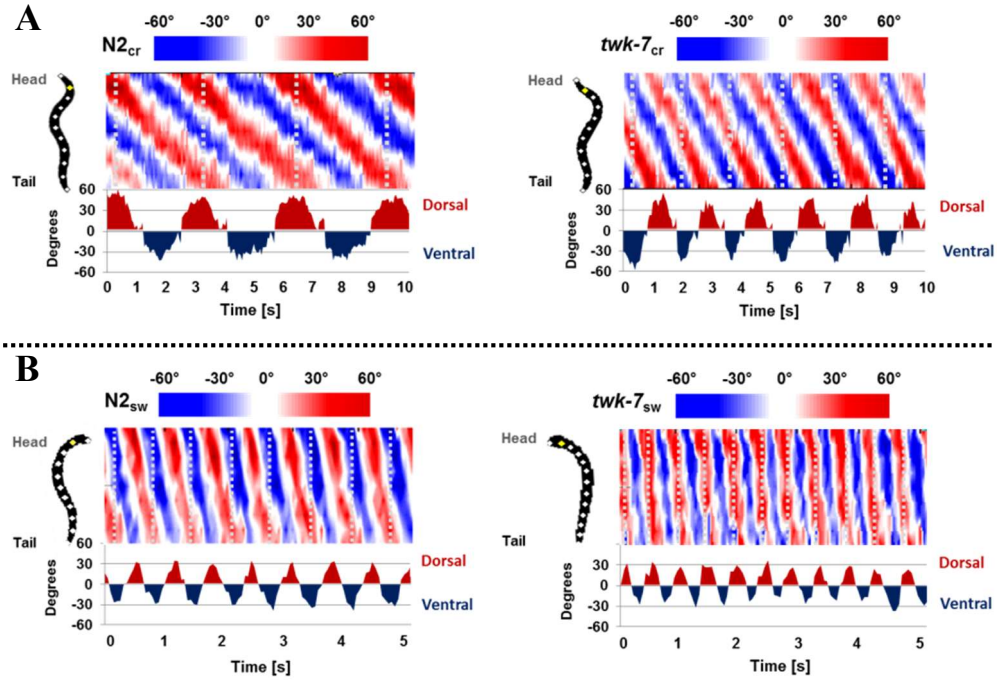

Figure 3: The *C*- and *S*-shape conformations visualized using the curvature matrices of swimming and crawling worms.
Sequence continuities indicate that *twk-7(nf120)* worms crawled **(A)** and swam **(B)** in a coordinated manner similar to wild-types although with higher body bending frequencies. The color code illustrates the dorsal (D, red) and ventral (V, blue) changes of body shape angles (up to 40° for swimming and 60° for crawling, respectively) over time during locomotion (for details see Material and Methods). The sinusoidal curves below depict the corresponding rhythmic curvature of the neck (for swimming) and midbody segment (for crawling) over time (segments are marked in yellow).

2.1.2 An intact potassium pore is required for the function of TWK-7 in maintaining normal swimming and crawling activity

To further investigate the function of TWK-7 in locomotor activity, the *twk-7(nf120)* null mutant was transformed either with the *twk-7* containing cosmid F22B7 or with the construct *cauEx[twk-7p(3000)::TWK-7::mCherry::let-858(3'UTR)]* that consists of the full genomic region of *twk-7* including 3000 bp of the promoter. Analysis of the resulting transgenic worms showed that these constructs rescued both the accelerated crawling and swimming activity of *twk-7(null),* even slightly below wild-type level **(Fig. 4A-C; Mov. M5).** In contrast, the activity of the two locomotory gaits was not affected in the non-transgenic siblings.

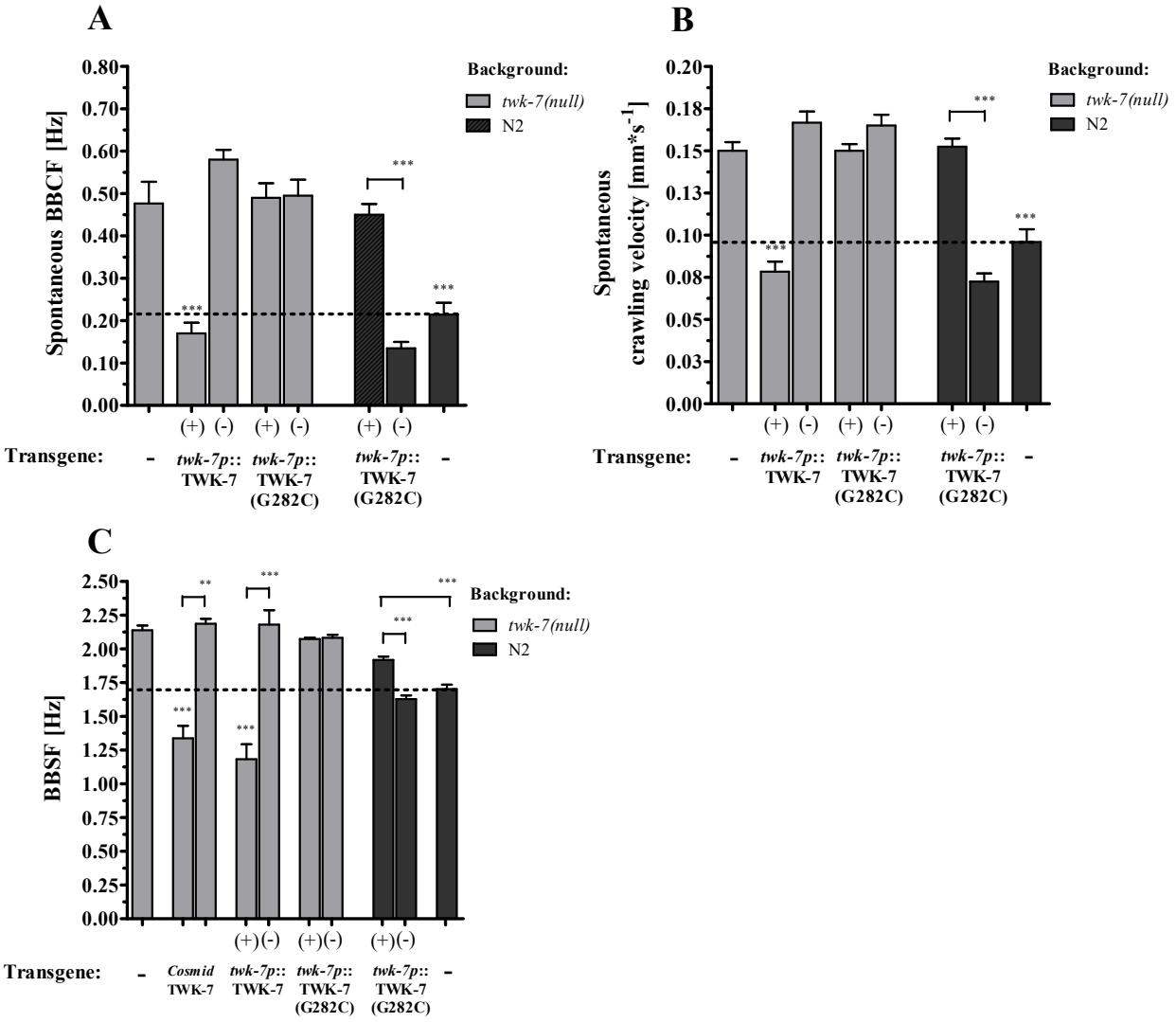

Figure 4: TWK-7 functions in motor neurons to affect locomotor activity.

(A) The body bending crawling frequencies and **(B)** the respective crawling velocities of transgenes (+) expressing TWK-7 and the selectivity filter mutant TWK-7($G^{282}C$) under its own promoter. The values for the corresponding non-transgenic siblings (-) are shown. **(C)** The body bending swimming frequencies (BBSF) of transgenic *twk-7(nf120)* and transgenic N2 wild-type worms are depicted. Transgenes (+) are directly compared with non-transgenic (-) siblings. Overexpression of TWK-7 in a *twk-7(null)* background restores the BBSF even below wild-type level. In contrast, the selectivity filter mutant TWK-7($G^{282}C$) did not affect the swimming rate of *twk-7(nf120)*, but has a dominant negative effect on the swimming activity in a N2 genetic background.

In a functional K_2P channel dimer, the pore domains P1 and P2 of both subunits contribute to the formation of one conductance pore specific for K^+ (ENYEDI and CZIRJAK 2010). Single amino acid substitutions within the ion selectivity filter of pore domain P1 inactivates channel function due to suppression of K^+ conductance (KOLLEWE *et al.* 2009). Here, we introduced the respective mutations into our *twk-7* construct *cauEx[twk-7p(3000)::TWK-7::mCherry::let-*

858(3'UTR)] to analyze whether the potassium pore of TWK-7 is required for locomotor function. We found that neither mCherry tagged mutant channel TWK-7($G^{282}C$) nor TWK-7($T^{279}K$) is able to rescue *twk-7(null)* locomotion phenotypes **(Fig. 4A-C; Fig. S3A, B)** that is indicative for a disrupted TWK-7 channel function. Confocal microscopy analysis showed an expression pattern of the TWK-7($G^{282}C$)::mCherry mutant channel similar to that of wild-type TWK-7::mCherry. Remarkably, expression of TWK-7($G^{282}C$)::mCherry in wild type worms resulted in an elevation of both crawling and swimming activity when compared with non-transgenic siblings or non-transformed wild-type worms **(Fig. 4A-C)**. Because the two-pore domain K^+ channels are obligate dimers whose pore domains form a single ion pore, our data indicate a successful expression of a dominant-negative TWK-7 mutant protein that most probably suppresses potassium conductance owing to an impaired ion selectivity filter. We conclude that an intact channel function of TWK-7 is necessary for its physiological role to affect locomotor activity.

2.1.3 TWK-7 is expressed in all types of motor neurons of the ventral nerve cord

To determine the expression pattern of TWK-7, we employed the *ohEx[twk-7p(3000)::DsRed::let-858(3'UTR)]* construct (KRATSIOS *et al.* 2012) expressing a cytosolic DsRed reporter protein under the control of the *twk-7* promoter. For co-localization studies, we used the *vsIs48[unc-17p::GFP::let-858(3'UTR)]* construct that expresses a GFP reporter protein in the entire set of cholinergic neurons with the exception of VC neurons (KRATSIOS *et al.* 2012). Laser scanning microscopy of transgenic worms revealed that the *twk-7* promoter drives DsRed reporter expression in some head and tail neurons as well as in all A-, B-, and AS-type motor neurons of the ventral nerve cord **(Fig. 5A-C; Fig. S4A-D)**. In addition, *Ds*Red expression was seen in GFP-negative neurons. According to their number and stereotypic position, these TWK-7 expressing cells were identified as the 13 ventral and 6 dorsal GABAergic D-type motor neurons of the ventral nerve cord. The cell type specific expression pattern of TWK-7 was confirmed in worms that express a C-terminal tagged TWK-7::mCherry fusion protein under the control of the *twk-7* promoter. TWK-7::mCherry was localized in punctuated intracellular structures and in the plasma membrane **(Fig. 5D, E; Fig. S4E-G)** suggesting that TWK-7 is trafficked by the secretory Golgi-dependent pathway and functions in the membrane as a channel protein. Taken together, in accordance to the unraveled impact of TWK-7 on locomotor activity, TWK-7 is expressed in all types of motor neurons of the ventral nerve cord that control body wall muscle activity.

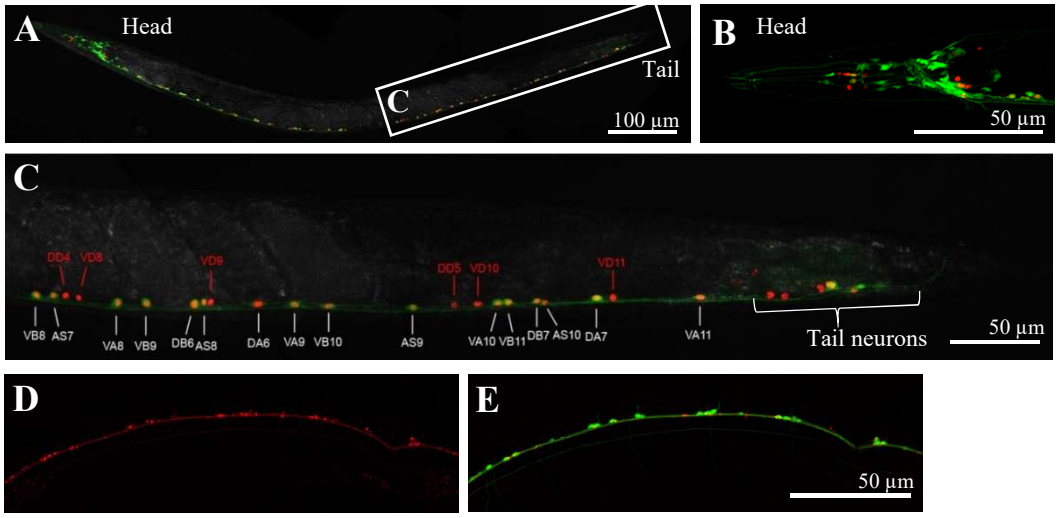

Figure 5: Co-localization of TWK-7 expression patterns along the ventral nerve cord, head and tail neurons.

(A) Cytosolic DsRed expression driven by the *twk-7* promoter is overlaid with the cholinergic neuron specific cytosolic GFP expression mediated by the *unc-17* promoter. Co-expression is indicated by yellow color. **(B)** Maximum projection of Z-series through the head region reveled that DsRed fluorescence is seen in cholinergic and non-cholinergic head neurons are depicted. **(C)** Maximum projection of Z-series through the cholinergic region of the ventral nerve cord. Detailed co-expression analyses of TWK-7 and UNC-17 expressing cells in the ventral nerve cord indicates that TWK-7 is present in the cholinergic A-, AS- and B-type motor neurons as well as in UNC-17 negative cells. According to their stereotypic positions, these were identified as GABAergic D-type motor neurons and unidentified tail neurons. **(D)** Maximum projection of Z-series through the cholinergic region of the ventral nerve cord are shown. Expression of a TWK-7::mCherry fusion protein which includes the entire TWK-7 channel protein leads to a punctate subcellular and membrane associated localization, which is overlaid in **(E)** Co-expressed cytosolic green fluorescence is generated by the cholinergic neuron specific *unc-17* promoter.

2.1.4 TWK-7 is required in excitatory cholinergic motor neurons to maintain normal spontaneous crawling activity

Cholinergic B-type and A-type motor neurons excite muscles on each side of the body during forward and, respectively, backward crawling while indirectly inhibiting muscles through excitation of GABAergic D-type motor neurons on the complementary side (CHALFIE *et al.* 1985; SENGUPTA and SAMUEL 2009). The B-type neurons act like a single command unit switching local segment oscillations *on* or *off* and modulate the speed and amplitude of the local segment waves (BRYDEN and COHEN 2008). Here we asked whether TWK-7 functions in a certain subset of neurons to maintain normal locomotor activity. Expression of TWK-7::mCherry exclusively in cholinergic excitatory motor neurons of the ventral nerve cord reduced both the crawling and swimming activity of *twk-7(null*) comparable to the values

obtained for transgenic worms expressing *twk-7* under its own promoter **(Fig. 6A, B)**. Interestingly, both slow crawling transgenic strains frequently showed an additional wave causing two overlapping S-shape curvatures along the body axis **(Fig. 6C; Mov. M5)**.

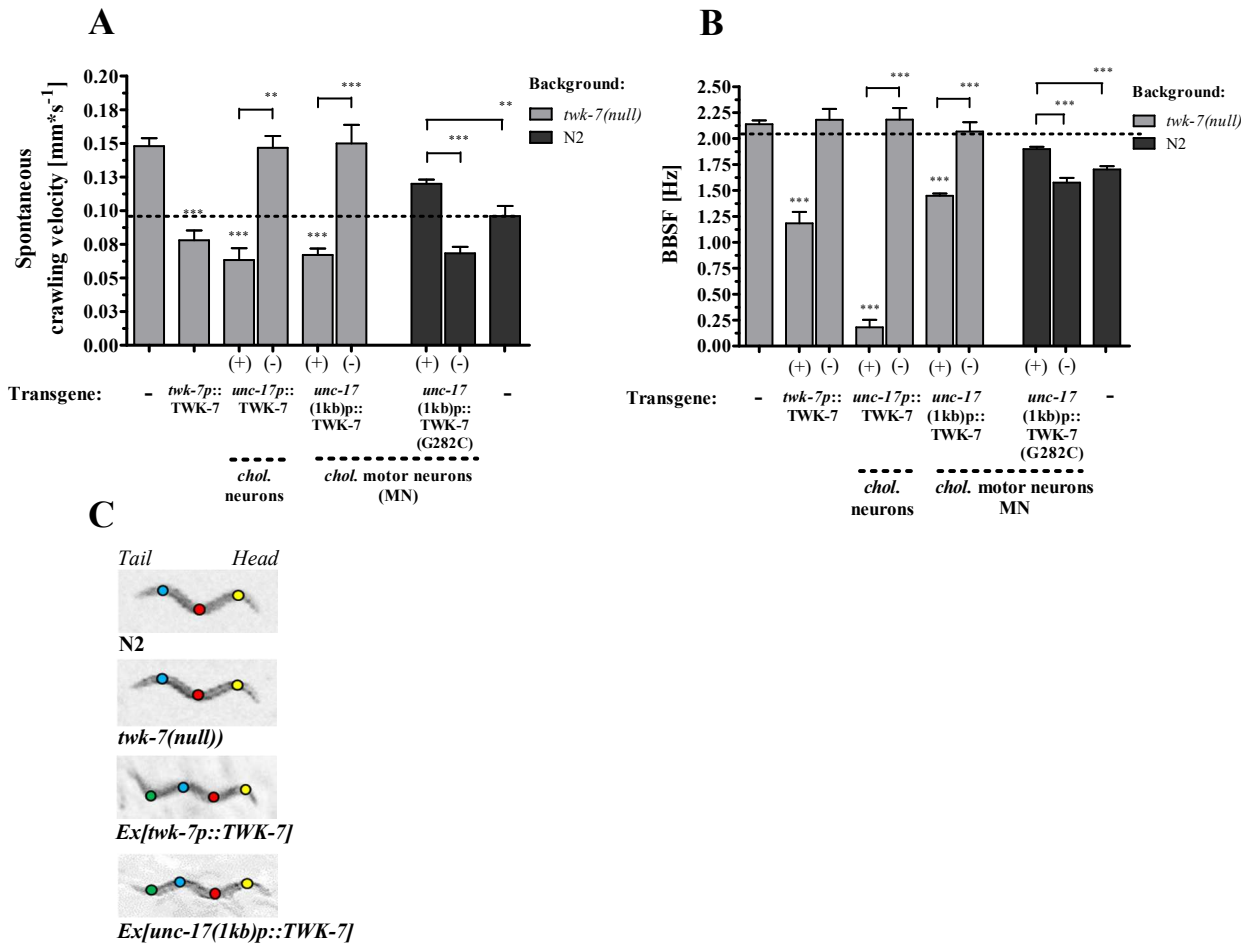

Figure 6: TWK-7 expressed cholinergic motor neurons is sufficient to affect locomotor activity.

(A) Crawling and **(B)** swimming activity analyses of transgenes expressing TWK-7 cell specifically. By employing two different *unc-17* promoter constructs, TWK-7 and the dominant negative selectivity filter mutant channel TWK-7($G^{282}C$) were cell-specifically expressed in all cholinergic neurons (*unc-17p(4.2kb)p*) or solely in the subset of cholinergic motor neurons (*unc-17(1 kb)p*). For each transgene (+) the corresponding locomotor activity of non-transgenic sibling (-) are shown. The spontaneous BBCF of the animals in (A) are listed in Suppl. Fig S5C. The values represent the means (± SEM) of at least N ≥ 3 independent experiments involving n ≥ 30 animals. *p < 0.05;**p < 0.01; ***p < 0.001 (Student's t-test). **(C)** *S*-shape curvature of wild-type N2 and the *twk-7(nf120)* mutant during crawling. Worms overexpressing TWK-7 under the control of the *twk-7* promoter (*Ex[twk-7p::TWK-7]*) or the cholinergic motor neuron specific *unc-17* promoter (*Ex[unc-17(1kb)p::TWK-7]*) show two overlapping S-shape curvatures during crawling generating an additional phase (green dot). The colored dots mark the phases (yellow: 0, red: π, blue: 2π, green: 3π) of wave propagation.

This may indicate a reduced excitability of cholinergic motor neurons resulting in a slowed and periodically arrhythmic propagation of the wave. Ectopic expression of TWK-7::mCherry in all cholinergic neurons of *twk-7(null)* resulted in uncoordinated and almost immobile swimming animals (**Fig. 6B**) indicating that a correct spatial expression of TWK-7 is critical for its locomotory function. Complementary to the results of the rescue approach, expression of the dominant negative TWK-7($G^{282}C$)::mCherry mutant channel in cholinergic excitatory motor neurons of wild-type worms led to an increased crawling and swimming activity **(Fig. 6A, B)**. Thus, TWK-7 might function in excitatory cholinergic motor neurons (A- and B-type) to maintain normal locomotor activity.

2.1.5 TWK-7 is required in cholinergic B-type and GABAergic D-type motor neurons to maintain normal spontaneous crawling activity

In order to match the role of TWK-7 in single subtypes of the cholinergic and GABAergic neurons, we expressed the wild-type variant of TWK-7 in the *twk-7(null)* background, and the dominant negative TWK-7($G^{282}C$) variant in the N2 wild-type background under the control of the *unc-4* (cholinergic A-type moto neurons), *acr-5* (cholinergic B-type moto neurons) and *unc-47* (GABAergic D-type moto neurons) promoter , respectively. Expression in the A-type motor neurons did not induce any changes in the spontaneous forward crawling behavior compared with corresponding non-transgenic animals **(Fig. 7A, B).** In contrast, worms with *twk-7(null)* background expressing *acr-5*p::TWK-7 (B-type motor neurons) or the *unc-47*p::TWK-7 (D-type motor neurons) construct exhibited markedly decreased locomotion rates **(Fig. 7A, B)**. The spontaneous crawling activities of *acr-5*p::TWK-7 (0.18 ± 0.05 Hz; 0.08 ± 0.01 mm*s^{-1}) and *unc-47*p::TWK-7 (0.21 ± 0.01 Hz; 0.09 ± 0.01 mm*s^{-1}) transgenes were similar to those of wild-type animals (0.23 ± 0.06 Hz; 0.09 ± 0.01 mm*s^{-1}), but significantly reduced in comparison with the *twk-7(null)* mutants (0.46 ± 0.07 Hz; 0.13 ± 0.02 mm*s^{-1}). Consistently, the dominant negative effect induced by the *acr-5*p::TWK-7($G^{282}C$) in wild-type background led to notably elevated spontaneous locomotion rates (0.47 ± 0.05 Hz; 0.13 ± 0.02 mm*s^{-1}) compared with the N2 control animals (0.23 ± 0.06 Hz; 0.09 ± 0.01 mm*s^{-1}) **(Fig. 7A, B)**. However, TWK-7($G^{282}C$) did not accelerate locomotion of wild-type worms when expressed in D-type motor neurons. Thus, TWK-7 functions in cholinergic B-type and GABAergic D-type motor neurons of the ventral nerve cord to maintain the activity of normal spontaneous crawling.

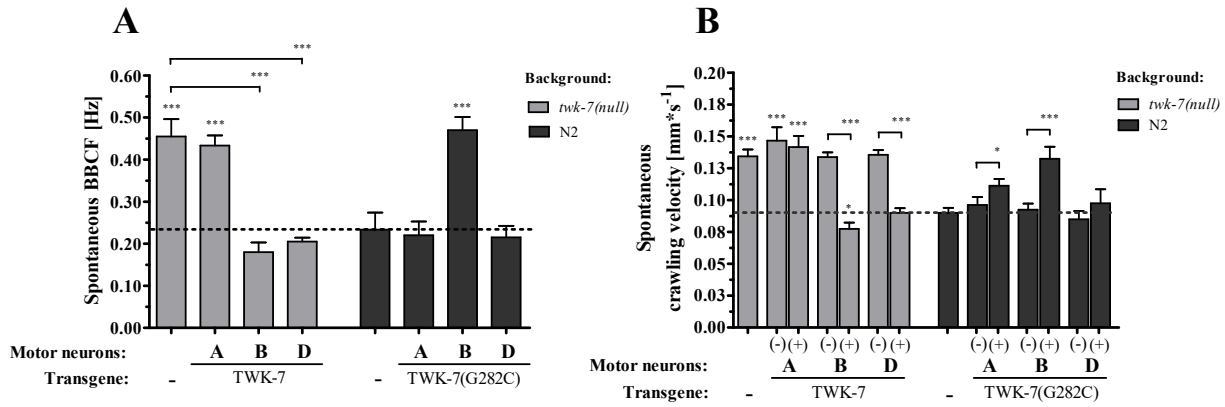

Figure 7: TWK-7 expressed in cholinergic B-type and GABAergic D-type motor neurons affects spontaneous crawling activity.

The BBCF **(A)** and velocity **(B)** of crawling were analyzed focusing on the A, B and D-type motor neurons of animals overexpressing *twk-7*wild-type and the dominant negative allele in *twk-7(null)* and wild-type background, respectively. The transgene worms (+) are directly compared with the non-transgenic (-) siblings. Dotted lines indicate the respective wild-type level. The values represent the means (± SEM) of at least N ≥ 3 independent experiments involving n ≥ 30 animals. *p < 0.05;**p < 0.01; ***p < 0.001 (Student's t-test).

2.1.6 TWK-7 abundance in cholinergic B-type and GABAergic D-type motor neurons affects the wave parameters during spontaneous crawling

The crawling pattern of *C. elegans* and other nematodes is determined by a sinusoidal wave propagated along the body from the head to the tail, where each segment of the worm's body follows the preceding segment (GRAY and LISSMANN 1964; PARK *et al.* 2008). In this context we were interested to know, to what extent the elevated speed of progression of *twk-7(null)* worms might affect parameters (i.e. amplitudes and wave lengths) which determine the shape of the sinusoidal wave propagated along the body **(Fig. S6A, B)**. To compare worm strains with different body proportions **(Fig. S6C)**, we calculated the respective wave parameters in percentage of body lengths. Dissecting these parameters we found that *twk-7(null)* mutants moved with about 15 % lower amplitude to body length ratios than wild-types **(Fig. 8A)**, whereas the wave length to body length values of both strains were similar **(Fig. 8B)**. Therefore, since the propagation speed of the wave along the body is determined by the frequency and the wave length, the higher bending frequency of *twk-7(null)* animals **(Fig. 7A)** was linearly translated into an increased wave velocity **(Fig. S6D)**. To further unravel the relationship between TWK-7 and the wave shape modulation process, we next analyzed the effects of an impaired TWK-7 function and TWK-7 overexpression on amplitudes and wave lengths at the level of motor neurons. Similar to *twk-7(null)* mutants, transgenic wild-type worms expressing

the dominant negative TWK-7($G^{282}C$) allele in the cholinergic motor neurons (driven by the *unc-17*(1 kb) promoter) or solely in B-type motor neurons (driven by the *acr-5* promoter) moved with about 13 % reduced amplitude to body length ratios when compared to wild-type **(Fig. 8A)**. The amplitude to body length ratios were not affected by TWK-7($G^{282}C$) expression in A-type (driven by the *unc-4* promoter) or D-type motor neurons (driven by the *unc-47* promoter). Moreover, for all transgenic wild-types expressing the dominant negative TWK-7($G^{282}C$) the wave length to body length ratios were wild-type-like (**Fig. 8B)**.

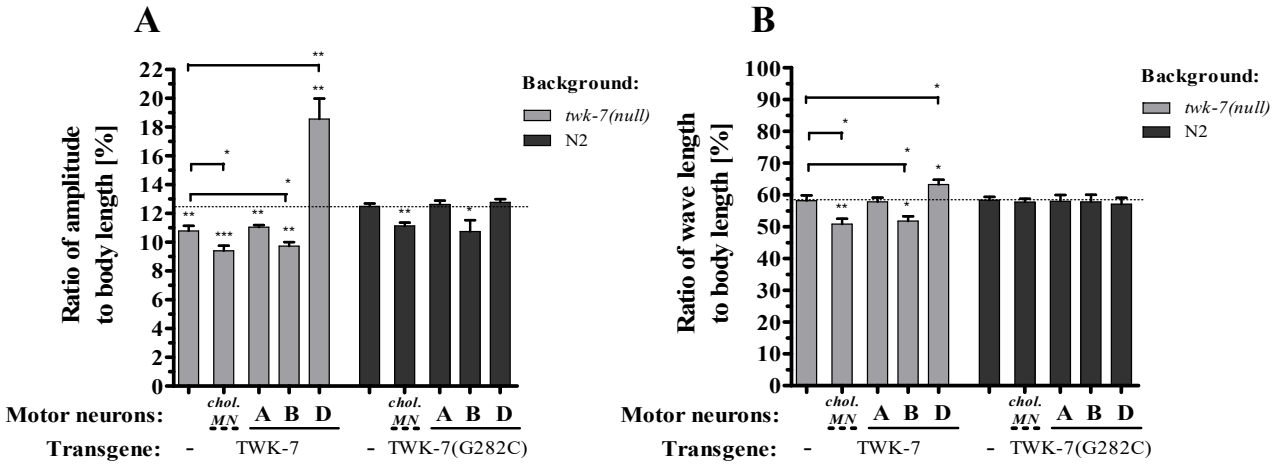

Figure 8: TWK-7 acts in cholinergic B-type and GABAergic D-type motor neurons to affect the wave parameters during spontaneous crawling.

The **(A)** amplitude- and **(B)** wave length to body length ratios of crawling were analyzed on the level of the A, B and D-type motor neurons by expressing *twk-7*wild-type and the dominant negative allel in *twk-7(null)* and wild type background. Dotted lines indicate the respective wild-type level. The values represent the means (± SEM) of at least N ≥ 3 independent experiments involving n ≥ 30 animals. *p < 0.05;**p < 0.01; ***p < 0.001 (Student's t-test).

When the wild-type form of TWK-7 was overexpressed in the cholinergic motor neurons (*unc-17* (1 kb) promoter) or solely in the B-type motor neurons (*acr-5* promoter) of *twk-7(null)* mutants, the amplitude to body length ratios were reduced by about 10 % and 20 % when compared to non-transgenic *twk-7(null)* and wild type animals, respectively **(Fig. 8A).** Moreover, these animals often initiated an additional wave along their bodies during spontaneous crawling **(Fig. 6C)** thereby showing reduced wave length to body length ratios **(Fig. 8B)**. Notably, the overexpression of the wild-type form of TWK-7 in D- type motor neurons of *twk-7(null)* worms (driven by the *unc-47* promoter) induced drastic increases of the amplitude to body length ratios that were found to be about 35 % and 40 % higher than in wild-type and *twk-7(null)* animals, respectively **(Fig. 8A)**. Moreover, the wave length to body length

ratios were increased by about 10 % in these transgenes when compared to the corresponding non-transgenes **(Fig. 8B)**. Remarkably, expression of wild-type form of TWK-7 in cholinergic A-type motor neurons of *twk-7(null)* worms (driven by the *unc-4* promoter) did not affect the wave parameters. These animals exhibited *twk-7(null)* phenotype. All transgenes with reduced crawling activity **(Fig. 7A)** also had decreased wave velocities **(Fig. S6D)**.

Summarizing, the abundance of functional TWK-7 at the level of B- and D-type motor neurons affects the wave lengths and amplitudes during spontaneous crawling. An impaired TWK-7 in B-type neurons is sufficient to reduce the wave amplitude, whereas overexpression of wild-type TWK-7 in D-type motor neurons is sufficient to elevate the wave amplitude. As shown for the unc-17(1kb)::TWK-7 transgenes **(Fig. 6C)**, increasing the TWK-7 expression specifically in B-type neurons was sufficient to frequently induce an additional wave during spontaneous crawling.

2.1.7 TWK-7 abundance in cholinergic B-type and GABAergic D-type motor neurons affects the duration of spontaneous forward crawling

A more detailed dissection of the crawling activity revealed that the body bending frequency of the two *twk-7(null)* mutant strains was preferentially enhanced during crawling forwards but was not significantly affected during crawling backwards **(Fig. S5A, B)**. This finding prompted us to investigate whether the temporal distributions of crawling forwards, crawling backwards, and resting are affected in the TWK-7(null) mutants. Compared to wild-type, these animals spent more time on crawling forwards in expense of reduced resting times, while the relative duration of crawling backwards was not altered **(Fig. 9A)**. Wild-type worms crawled 41.9 ± 17.5 % of their time in the forward mode and 54.5 ± 15.8 % of their time they rested, whereas, the respective values of *twk-7(nf120)* were 63.7 ± 14.9 % and 31,0 ± 12.7 %. Mutants carrying the *twk-7(gk760044)* allele also allocated their time preferentially to crawling forwards (62.1 ± 9.7 % crawling forwards, 30.8 ± 9.1 % resting). Remarkably, expression of TWK-7 under its own promoter as well as under the cholinergic motor neuron specific promoter completely rescued the crawling behavior phenotype of TWK-7(null) **(Fig. 9A)**. In accordance to this rescue approach, impairing TWK-7 channel function by expressing the dominant negative mutant variant TWK-7($G^{282}C$) in cholinergic motor neurons of wild-type worms led to a temporal distribution of crawling behaviors similar to TWK-7(null) **(Fig. 9A)**. Regarding the subtype level of motor neurons, transgenic *twk-7(nf120)* animals expressing *acr-5*p::TWK-7 (B-type motor neurons) and *unc-47*p::TWK-7 (D-type) spent more time on resting and less time

on forward crawling than the TWK-7(null). Wild-type worms carrying the dominant negative TWK-7($G^{282}C$) in the B-type motor neurons exhibited similar increased forward crawling activity like the twk-7*(null)* mutants. These transgenes spent more time in the state of forward crawling and exhibited shorter resting periods than the non-transgenic wild-types **(Fig. 9B)**. The dominant negative TWK-7($G^{282}C$) construct expressed in GABAergic D-type neurons had no influence on the duration of forward crawling and resting. Overall, the expression of TWK-7 in cholinergic B-type and GABAergic D-type motor neurons of the ventral nerve cord affects the persistence of forward crawling.

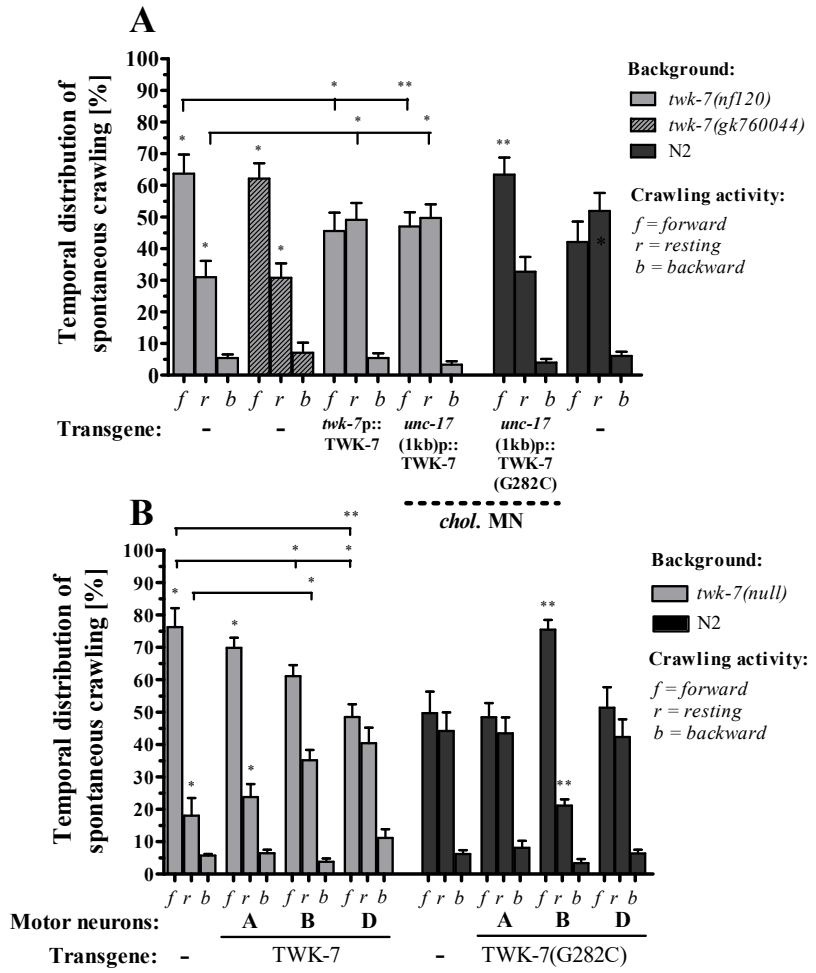

Figure 9: Inactive TWK-7 in cholinergic and GABAergic motor neurons increase the duration of spontaneous forward crawling.

The persistence of forward crawling and resting periods was analyzed in animals overexpressing selectively wild-type *twk-7* and the dominant negative allel in the **(A)** *twk-7*-specific neurons, all cholinergic motor neurons and **(B)** in the motor neuron subtypes A-, B-, and D with *twk-7(null)* and wild type background. The dotted lines indicate the respective wild-type level. The values represent the means (± SEM) of at least N ≥ 3 independent experiments involving n ≥ 30 animals. *p < 0.05;**p < 0.01; ***p < 0.001 (Student's t-test).

2.1.8 TWK-7 abundance in cholinergic B-type and GABAergic D-type motor neurons affects the straightness of forward crawling

We noticed that the straightness of crawling forwards was improved in TWK-7(null) mutants **(Fig. 10A)**. The ratio of distance to track length was found to be 43.1 ± 11.8 % for wild-type compared to 64.5 ± 11.6 % for *twk-7(null)* and 67.5 ± 16.8% for *twk-7(gk760044),* respectively **(Fig. 10B)**.

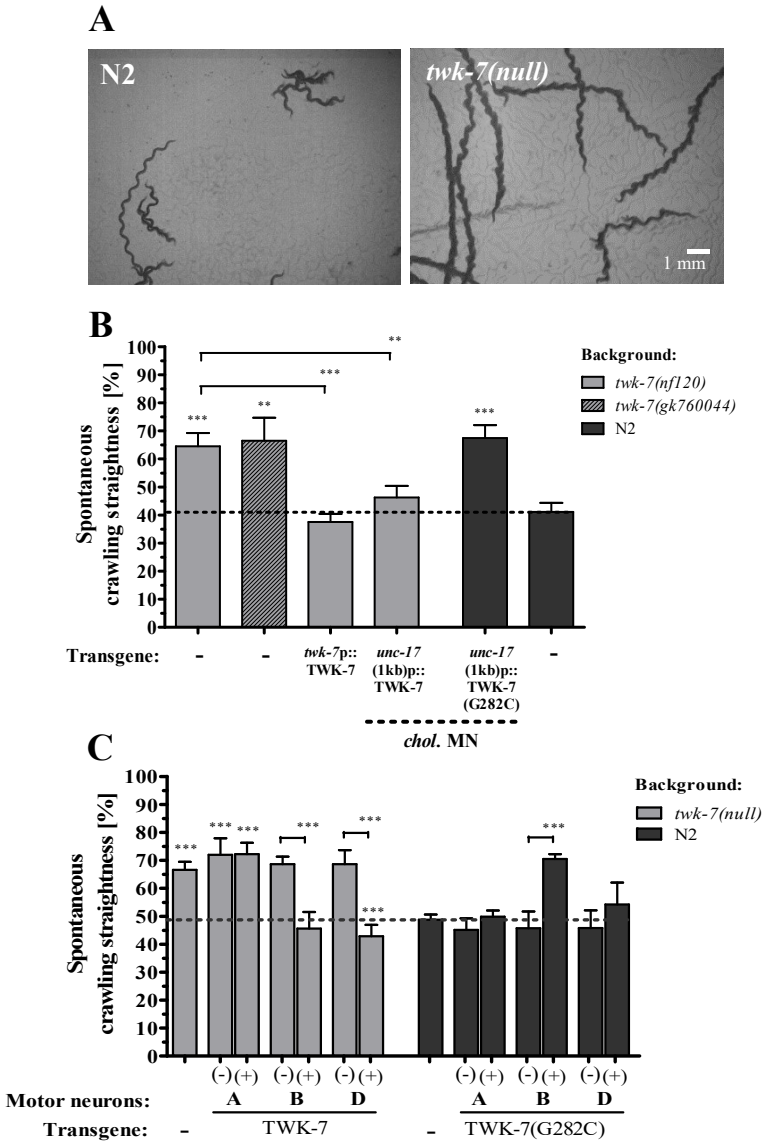

Figure 10: **Inactive TWK-7 in cholinergic and GABAergic motor neurons increase the straightness of spontaneous forward crawling.**
(A) Locomotion tracks (1 min. at 20°C, *ad libitum* feeding) of *twk-7(null)* and N2 wild types. The straightness of forward crawling was analyzed in worms overexpressing selectively wild type *twk-7* and the dominant negative allel $G^{282}C$ in **(B)** the TWK-7 specific neurons, cholinergic motor neurons and **(C)** in the cholinergic and GABAergic motor neuron subtypes with *twk-7(null)* and wild type background. The transgenes (+) are directly compared with non-transgenic (-) siblings. Dotted lines indicate the respective wild-type level. The values represent the means (± SEM) of at least N ≥3 independent experiments involving n ≥30 animals. *p < 0.05;**p < 0.01; ***p < 0.001 (Student's t-test).

This crawling behavior phenotype was rescued by TWK-7 expression driven by its own, by the cholinergic motor neuron specific, by the B-type motor neuron specific, and by the D-type motor neuron specific promoter, respectively **(Fig. 10B, C)**. Overexpression of both TWK-7 and TWK-7($G^{282}C$) in A-type motor neurons of TWK-7(null) and wild-type, respectively, had no influence on the straightness of forward crawling. However, when expressed in the B-type motor neurons of wild-type worms, the dominant negative TWK-7($G^{282}C$) construct initiated an improved straightness similar to *twk-7(null)*, while its expression in GABAergic D-type neurons had no influence on the straightness of forward crawling. Taken together, these data indicate that TWK-7 functions in the cholinergic excitatory B-type and inhibitory GABAergic D-type motor neurons of the ventral nerve cord not only to affect locomotion activity but also the locomotion behavior.

2.1.9 Loss of TWK-7 function affects locomotion parameters in a manner characteristic for stimulated locomotion behavior.

Compared to wild-type, crawling of TWK-7 deficient mutants and of transgenes overexpressing a dominant negative from of TWK-7 is characterized by (i) an increased activity preferentially on crawling forwards, (ii) an extended time spent on crawling forwards, and (iii) an improvement of the straightness of crawling forwards. Thus, the *twk-7(null)* mutants gave the impression to be "on the run" and, consequently, it is tempting to speculate that TWK-7 might be involved in a forward escape or foraging behavior (compare, (BHATTACHARYA *et al.* 2014; CALHOUN *et al.* 2014; FUJIWARA *et al.* 2002; WAKABAYASHI *et al.* 2004). Consistently with this hypothesis, the inspection of tracks generated by the TWK-7(null) mutant over a extended time period (17 hours) revealed that the area explored by the mutant worms were noticeably larger than the area covered by the wild types animals **(Fig. 11A).**

To underscore our hypothesis, we have developed a forward escape score that is based on the distribution of time spent on spontaneous crawling forwards, the straightness of spontaneous forward movement, and the spontaneous velocity. This escape score is approximately four times higher in both TWK-7(null) mutants compared to wild-type **(Tab. 1)**. Expression of TWK-7 under its own promoter as well as under the cholinergic motor neuron specific promoter rescued the increased escape score of TWK-7(null) mutants to the wild-type level **(Tab. 1)**. In contrast to that and consistent with the results presented above, the escape score of N2 wild-type worms that expressed the dominant negative TWK-7($G^{282}C$) mutant protein in TWK-7-specific neurons or in cholinergic motor neurons was found to be similarly elevated as seen for

TWK-7(null) **(Tab. 1)**. In contrast to the escape behavior, TWK-7 did not affect the food-dependent basal slowing response, another adaptive locomotion response observed in *C. elegans* (SAWIN *et al.* 2000). Well-fed TWK-7(null)animals reduced their crawling frequency upon entering areas of food similar to wild-type (**Fig. S8**). These results underline our hypothesis that TWK-7 may be specifically involved in escape-like locomotion behaviors by enhancing the activity, duration, and straightness and adjusting the wave parameters of moving forwards.

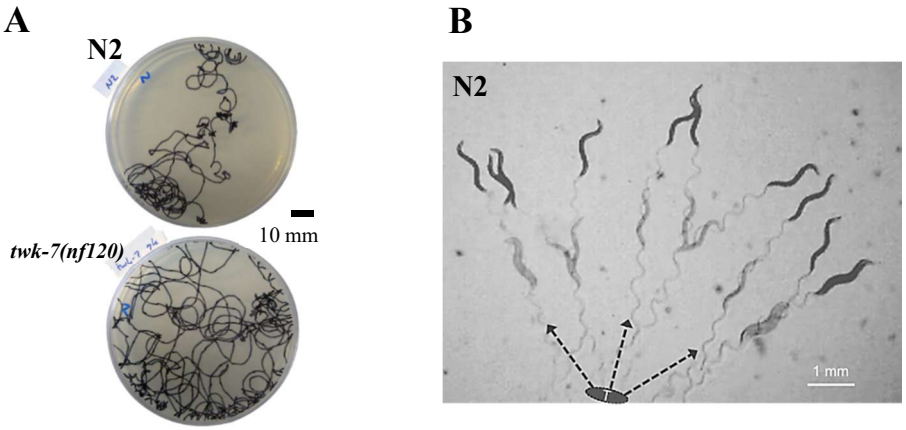

Figure 11: Tracks of spontaneous and stimulated moving worms.
(A) Tracks of spontaneous crawling activity were recorded for single worms after incubation overnight (17 hours, at 20°C and ad libitum feeding condition). **(B)** To assay the stimulated crawling activity, groups of approximately 10 young adult worms (age 72 h) were transferred to a new NGM agar plate and recorded immediately by camera. As shown here for wild-type worms, the animals leave the transfer point "T" by crawling straight forward (indicated by dotted arrows).Two pictures of the same movie are overlaid, showing the time span of 10 s between pale (0 s) and dark worms (+10 s).

Next, we investigate how wild-type animals change their locomotor activity, wave form and behavior in response to an external stimulus. Stimulated forward locomotion was initiated by transferring groups of 10 worms with a platinum wire on *ad libitum* seeded NGM plates (adapted from GAGLIA and KENYON, 2009) **(Fig. 11B; Fig. S7; Mov. M6, M7)**. We found that the stimulated wild-type animals dramatically increased their crawling frequencies about 5-fold **(Fig. 2A; Fig. 7A Fig. 12A, B)** and straightness rates about 2-fold **(Fig. 10B, C; Fig.12E, F)**. Notably, they reduced their amplitude to body length ratios by about 15 % to the level of spontaneously crawling TWK-7(null) mutants **(Fig. 8A; Fig.13A)**. Similar with the spontaneous condition, the wave length to body length ratios of wild-type worms were not affected **(Fig. 8B; Fig. 13B)**.

Then, we investigated how the constitutively hyperactive straightforward phenotype of TWK-7(null) mutants is affected by external stimulation. These animals further increased their activity about 2-fold **(Fig. 2A; Fig. 7A; Fig. 12A, B)** and straightness rates about 1.5-fold **(Fig. 10B, C; Fig. 12E, F)**, however, only up to the level of the stimulated wild-type worms. The amplitude to body length ratios of TWK-7(null) worms remained unchanged after stimulation when compared to the spontaneous crawling conditions **(Fig. 8A; Fig. 13A)**. Hence, the locomotion parameters of stimulated wild-type match those of stimulated TWK-7(null) animals. Consistently, the expression of the dominant negative TWK-7($G^{282}C$) in wild-types did not induce any significant effects on the stimulated wild-type crawling **(Fig. 12A-F)**.

Table 1: Escape scores of TWK-7(null) animals compared to N2 wild types and transgenic strains expressing the wild-type TWK-7 or the mutant channel TWK-7($G^{282}C$).

The velocity rate V reflects the ratio between stimulated (v) and spontaneous velocity (v_s). The values T_{fw}, St and V represent the means ± SD.

Allele/Transgene	% Time forward (T_{fw})	Straightness (St)	Velocity Rate V(v/v_s)	Escape Score (T_{fw} x St x V)
N2	0.42 ± 0.17	0.43 ± 0.12	0.41 ± 0.07	0.07
twk-7(nf120)	0.64 ± 0.15	0.65 ± 0.12	0.64 ± 0.05	0.26
twk-7(gk760044)	0.62 ± 0.10	0.68 ± 0.17	0.64 ± 0.03	0.27
*Ex[twk-7p:*TWK-7*]**	0.46 ± 0.14	0.38 ± 0.07	0.33 ± 0.06	0.06
*Ex[twk-7p:*TWK-7($G^{282}C$)*]**	0.63 ± 0.04	0.71 ± 0.06	0.64 ± 0.01	0.29
Ex[twk-7p:TWK-7($G^{282}C$)]§	0.61 ± 0.09	0.73 ± 0.07	0.64 ± 0.01	0.28
*Ex[unc-17(1kb)p:*TWK-7*]**	0.47 ± 0.12	0.46 ± 0.11	0.29 ± 0.01	0.06
*Ex[unc-17(1kb)p:*TWK-7($G^{282}C$)*]*§	0.63 ± 0.14	0.67 ± 0.12	0.51 ± 0.01	0.22

* *twk-7(nf120)* and § N2 background, respectively

Notably, rescued TWK-7(null) mutant worms that overexpressed wild type TWK-7 under the *twk-7* promoter were not able to reach the stimulated forward crawling activity exhibited by wild-type as well as by *twk-7(null)* animals **(Fig. 12A, C; Movie M8)**. This effect was also observed by overexpression of TWK-7 in the entire set of cholinergic, B-type or D-type motor neurons **(Fig. 12B, D)**. However, the effects of the rescue constructs during spontaneous crawling were less enhanced by external stimulation when compared to the spontaneous condition **(Fig. 7A, B; Fig. 12B, D)**.

Overall, we conclude that wild-type worms respond to external stimulation by changing crawling parameters reminiscent to the spontaneous hyperactive locomotion phenotype of TWK-7(null).

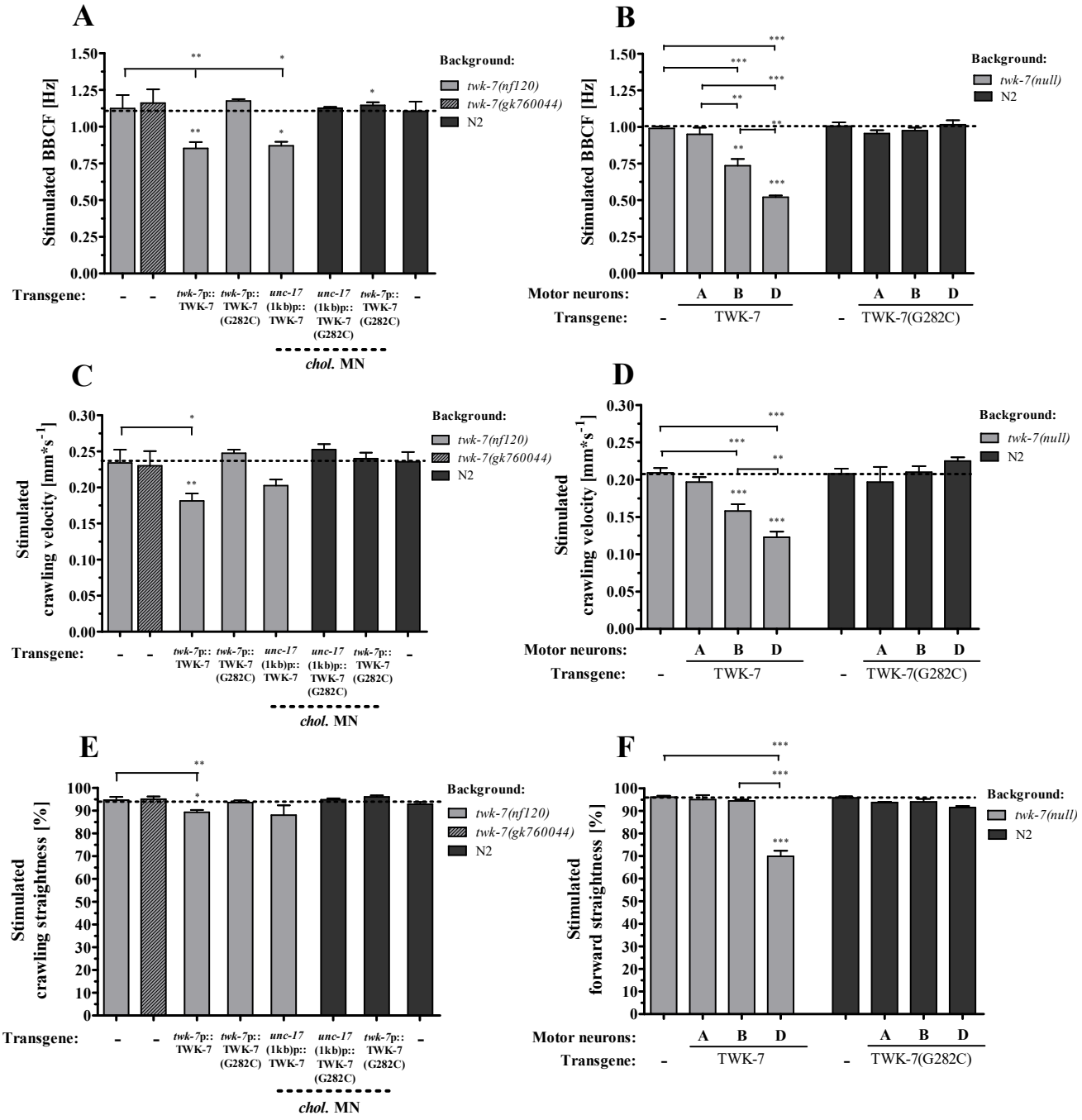

Figure 12: Stimulation affects the locomotion parameters in a manner typical for TWK-7 during spontaneous crawling.

The stimulated BBCF **(A, B)**, and the respective velocities **(C, D)** of forward crawling were determined immediately after stimulation for wild-type, *twk-7(nf120)* and transgene animals. The straightness rates **(E, F)**, of stimulated non-transgenes and transgenes are depicted. Dotted lines indicate the respective wild-type level. The values represent the means (± SEM) of at least N ≥ 3 independent experiments involving n ≥ 30 animals. *p < 0.05;**p < 0.01; ***p < 0.001 (Student's t-test).

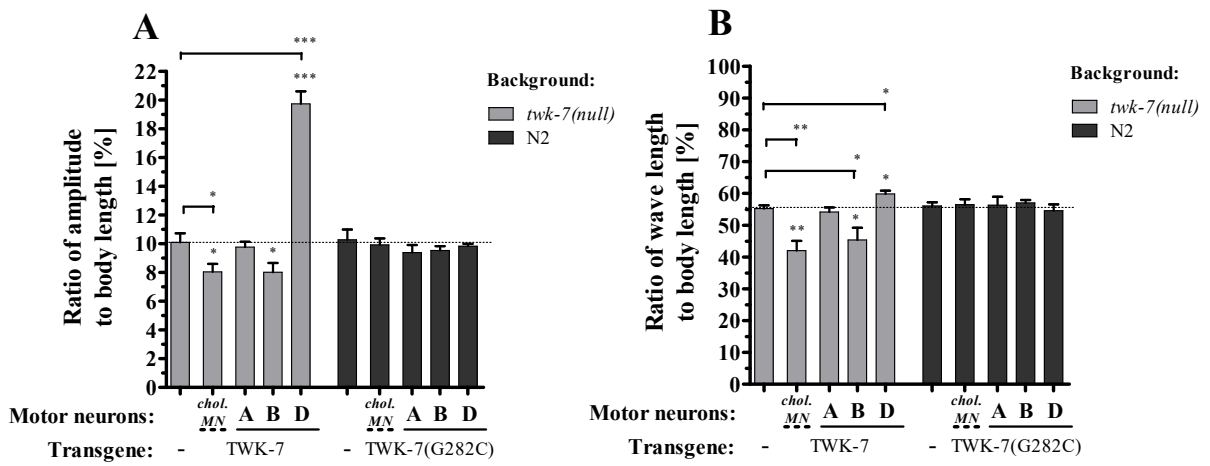

Figure 13: The wave parameters of transgenes and non-transgenes during stimulated crawling.

The **(A)** amplitude to body length ratios and the **(B)** wave length to body length ratios of transgenes and non-transgenes after stimulation are depicted. Dotted lines indicate the wild-type level. The values represent the means (± SEM) of at least N ≥ 3 independent experiments involving n ≥ 30 animals. *p < 0.05; **p < 0.01; ***p < 0.001 (Student's t-test).

2.2 The canonical Gαs pathway acts in *C. elegans* GABAergic motor neurons epistatically through TWK-7 to modulate locomotion behavior

2.2.1 Isolation of a novel *kin-2(cau1)* allele with enhanced locomotor activity

In a genetic screen for *C. elegans* worms with an enhanced and coordinated body bending swimming frequency we isolated the *kin-2* allele *cau1*. Compared to wild-type animals with a bending rate of 1.71 ± 0.1 Hz, the value of *cau1* worms was increased by about 0.52 Hz **(Fig. 14A)**. The *kin-2(cau1)* mutant strain also crawled on agar plate with an elevated spontaneous body bending rate (0.20 ± 0.05 Hz *vs* 0.53 ± 0,15 Hz) **(Fig. 14B)** resulting in an increased average crawling velocity of 0.15 ± 0,02 mm*s^{-1} when compared with the spontaneous velocity of wild-type worms (0.10 ± 0,01 mm*s^{-1}) **(Fig. 14C)**.

KIN-2/RIβ represents the cAMP dependent regulatory subunit of KIN-1/PKA-1. The *cau1* allele carries a G to A transition at nucleotide 275 of the coding region resulting in a $R^{92}H$ substitution in the polypeptide sequence. The R^{92} is part of the pseudo-substrate site of the inhibitory domain of KIN-2 (SCHADE *et al.* 2005). In good accordance with that, the strong reduction-of-function allele *ce179* of *kin-2* (SCHADE *et al.* 2005), which contained a similar $R^{92}C$ exchange in this small pseudo-substrate domain **(Fig. S9A)**, was suggested to cause enhanced activation of KIN-1/PKA and was characterized as hyperactive on plate. Our data revealed that the *kin-2(ce179)* with a $R^{92}C$ and the *kin-2(cau1)* with a $R^{92}H$ exchange exhibited similar increased swimming and crawling activity **(Fig. S9B-D)**.

2.2.2 Gαs*(gf)* mutants phenocopy the spontaneous locomotor activity and locomotion behavior of *twk-7(null)* mutants.

Catalytic KIN-1/PKA-1 and regulatory KIN-2/RIβ units are part of the Gαs signaling pathway. Being a negative regulator of KIN-1, a reduction of KIN-2 activity causes a gain-of-function *(gf)* of Gαs signaling. Hence, we next tested the corresponding upstream G-protein GSA-1 and the phosphodiesterase PDE-4, a negative regulator of Gαs signaling, for their effects on locomotor activity. Consistent with previous reports (CHARLIE *et al.* 2006; HU *et al.* 2011), the two Gαs*(gf)* mutant alleles *gsa-1(ce94)* and the *pde-4(ce286)* also showed enhanced spontaneous crawling activities similar to *kin-2(cau1)* and *kin-2(ce179)*. Most importantly, the

BBCF and velocities of all $G\alpha_s$*(gf)* mutants were remarkably similar to those of TWK-7(null) mutants (**Fig. 14A-C)**.

$G\alpha_s$*(gf)* mutant worms are smaller (**Fig. S9E**) and consequently moved with significantly reduced amplitudes (**Fig. S10A**) and wave lengths (**Fig. S10B**) during spontaneous forward crawling when compared with wild-type animals (absolute values). To compare wave shape parameters in animals of different body lengths, we calculated the amplitudes and wave lengths **(Fig. S10A, B)** in percentage of body lengths and found a reduced amplitude to body length ratio for the *kin-2(cau-1)* mutants (9.67 ± 0.38 % of body length) compared to the wild-type worms (12.15 ± 0.96 % of body length) (**Fig. 14D**). The ratios of wave lengths to body lengths revealed no significant differences among the tested strains (**Fig. 14E**). Although *twk-7(null)* worms were of the same body size as wild-types, their wave amplitudes during spontaneous crawling were reduced. The ratio of amplitude to body length (9.63 ± 0.55 % of body length) was similar to *kin-2(cau-1)* mutants (**Fig. 14D**).

Next, a detailed analysis of spontaneous crawling behavior revealed that $G\alpha_s$*(gf)* mutants spent significantly more time on fast crawling forwards (about 35 %) in expense of resting periods (about 35 %) **(Fig. 14F)** and exhibited increased straightness rates (about 20 %) in comparison with wild-type worms **(Fig. 15B**). Notably, this spontaneous fast straightforward locomotion behavior of $G\alpha_s$*(gf)* mutants was essentially indistinguishable from that of TWK-7(null) worms **(Fig 15A)**.

Taken together, mutants with an activated $G\alpha_s$ pathway and TWK-7(null) mutants resemble each other in their locomotor activities, body shape modulations and locomotion behaviors during spontaneous crawling affecting four different motor outputs – velocity/frequency (DE BONO and BARGMANN 1998; GLORIA-SORIA and AZEVEDO 2008), amplitude (BRYDEN and COHEN 2008; MCINTIRE *et al.* 1993a; YANIK *et al.* 2004), direction (CALHOUN *et al.* 2015; NAGY *et al.* 2015) and persistence (BENDESKY *et al.* 2011; WAKABAYASHI *et al.* 2004).

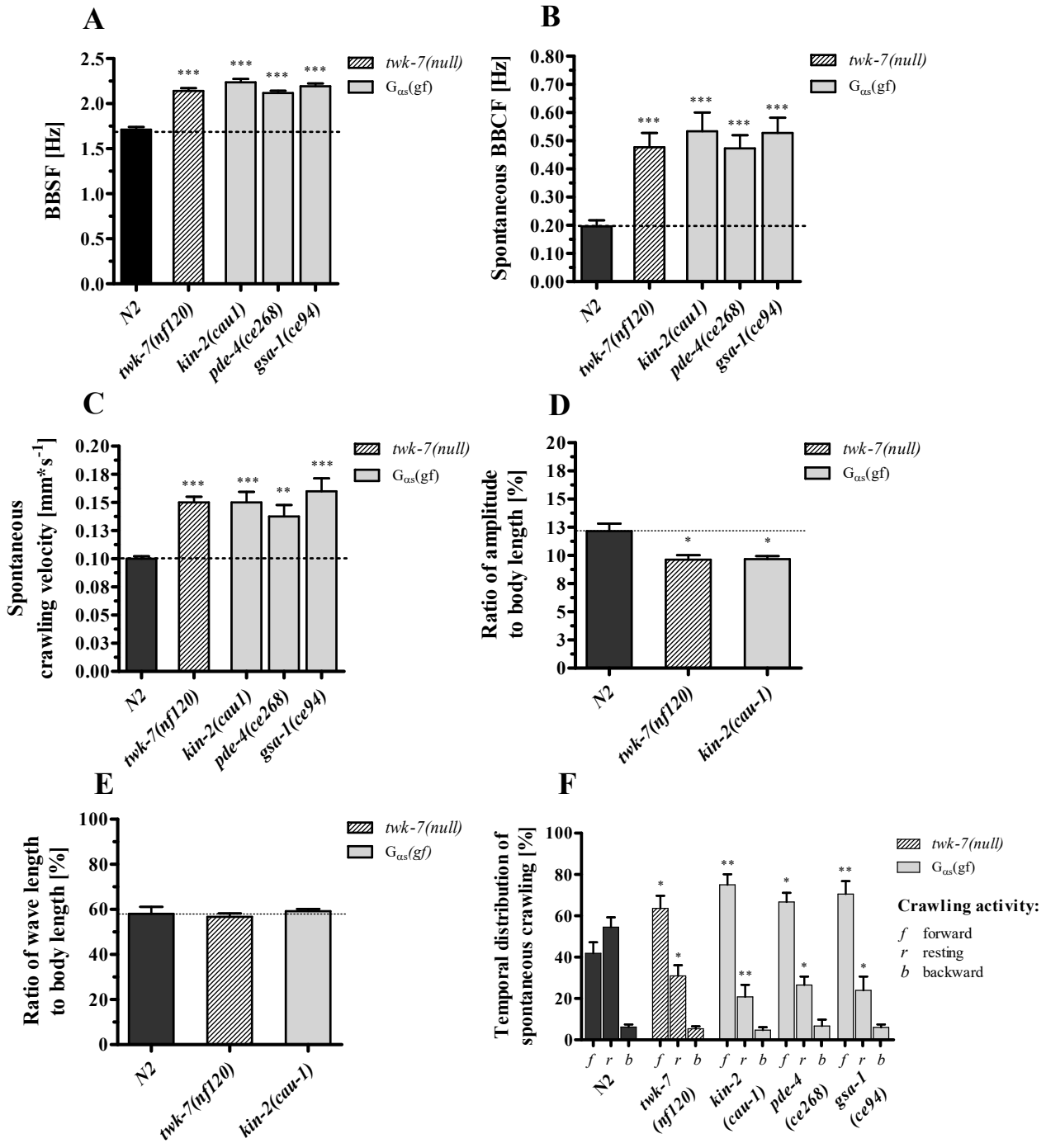

Figure 14: The spontaneous locomotor activities and behaviors of Gα$_s$*(gf)* and TWK-7(null) mutants.

Animals carrying alleles that cause a gain of function in the Gα$_s$ pathway and TWK-7(null) mutants exhibited similar hyperactivity. The **(A)** BBSF, **(B)** BBCF and the **(C)** crawling velocities are depicted. Compared with the wild-type worms, the **(D**) ratios of amplitudes to body lengths of *kin-2(cau-1)* and *twk-7(null)* mutants are slightly lower. The **(E)** ratios between wave lengths and body lengths are similar and wild-type like. The TWK-7(null) *and* Gα$_s$*(gf)* animals spend **(F)** more time on fast forward crawling and less time on resting. Dotted lines indicate the wild-type level. All values represent the means (± SEM) of at least N ≥ 3 independent experiments involving n ≥ 30 never starved animals. *p < 0.05;**p < 0.01; ***p < 0.001 (Student's t-test).

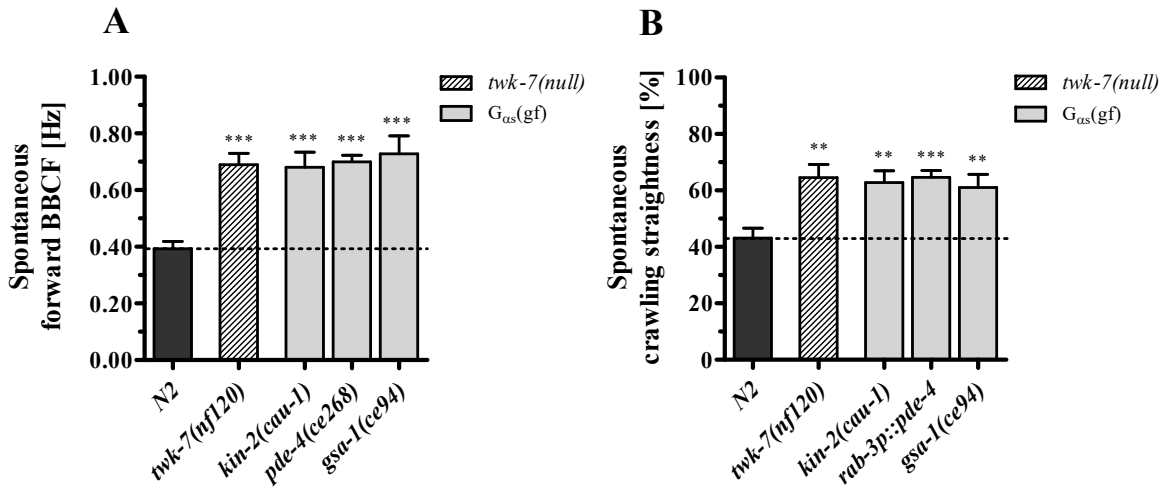

Figure 15: The straightforward movement characteristic for of Gα$_s$*(gf)* and TWK-7(null) mutant worms.
Hyperactive Gα$_s$*(gf)* and TWK-7(null) animals exhibit **(A)** elevated forward BBCF (when resting periods and backward movement are excluded) and **(B)** enhanced straightness rates when compared to wild-type. Dotted lines indicate the wild-type level. All values represent the means (± SEM) of at least N ≥ 3 independent experiments involving n ≥ 30 never starved animals. *p < 0.05;**p < 0.01; ***p < 0.001 (Student's t-test).

2.2.3 Hyperactive Gα$_{q/0}$ mutants differed from hyperactive Gα$_s$*(gf)* and TWK-7(null) worms in their locomotion behavior during spontaneous crawling.

Previous studies reported that Gα$_q$ and Gα$_0$ mutants with elevated DAG- and acetylcholine levels have a hyperactive phenotype (BHATTACHARYA *et al.* 2014; MILLER *et al.* 1999; SCHADE *et al.* 2005). However, although these animals crawled with an enhanced body bending frequency similar to Gα$_s$*(gf)* and TWK-7(null) mutants **(Fig. S11A, B)**, our more detailed analyses revealed a very distinct locomotion phenotype. Compared to wild-type animals, *goa-1(e1134)* and *dgk-1(nu62)* mutants did not exhibit elevated swimming activity **(Fig. S11C)**. Moreover, during spontaneous crawling these mutants spent significantly less time on crawling forwards and more time on resting and moving backwards **(Fig. S11D)** showing lower straightness rates **(Fig. S11E)** than the wild-types, Gα$_s$*(gf)* mutants and TWK-7(null).

2.2.4 TWK-7 requires the canonical Gα$_q$ pathway for its modulatory function.

It has been previously shown that the stimulating effect of an activated PKA on the locomotion of *C. elegans* is strongly dependent on the canonical Gα$_q$ pathway (REYNOLDS *et al.* 2005). Gα$_q$ influences the crawling activity of *C. elegans* by altering the intracellular concentration of the second messenger diacylglycerol (DAG) and, hence, the acetylcholine priming and release process (LACKNER *et al.* 1999; MILLER *et al.* 1999; NURRISH *et al.* 1999; REYNOLDS *et al.* 2005).

To test whether a hyperactive TWK-7(null) is able to affect the lethargic phenotype with extremely low spontaneous crawling activity of the strong $G\alpha_q$ reduction-of-function allele egl-*30(ad805)*, the respective double mutant was generated by introducing the *twk-7(nf120)(lf)* allele. Analyses of spontaneous crawling revealed that the TWK-7(null) allele was not able to substantially increase neither the declined locomotor activity **(Fig. 16A, B)** nor the increased resting periods **(Fig. 16C)** of the $G\alpha_q$*(lf)* mutant *egl-30(ad805)*. These results indicate that similar to the data reported for activated PKA (REYNOLDS *et al.* 2005) the stimulating impact of an inactive TWK-7 on *C. elegans* locomotion completely depends on a functional $G\alpha_q$ pathway.

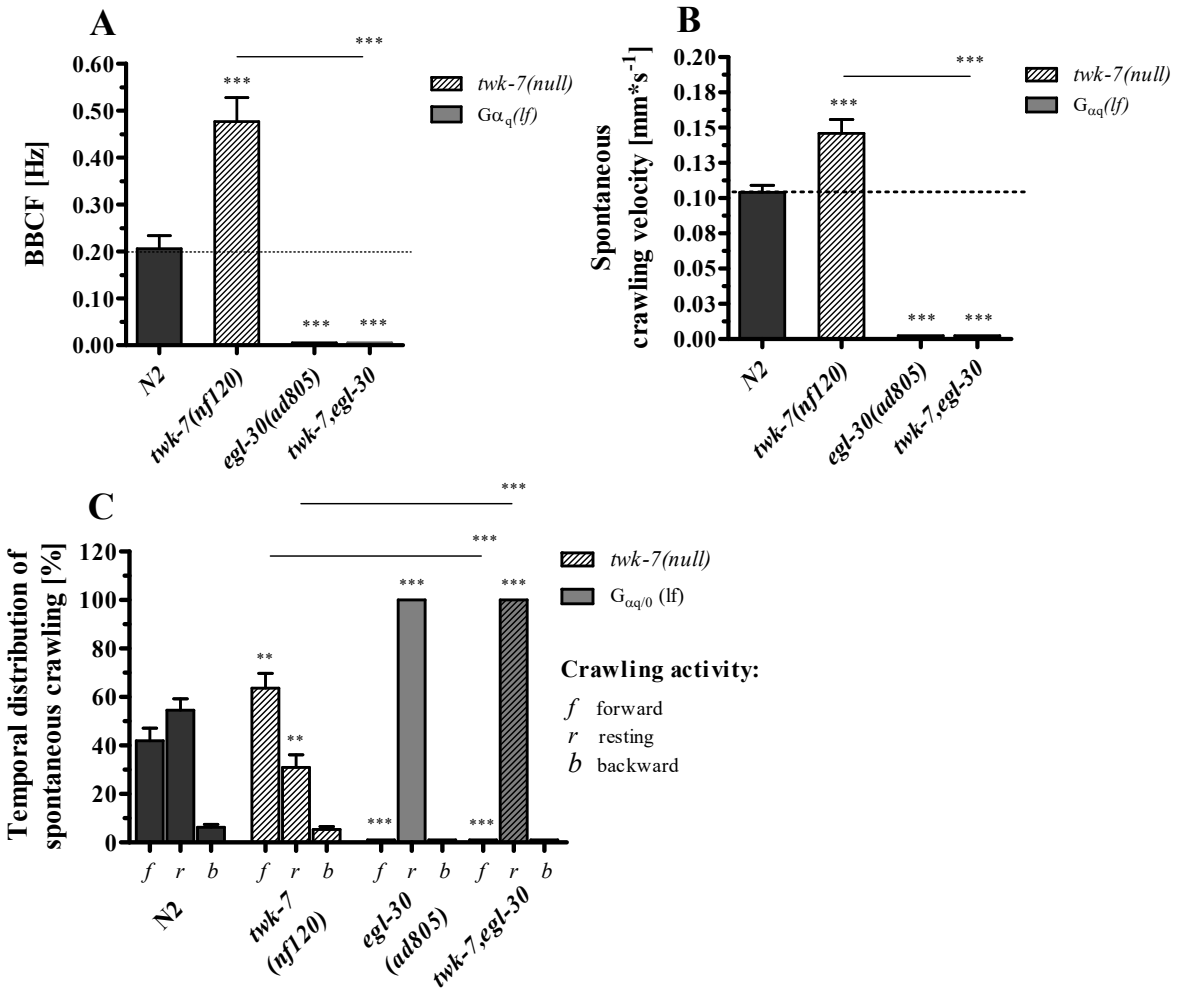

Figure 16: $G\alpha_{q/0}$ signaling is required for the function of TWK-7.

Inhibition of the $G\alpha_{q/0}$ pathways by the loss-of-function *egl-30(ad805)* allel caused decreased **(A)** bending frequencies and **(B)** crawling velocities in the respective single- and double mutant animals. The **(C)** periods of resting shown by worms with suppressed $G\alpha_{q/0}$ signaling are significantly increased in expense of shorter crawling phases. All values represent the means (± SEM) of at least N ≥ 3 independent experiments involving n ≥ 30 never starved animals. Dotted lines indicate the wild-type level. *p < 0.05;**p < 0.01; ***p < 0.001 (Student's t-test).

2.2.5 The Gαs*(gf)* and TWK-7(null) mutants showed wild-type-like responses in synaptic transmission assays

To test whether the elevated body bending rates of TWK-7(null) and Gαs*(gf)* animals that reflect increased body-wall muscle activity are caused by an alteration in the neuromuscular synaptic transmission of the major excitatory neurotransmitter acetylcholine, we employed a sensitivity assay with the choline esterase inhibitor aldicarb (BOULIN *et al.* 2008; FLEMING *et al.* 1997; LEWIS *et al.* 1980; MAHONEY *et al.* 2006; NGUYEN *et al.* 1995; OPPERMAN and CHANG 1991) Accumulation of acetylcholine in the synaptic cleft due to inhibition of its hydrolysis results in over-activation of postsynaptic cholinergic receptors and paralysis of worms. Consistent with previous studies, the control mutant alleles *dgk-1(nu62)* and *egl-8(e2917)* representing *(gf)* and *(lf)* alleles of the Gαq pathway were found to be hypersensitive or resistant, respectively, to the paralyzing effect of aldicarb, which is indicative for an enhanced or decreased steady state acetylcholine concentration, respectively. Remarkably, the time-course of aldicarb-induced paralysis was unchanged in the hyperactive allele *twk-7(nf120)* when compared with wild-type worms **(Fig. 17A)**. The enhanced locomotor activity of *kin-2(cau1)* worms was associated with a slightly increased sensitivity to the choline esterase inhibitor, however, a significant difference ($p = 0{,}038$) was found only at time point 90 min.

To examine postsynaptic processes, sensitivity assays using the acetylcholine agonist levamisole were performed. Levamisole activates nicotinic acetylcholine receptors of body-wall muscle which causes paralysis. In accordance with previous studies, the control allele *unc-29(e403)* encoding a defective postsynaptic acetylcholine receptor subunit showed a resistant phenotype. Compared to wild-type worms, the time course of levamisole induced paralysis was unchanged in TWK-7(null) **(Fig. 17B)**. Both Gαs pathway *(gf)* mutant alleles *kin-2(cau1)* and gsa-*1(ce94)* exhibited a slightly, however at no time point significant, increased sensitivity to levamisole.

Taken together, the *twk-7(nf120)*, *kin-2(cau1)* and *gsa-1(ce94)* mutant worms, although being hyperactive in swimming and crawling assays, did not show pronounced phenotypes in these pharmacological synaptic transmission assays. This striking discrepancy between the hyperactive locomotion phenotype and their wild-type like sensitivity to aldicarb and levamisole implicates that in contrast to the Gαq and Gα0 pathway, TWK-7 and Gαs may affect locomotion activity without altering the levels of steady-state acetylcholine release. However, one has to keep in mind that for unknown reasons, in some mutants changes of locomotion

behavior and aldicarb sensitivity do not necessarily reflect a change in acetylcholine release (SIEBURTH *et al.* 2007).

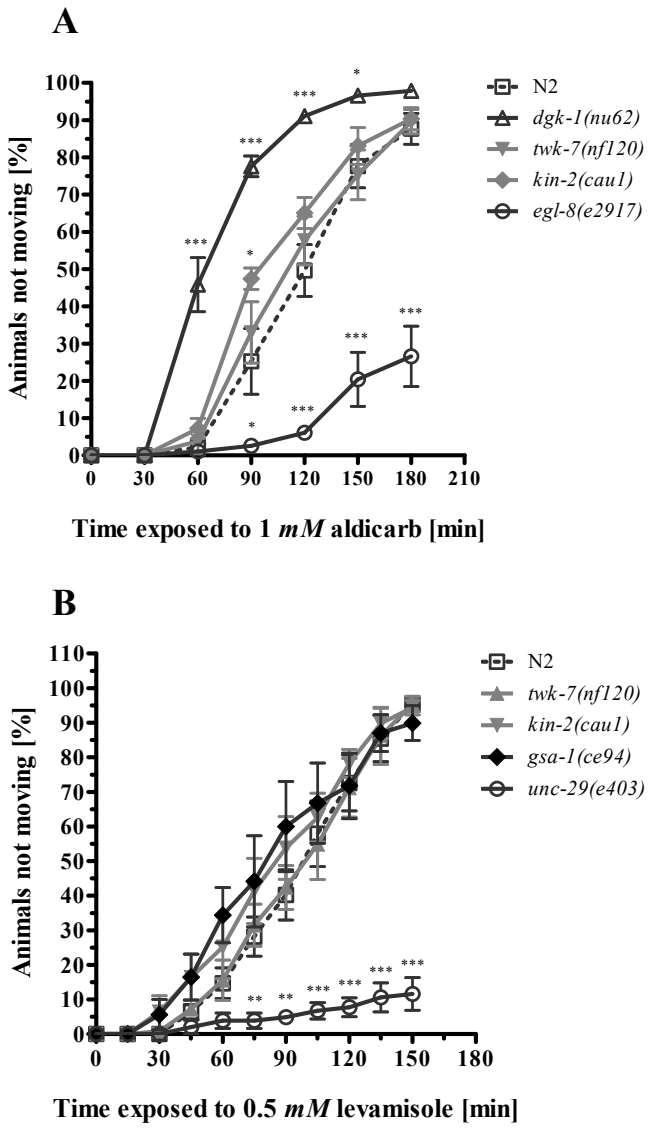

Figure 17: Synaptic transmission analysis assay.

Wild-type, *twk-7(null)* and *kin-2(cau-1)* worms exposed to **(A)** aldicarb and **(B)** levamisole revealed similar sensitivity for paralysis when compared to the *egl-8(e291)* and *unc-29(e403)* controls, respectively. All values represent the means (± SD) of at least N ≥ 3 independent experiments involving n ≥ 30 never starved animals. Dotted lines indicate the wild-type level. *p < 0.05;**p < 0.01; ***p < 0.001 (Student's t-test).

2.2.6 An activated Gαs pathway and TWK-7(null) did not act synergistically to modulate the locomotor activity and locomotion behavior during spontaneous crawling

The high degree of similarity between the spontaneous locomotion parameters of Gαs*(gf)* and TWK-7(null) mutants prompted us to examine whether the Gαs pathway interacts genetically with TWK-7. We generated *twk-7(null),kin-2(cau1)* and *twk-7(null),gsa-1(ce94)* double mutants and found that the Gαs*(gf)* alleles did not additionally increase the spontaneous bending frequencies **(Fig. 18A)** and velocities **(Fig. 18B)** in the *twk-7(null)* genetic background when compared to the respective single mutants. Accordingly, the activity of TWK-7(null) mutants was not affected by the insertion of the *kin-2(cau-1)* allele in the corresponding *twk-7(null)* genetic background.

The body sizes of *twk-7(null),kin-2(cau-1)* double mutants were as small as those of the *kin-2(cau-1)* single mutants **(Fig. S9E)** leading to similar absolute amplitude **(Fig. S10A)** and wave length values **(Fig. S10B)**. Accordingly, the double mutants exhibited comparable amplitude to body length ratios as calculated for the respective single mutants, *kin-2(cau1)* and *twk-7(null)* **(Fig. 18C)**. The wave lengths to body length ratios were not affected in the double mutants **(Fig. 18D)**. Thus, the wave shape parameters of TWK-7(null) mutants were not influenced by crossing the *kin-2(cau-1)* allel in the *twk-7(null)* genetic background.

We next found that the Gαs*(gf),twk-7(null)* double mutants and the respective single mutants spent similarly more time on fast forward crawling and less time on resting during spontaneous behavior **(Fig. 18E)**. Moreover, the values of spontaneous straightness were not further increased in the Gαs*(gf),twk-7(null)* double mutants **(Fig. 18F)**. Consequently, the locomotion behavior of TWK-7(null) mutants was not affected by introducing the *kin-2(cau-1)* allel in the *twk-7(null)* genetic background.

Summarizing, the enhanced locomotor activities and locomotion behaviors during spontaneous crawling caused by an inactive TWK-7 cannot be further affected by an activated Gαs pathway. Thus, the canonical Gαs and TWK-7 might share the same genetic pathway generating multiple phenotypes of high similarity in an epistatic manner.

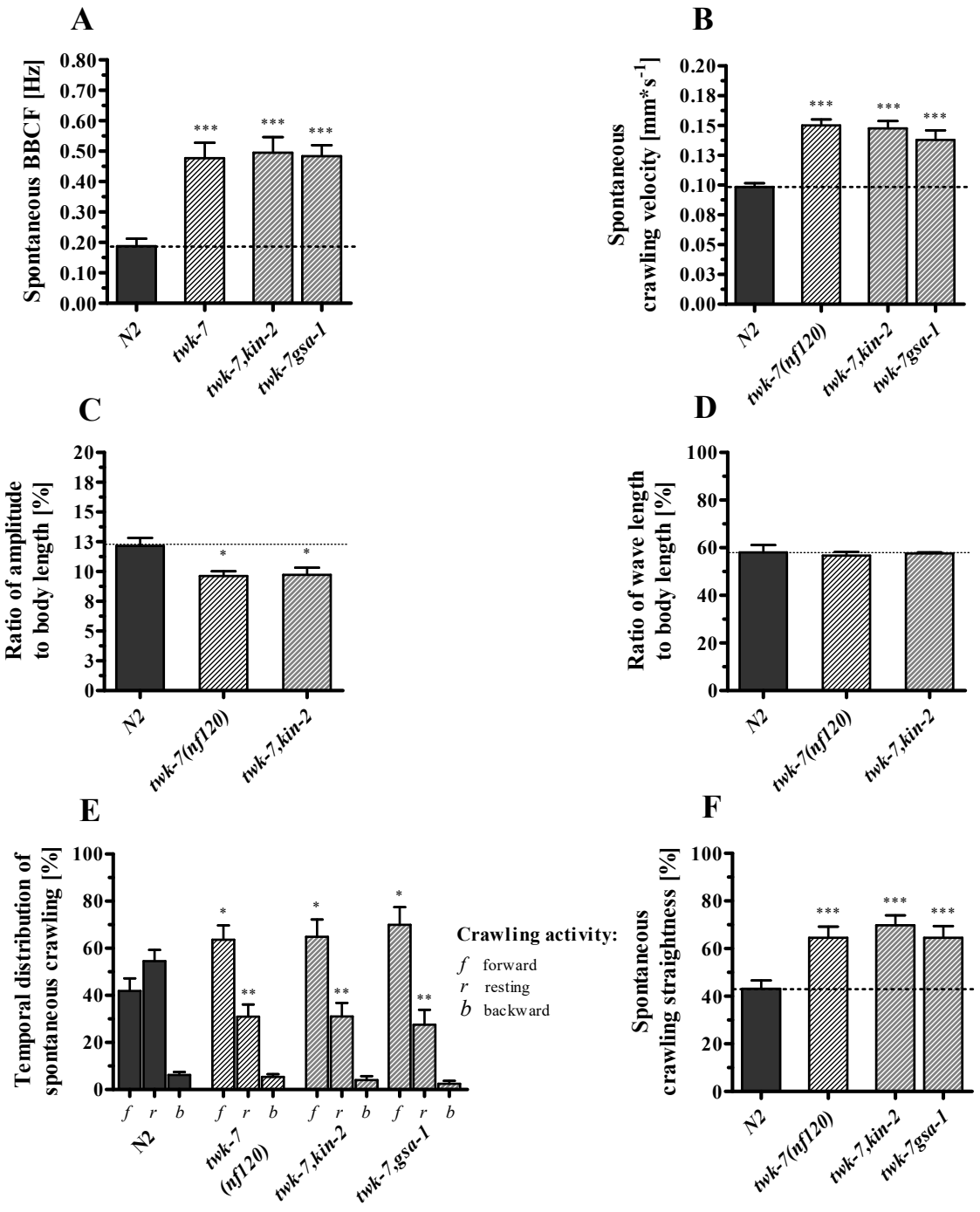

Figure 18: The spontaneous locomotor activities and locomotion behaviors of the *twk-7(null)*,Gα_s*(gf)* double mutants.

The *twk-7(null),*Gα_s*(gf)* double mutants exhibit **(A)** bending frequencies and **(B)** crawling velocities that are similar to those of the corresponding single mutants. Compared with wild-type animals, the **(C)** ratios amplitudes to body lengths of *twk-7,kin-2* double mutants are lower but similar to those of the respective single mutant worms. The **(D)** ratios of wave length to body length were nearly identical between wild-type, single- and double mutants. Similar to the single mutant worms, the double mutants of *twk-7* and Gα_s*(gf)* spend **(E)** more time on crawling forwards in expense of resting periods exhibiting markedly increased straightness rates **(F)** during spontaneous crawling when compared to the wild-type animals. Dotted lines indicate the wild-type level. All values represent the means (± SEM) of at least N ≥ 3 independent experiments involving n ≥ 30 never starved animals. *p < 0.05;**p < 0.01; ***p < 0.001 (Student's t-test).

2.2.7 Absent TWK-7 pores restore the locomotor activity and locomotion behavior phenotype induced by an suppressed *Gα$_s$* pathway in GABAergic motor neurons

To further investigate the interaction between the Gα$_s$ pathway and TWK-7 in *C. elegans* locomotion, we chose a cell-specific expression approach. TWK-7 has been previously shown in this study to be expressed in A-, B-, AS- and D-type motor neurons of the ventral nerve cord and some unidentified head neurons. We have demonstrated that overexpression of functional TWK-7 solely in GABAergic motor neurons of TWK-7(null) animals is sufficient to cause a drastically reduced spontaneous locomotor activity with increased amplitude to body length ratios. The same effects on spontaneous locomotion were observed not only in wild-type, but also in a *kin-2(cau1)* single and *twk-7(null),kin-2(cau1)* double mutant background. Hence, an elevated *twk-7* expression in GABAergic motor neurons is sufficient to mitigate the locomotion phenotypes induced by a generally activated PKA-1/KIN-1.

We next asked whether the inactivation of the Gα$_s$ pathway specifically in GABAergic motor neurons had a similar effect on the spontaneous locomotor activity of worms as the expression of *twk-7*. To this end, we employed the dominant negative *unc-47*p*::kin-2(G^{310}D)* construct generated by Wang and Sieburth (2013). Owing to the G^{310}D exchange the mutated KIN-2 is insensitive to cAMP and hence inhibits the PKA-1/KIN-1 pathway by preventing the dissociation of the PKA-1/KIN-1 holoenzyme (WANG and SIEBURTH 2013). Notably, the *unc-47*p*::kin-2(G^{310}D)* construct rescued the elevated locomotor activity of *kin-2(cau1)* mutants **(Fig. 19A, B)** and led to increased amplitude to body length ratios **(Fig. 19C)**. Interestingly, stimulated transgenic worms further increased their amplitude to body length ratios in contrast to the stimulated wild-type animals which reduced the corresponding amplitude ratios approximately to the level of *kin-2(cau-1)*, *twk-7(null)* and the respective double mutants **(Fig. 19C; Fig. 21B).** However, in a *twk-7(null)* or *twk-7(null),kin-2(cau1)* background, expression of *kin-2(G^{310}D)* in GABAergic motor neurons did not change the enhanced velocity, increased BBCF and reduced amplitude to body length ratio **(Fig. 21A)**. Hence, the loss of TWK-7 completely reverses the spontaneous locomotion activity and amplitude phenotypes caused by an inactivated Gα$_s$ pathway in GABAergic neurons **(Movie M9-M13)**.

When analyzing the spontaneous crawling behavior, we found that the persistent straightforward locomotion exhibited by *twk-7(null)* and *kin-2(cau-1)* single mutant animals

became drastically altered when *twk-7* was overexpressed in their GABAergic motor neurons. The time spent on crawling forward was reduced by almost 50 % in transgenic worms **(Fig. 20A)** and their straightness dropped from about 80 % to about 50 % **(Fig. 20B)**. Similar effects were observed in *kin-2(cau-1)* transgenic animals expressing the dominant negative *kin-2(G^{310}D)* allele in GABAergic motor neurons **(Fig. 20A, B)**. However, when introducing *unc-47*p::*kin-2(G^{310}D)* in a *twk-7(null)* single or *twk-7(null),kin-2(cau1)* double mutant background the time spent on crawling forwards and the straightness of forward crawling during spontaneous locomotion remained unchanged when compared to the elevated values obtained for the corresponding non-transgenes **(Fig. 20A, B)**.

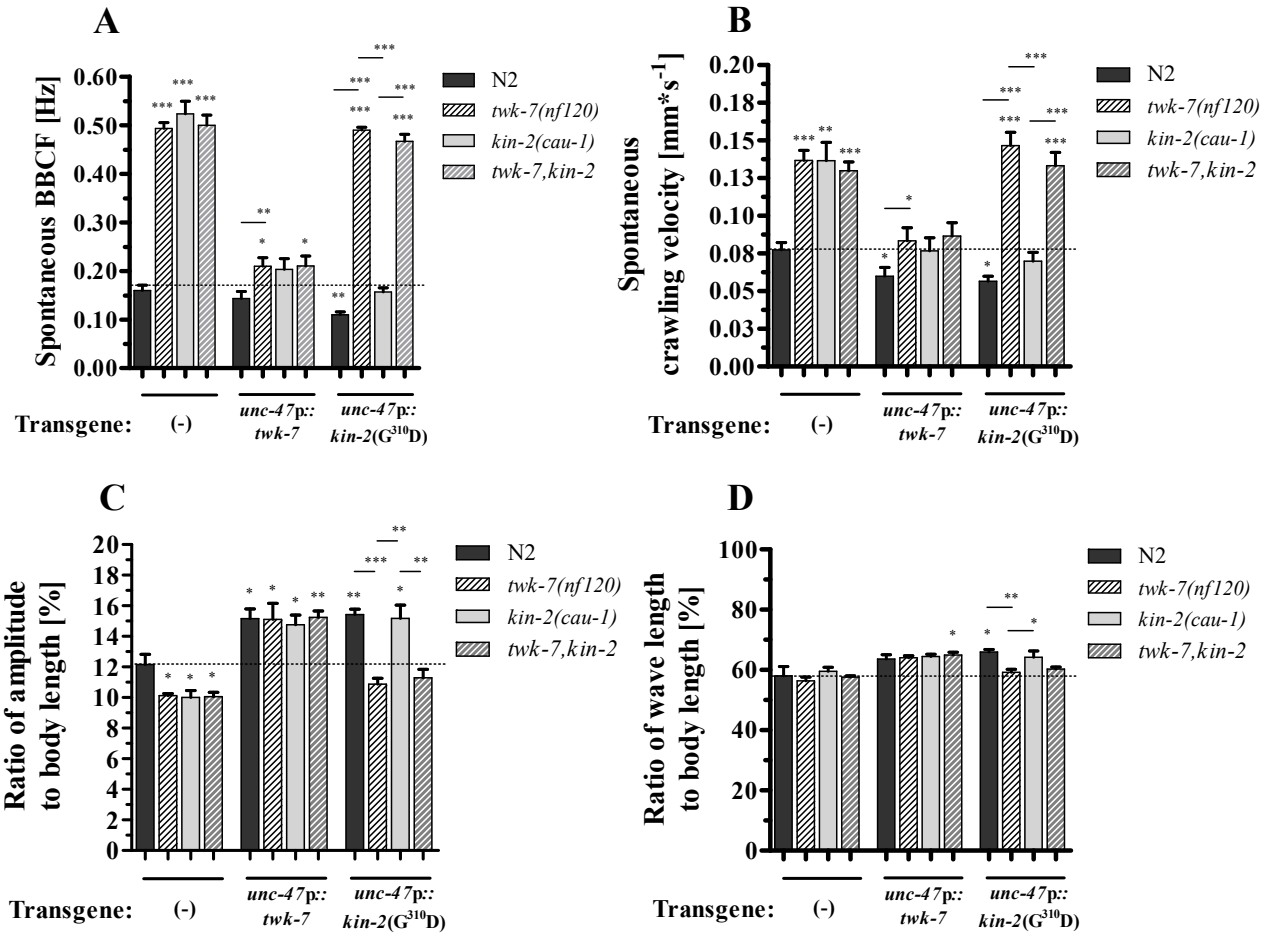

Figure 19: The spontaneous locomotor activities of *twk-7(null)* and *kin-2(cau-1)* transgenes with suppressed GABAergic signaling.
Animals overexpressing the wild-type *twk-7* and the dominant negative *kin-2(G^{310}D)* allele in the GABAergic neurons exhibit noticeably decreased **(A)** bending frequencies and **(B)** velocities during spontaneous crawling. These transgene animals also present **(C)** elevated bending amplitudes and **(D)** slightly increased wave lengths. Notably, the amplitudes of animals carrying dominant negative *kin-2* in *twk-7(null)* genetic background present normal amplitudes. All values represent the means (± SEM) of at least N ≥3 independent experiments involving n ≥30 never starved animals. *p < 0.05;**p < 0.01; ***p < 0.001 (Student's t-test).

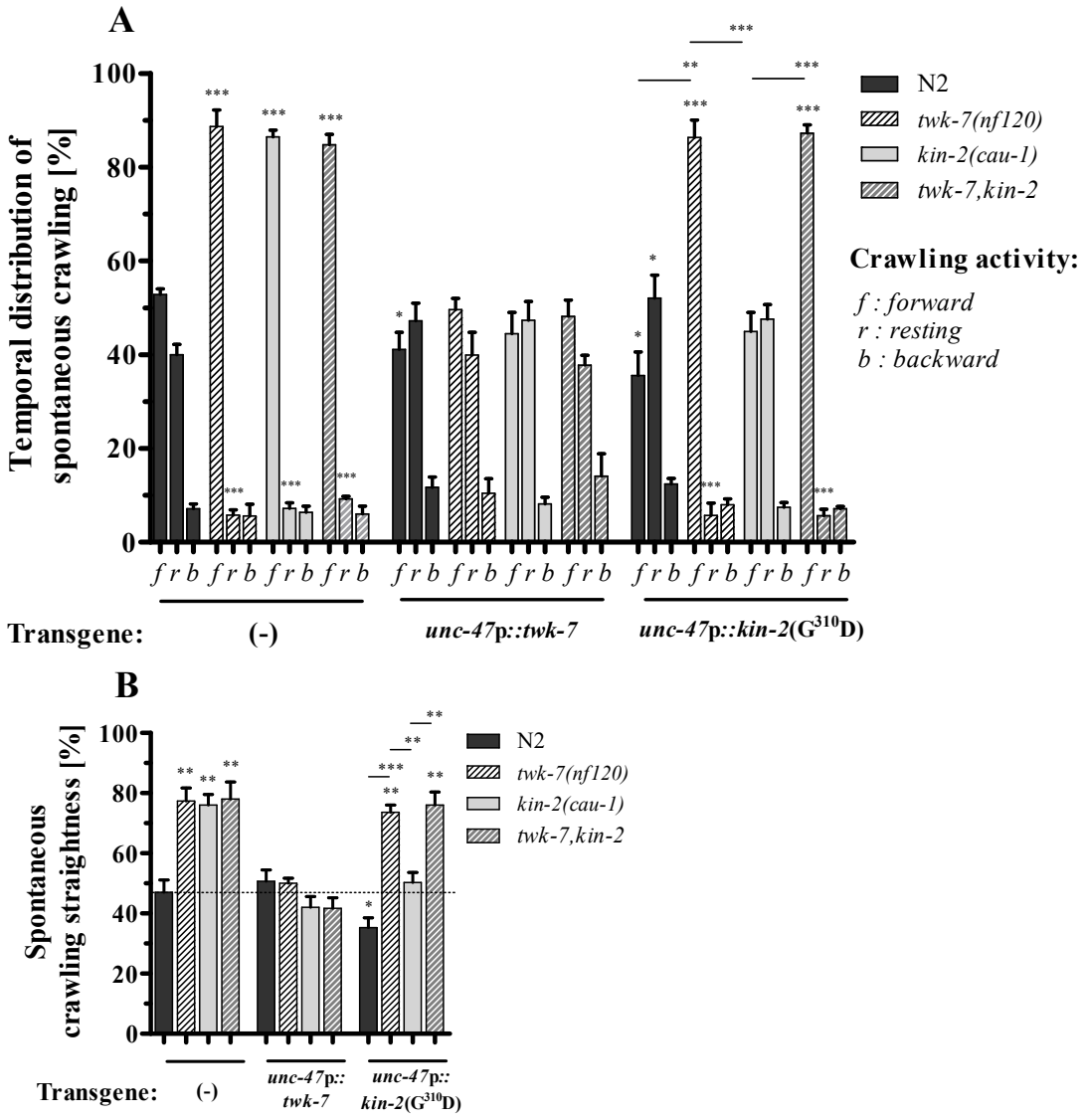

Figure 20: The spontaneous locomotion behaviors of *twk-7(null)* and *kin-2(cau-1)* transgenes with suppressed GABAergic signaling.
Compared with the corresponding non-transgenes, animals overexpressing the wild-type *twk-7* and the dominant negative *kin-2* allele spend **(A)** more time on resting in expense of crawling periods, exhibiting decreased **(B)** straightness rates. Decisively, the *twk-7(null)* and *twk-7, kin-2* mutants carrying the dominant negative *kin-2* are not affected **(A, B)**. Dotted lines indicate the wild-type level. All values represent the means (± SEM) of at least N ≥ 3 independent experiments involving n ≥30 never starved animals. *p < 0.05;**p < 0.01; ***p < 0.001 (Student's t-test).

Again, the loss of TWK-7 (most probably equivalent to a closed channel) counteracts the locomotion effects of an inactive PKA pathway in GABAergic motor neurons, while an activated PKA-1/KIN-1 pathway is not able to mitigate the effects of GABAergic motor neuron specific *twk-7* expression.

Taken together, in GABAergic motor neurons an impaired PKA pathway and overexpressed TWK-7 confer similar lethargic locomotion phenotypes with increased bending amplitudes. In both cases, these phenotypes were affected by an activated PKA-1/KIN-1 background. In contrast, the hyperactivity caused by a loss of TWK-7 (most probably equivalent to a closed channel) completely masked the locomotion phenotype of a suppressed GABAergic PKA-1/KIN-1 pathway. This indicates that TWK-7 functions epistatic to KIN-1/PKA-1 to affect the spontaneous as well as the stimulated locomotion parameters - activity, wave shape, and behavior (i.e. duration and straightness of forward crawling). Especially, the amino acid sequence of TWK-7 contains phosphorylation sites at the positions 2, 13, 81, 444 and 502 which are highly specific for the PKA **(Tab. S1)**. Interestingly, the enhanced straightness rates induced by activated PKA and/or closed TWK-7 pores might compensate the overall loss of locomotor efficiency caused by hyperactivity on the level of the GABAergic motor neurons **(Fig. 20B; Fig. S13; Fig. 19A, B).**

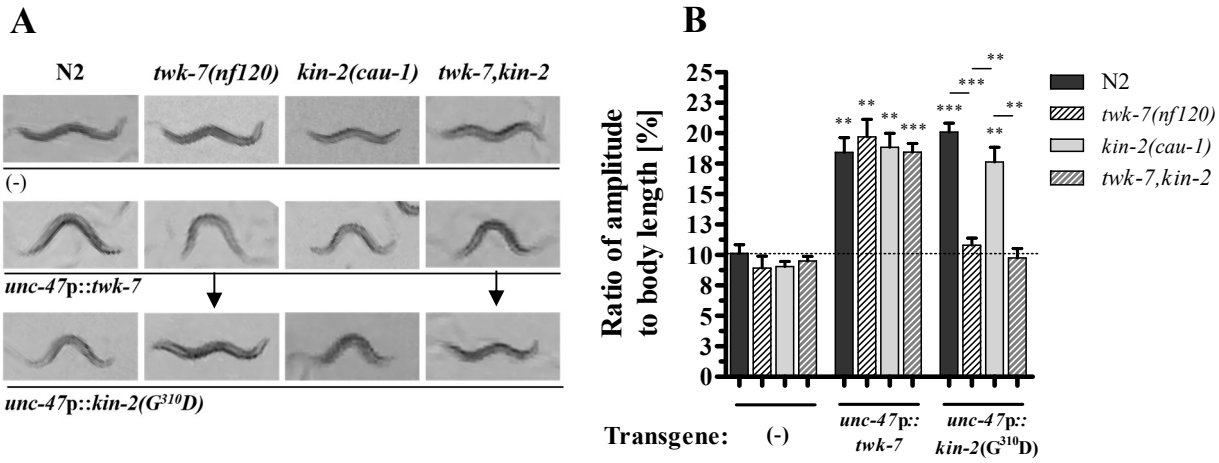

Figure 21: The amplitudes of *twk-7(null)* and *kin-2(cau-1)* transgenes with suppressed GABAergic signaling during stimulated crawling.
The amplitudes of stimulated animals **(A)** captured by camera during crawling are shown. The arrows indicate the rescue effect in worms with TWK-7(null) background expressing the *kin-2(G^{310}D)* allele. After stimulation wild-type animals reduced their **(B)** amplitudes to the level of spontaneous crawling *kin-2(cau-1)*, *twk-7(null)* mutants and double mutants (compare Fig, 19C), whereas worms overexpressing wild-type *twk-7* or dominant negative *kin-2* exhibit strongly elevated amplitudes. In contrast, the amplitudes of animals carrying dominant negative *kin-2* in *twk-7(null)* genetic background present normal amplitudes. Dotted lines indicate the wild-type level. All values represent the means (± SEM) of at least N ≥ 3 independent experiments involving n ≥ 30 never starved animals. *p < 0.05;**p < 0.01; ***p < 0.001 (Student's t-test).

3. Discussion

Here we have shown that the *C. elegans* two-pore domain potassium (K_2P) channel TWK-7 is required to maintain both normal spontaneous rhythmic locomotor activity and locomotion behavior. In spite of predicted biochemical similarities within the *C. elegans* TWK family (KRATSIOS *et al.* 2012; SALKOFF *et al.* 2001), we found that the locomotion phenotypes of the TWK-7(null) were distinct to several other neural expressed TWK-7 mutants. Our data indicate that these functions can be ascribed to a cholinergic B-type and GABAergic D-type neuron specific expression of TWK-7. In the past two decades by means of molecular and electrophysiological methods it has been recognized that the eukaryotic K_2P channels are regulatory background K^+ channels that modify the membrane potential of neurons and other cell types (ENYEDI and CZIRJAK 2010). Nevertheless, data defining the physiological role of K_2P channels in their native environments are still limited. In principle, activated K_2P channels restore the resting membrane potential by increasing potassium permeability. Diametrically opposed closure or a genetic knock out of K_2P channels depolarize the resting membrane potential resulting in an increased excitability of cells (ENYEDI and CZIRJAK 2010). Accordingly, we suggest that the enhanced spontaneous locomotion activity of TWK-7(null) animals is caused by an elevated excitability of neurons. This acceleration of TWK-7(null) worms also implicates that in wild-type worms TWK-7 is activated during spontaneous crawling. An activated K_2P channel lowers the excitability of cells and, to that effect, overexpressing TWK-7 reduced the locomotor activity of TWK-7(null) mutants even slightly below that of wild-type worms. Moreover, the additional wave that appears in worms with overexpressed TWK-7 channels can be explained by a reduced excitability of motor neurons that leads to decreased wave lengths and bending frequencies causing a slowed backward propagation of the wave, while the respective rhythmic wave initiation pattern appears to be periodically out of phase.

Since the activity of K_2P channels require a dimeric structure (ENYEDI and CZIRJAK 2010), the expression of TWK-7 mutant channels having a disabled potassium selectivity filter should have an antimorphic effect by binding and thus inactivating the normal wild-type channels. As expected the expression of the mutant channel TWK-7($G^{282}C$) solely in cholinergic excitatory B-type motor neurons did not influence the elevated locomotor activity of TWK-7 (loss of function) mutants but increased the activity of wild type worms. In good accordance with the proposed function of *C. elegans* TWK-7 in motor neurons, knock-out models and

pharmacological approaches in the fly and in mammals suggested that K_2P channels are involved in the regulation of rhythmic muscle activity (ALLER *et al.* 2005; DE LA CRUZ *et al.* 2003; DE LA CRUZ *et al.* 2014; DECHER *et al.* 2011; DONNER *et al.* 2011; KUNKEL *et al.* 2000; LALEVEE *et al.* 2006). For example, pharmacological activation of the K_2P channel TASK is associated with decreased motor neuronal excitability, which most likely contributes to the immobilizing effect of the anesthetics (LAZARENKO *et al.* 2010).

Worthy of note, in contrast to the classical *unc*oordinated *C. elegans* mutants (BRENNER 1974) which impair normal behavior and mainly define constitutive elements of neuromuscular functions, the *twk-7(null)* mutant shows coordinated, directed and accelerated locomotion within a physiological range. This indicates that TWK-7 may be involved in modulation of rhythmic and patterned muscle activity in cholinergic B-type motor neurons and GABAergic D-type motor neurons. These inhibitory GABAergic motor neurons have been reported to be not essential for rhythmic activity during forward crawling (MCINTIRE *et al.* 1993b). Here, we found that adequate TWK-7 expression is required in D-type GABAergic motor neurons to maintain both activity and straightness of forward locomotion suggesting that the excitability of these motor neurons may be important for specific locomotion behaviors. In particular, TWK-7 expression in D-type motor neurons was found to counteract the changes in locomotor activity and behavior of TWK-7(null) mutants. However, in contrast to the situation in the excitatory B-type motor neurons, an impaired TWK-7 channel was not able to increase the velocity, straightness and duration of forward movement in wild-type animals via D-type motor neuron expression. Given that B-type motor neurons activate the contralateral inhibitory D-type motor neurons, we assume that a specifically reduced excitability of D-type motor neurons due to TWK-7 expression may represent a limiting step in the otherwise elevated B-type driven rhythmic muscle contraction of TWK-7(null) mutants. On the other hand, an increased excitability of D-type motor neurons due to expression of an inactive TWK-7 channel will have no effect on the rhythm of unstimulated forward crawling in wild-type worms. This might be a result of suspected *all-or-nothing* inhibitory action potentials. We also observed that the TWK-7(null) worms expressing native TWK-7 in GABAergic neurons moved slow but uncoordinated, exhibiting larger S-shapes with higher amplitudes. A role of the GABAergic neurons in regulating shape and amplitude of the worms is in agreement with the literature (BRYDEN and COHEN 2008; MCINTIRE *et al.* 1993b; YANIK *et al.* 2004).

It is an interesting question how inactivation of TWK-7 in cholinergic motor neurons causes preferentially forward movement. It has been shown that distinct premotor interneurons (AVA, AVE, AVD, AVB, PVC) innervate the A- and B-type motor neurons to initiate backward and forward movement (CHALFIE *et al.* 1985; ZHENG *et al.* 1999). Moreover, the cross-inhibition between the forward and backward circuit and the premotor interneuron-motor neuron coupling via gap junctions has been demonstrated to establish an imbalanced motor neuron output in favor of forward locomotion (KAWANO *et al.* 2011; ZHENG *et al.* 1999). The forward circuit is generally active and represents the default mode of locomotion direction, whereas the backward circuit is rather proactive regulated by touch and other stimuli (CHALFIE *et al.* 1985). Similar models of the neuronal control of locomotion direction have been unraveled in *Drosophila* (BIDAYE *et al.* 2014), crickets (SCHONEICH *et al.* 2011), and cockroaches (BURDOHAN and COMER 1996). All of these models predict that higher excitability of the motor neurons reinforce the activity of the forward circuit. In line with this, we have shown that a closed TWK-7 channel solely in cholinergic B-type motor neurons is sufficient to enhance the duration of forward movement in expense of resting periods.

The regulation of velocity, duration, and direction of movement in response to external and internal cues is a hallmark of adaptive locomotion behavior. Escape behaviors and foraging are representative examples for this. In agreement with a previous report (GAGLIA and KENYON 2009), we found that the transfer of worms to new assay plates by a platinum wire stimulates fast straightforward crawling when comparing to spontaneous movement. Since this effect although declining persists **(Fig. S15)**, we suggest that it might reflect an escape-like behavior rather than an escape reflex. Although, our current data do not allow to draw unequivocally the conclusion that *twk-7* contributes to this stimulated escape-like behavior. Nevertheless, the high degree of similarity in 5 central aspects of locomotion - velocity/frequency, wave parameters, forward direction, duration, and straightness - that are constitutively affected by TWK-7 and induced in wild-type by external stimulation are quite remarkable. Thus, we suggest that TWK-7 may act as a putative player in the context of fast targeted forward locomotion.

Since the K_2P channels are regulated by a huge number of stimuli (ENYEDI and CZIRJAK 2010), preferentially the N- and C-terminal region of TWK-7 might constitute a direct target for regulators such as cAMP-dependent kinases. It was particularly important to test this hypothesis in order to get insight into the pathways regulating TWK-7.

Following the question of putative regulators of TWK-7, we have isolated a novel hyperactive allele of the *C. elegans kin-2* gene encoding the negative regulatory subunit of PKA-1/KIN-1. Detailed locomotion analyses revealed that the novel *kin-2(cau1)* allele and other known $G\alpha_s$-PKA*(gf)* mutants (CHARLIE *et al.* 2006; REYNOLDS *et al.* 2005; SCHADE *et al.* 2005) showed a fast **(Fig. 14B, C)** straightforward **(Fig. 15A, B)** spontaneous locomotion behavior spending more time on crawling forwards in expense of resting periods **(Fig. 14F)** thereby offering the impression to be "on the run" when compared to wild-type worms. In this study, we found similar phenotypes for mutants that lack the K_2P channel TWK-7. In good accordance, our genetic interactions studies provide evidence for epistasis between the $G\alpha_s$-PKA pathway and TWK-7 in affecting the locomotion activity and behavior of *C. elegans*.

The modulation of synaptic transmission by $G\alpha_s$-PKA signaling is a widespread mechanism of neuronal communication and activation of PKA is known to facilitate synaptic transmission by presynaptic mechanisms (CHEUNG *et al.* 2006; KUROMI and KIDOKORO 2005; NGUYEN and WOO 2003; TRUDEAU *et al.* 1996). Several studies in invertebrates and vertebrates have demonstrated that genes involved in cAMP signaling regulate rhythmic physiological processes including locomotor activity and locomotion behavior. Mutations in the *Drosophila* catalytic PKA-C1 subunit and its type II regulatory subunit PKA-RII (homologue of KIN-2) led to behavior-specific arrhythmia and altered spontaneous locomotion behavior (MAJERCAK *et al.* 1997; PARK *et al.* 2000). Mice exhibited hyperlocomotor activity when they were deficient in the regulatory subunit RIIβ of PKA (homologue of KIN-2) specifically in the dopamine receptor 2 expressing medium spiny neurons of the striatum, a brain region which regulates motor behaviors (ZHENG *et al.* 2013). In mammalian trigeminal motor neurons that participate in rhythmical motor behaviors including suckling, chewing, and swallowing an activated PKA induced a long-lasting increase in excitability (BAKHSHISHAYAN *et al.* 2013). Further, the β-adrenergic stimulation of the mammalian heart rate is mediated by PKA with the L-type Ca^{2+} channel Ca(V)1.2 representing one of the main downstream targets (HELL 2010). Recently, the ability of *C. elegans* PKA-1/KIN-1 to propagate patterned signaling through GABAergic neurons in the context of a rhythmic behavior (namely, the rhythmic defecation cycle) was elucidated in detail. PKA was found to be required in excitatory GABAergic AVL and DVB neurons for the generation of periodic synaptic calcium transients that elicit GABA release and subsequent enteric muscle contraction. The voltage-gated calcium channels (VGCC) UNC-2 (P/Q-type VGCC) and EGL-19 (L-type VGCC) are suggested to function downstream of PKA-1/KIN-1 to promote the presynaptic Ca^{2+} influx (WANG and SIEBURTH 2013). However,

in most cases downstream targets of PKA that affect the rhythmic locomotor output remain elusive.

Our phenotype- and genetic interaction studies indicate that $G\alpha_s$-PKA signaling may act in motor neurons upstream of TWK-7 affecting *C. elegans* locomotion activity and behavior. First, worms with an activated $G\alpha_s$-PKA/KIN-1 and TWK-7 deficient mutants showed a high degree of similarity in various aspects of spontaneous locomotion. Second, in *twk-7(null)*,$G\alpha_s$-PKA*(gf)* double mutants the frequencies, amplitudes and wave lengths of spontaneous crawling were highly synchronized without any significant additive / synergistic effects **(Fig. 18A-D)** and behavioral characteristics such as the duration and the straightness of crawling were very similar to the corresponding single mutants **(Fig. 18E, F)**. Third, *twk-7(null)* is able to restore a suppressed PKA activity in GABAergic D-motor neurons, which was elicited by overexpression of a dominant negative *kin-2($G^{310}D$)* allele. Contrary, an activated $G\alpha_s$ did not rescue *twk-7* overexpression in these neurons **(Fig. 19A-C; Fig. 20 A, B; Movie M12, M13)**. Together, this is a strong indication of an epistatic relationship. Unfortunately, employing the same strategy for epistatic analysis in cholinergic B-type motor neurons failed owing to dramatic mortality rates, egg-laying defects and sterility among the isolated transgenic F2 and F3 lines carrying a *acr-5p;;kin-2($G^{310}D$)* construct. Consistent, lethality caused by loss of PKA function has been described for *C. elegans* (KIM *et al.* 2012; KIM *et al.* 2013; LEE *et al.* 2014; WANG and SIEBURTH 2013).

Similar to PKA, K_2P channels have been reported to regulate rhythmic processes by modulating the presynaptic membrane potential (LALEVEE *et al.* 2006; RENIGUNTA *et al.* 2015). Most importantly, some reports have established K_2P channels as downstream targets of the $G\alpha_s$/PKA pathway (CZIRJAK and ENYEDI 2010; LESAGE *et al.* 2000; OLSCHEWSKI *et al.* 2006; PATEL *et al.* 1998). PKA activation resulted in the inhibition of the TREK-1 current in mammalian cell culture via phosphorylation at the conserved consensus PKA site Ser^{333} (PATEL *et al.* 1998). The K_2P channel TREK-1 is discussed to be involved in heart rate regulation (TERRENOIRE *et al.* 2001). Accordingly, studies on the human cardiac system provide mechanistic evidence to establish cardiac K_2P channels as antiarrhythmic drug targets (SCHMIDT *et al.* 2012). The activation of TASK-1, a K_2P channel of the human pulmonary artery smooth muscle cells, via PKA phosphorylation might represent an important mechanism underlying the vasorelaxing processes (OLSCHEWSKI *et al.* 2006). Thus, the modulation of the second messenger cAMP and concurrent PKA activity seems to be read out by certain K_2P channels resulting in

hyperpolarizations and depolarizations, respectively. In this regard it is remarkable, that an *in silico* analysis of the *C. elegans* TWK-7 amino acid sequence revealed two putative PKA-1/KIN-1 consensus phosphorylation sites Ser^{81} and Ser^{444} with markedly high scores **(Tab. S1)**. However, epistasis defines a relation between gene products and might not be sufficient to implicate any physical interaction between the resulting proteins (BARYSHNIKOVA *et al.* 2013; COSTANZO *et al.* 2010; ST ONGE *et al.* 2007). Therefore, further investigations including phosphorylation assays and site-directed mutation studies are necessary to prove the evidence of a physical interaction between PKA/KIN-1 and TWK-7 in *C. elegans* motor neurons.

Remarkably, the hyperactive *kin-2(cau-1)* and *twk-7(null)* mutant worms differ significantly in their behavior from hyperactive $G\alpha_{q/0}$ mutants. The respective $G\alpha_q$*(gf)* and $G\alpha_0$*(lf)* mutants with higher DAG levels and elevated acetylcholine release were hyperactive on plate during spontaneous crawling **(Fig. S11A, B)**, but exhibited decreased swimming activity **(Fig. S11C)**, spent less time on crawling forwards and moved with lower straightness rates **(Fig. 11D, E)**. Further, hyperactive *twk-7(null)* and *kin-2(cau-1)* mutants are characterized by reduced wave amplitudes during spontaneous crawling **(Fig. 14D)**. In sharp contrast, hyperactive animals with an elevated presynaptic acetylcholine release such as egl-30*(gf)* and goa-1*(lf)* (BRUNDAGE *et al.* 1996; HUANG *et al.* 2008; LACKNER *et al.* 1999) or an increased postsynaptic acetylcholine receptor sensitivity (BHATTACHARYA *et al.* 2014) moved with enhanced wave amplitudes. Remarkably, inactivation of PKA or overexpression of TWK-7 in GABAergic motor neurons in a wild-type or *kin-2(cau-1)* genetic background also led to elevated amplitudes during spontaneous crawling. In line with the suggested epistasis, a TWK-7(null) background was able to restore the amplitude of transgenic worms with a suppressed $G\alpha_s$-PKA signaling in their GABAergic motor neurons. Although $G\alpha_q$*(gf)* and $G\alpha_0$*(lf)* animals are characterized by an increased spontaneous body bending frequency on plate, these worms executed futile back and forth movements suggesting that a higher DAG level and concurrent increased acetylcholine output *per se* is not sufficient to promote a directed accelerated locomotion. Moreover, our pharmacological assay data suggest that, in contrast to the $G\alpha_{q/0}$ pathway, PKA-1/KIN-1 and TWK-7 affect locomotor activity and locomotion behavior without altering the levels of steady-state acetylcholine release **(Fig. 17A, B)**. Similar pharmacological results for $G\alpha_s$*(gf)* mutants have been presented previously (CHARLIE *et al.* 2006) and have been discussed to be in line with electrophysiological data from *Drosophila* $G\alpha_s$*(gf)* mutants (SUZUKI *et al.* 2002) where the resting spontaneous synaptic current frequency or the nerve-evoked synaptic currents did not

differ between wild-type and *dunce* (homologue of PDE) mutant embryos. On the other hand, the function of both, TWK-7 (shown in this study) and $G\alpha_s$-PKA pathway (SCHADE *et al.* 2005) largely depends on $G\alpha_q$, the core vesicle priming pathway, which is a constitutive element for proper locomotion. Hence, we suggest that the $G\alpha_s$-PKA-TWK-7 pathway affects the locomotor activity of *C. elegans* in the framework of a predetermined $G\alpha_q$ dependent acetylcholine output.

In the context of stimulated locomotion, neural ablation and genetic studies have shown that AIB and AIZ interneurons promote sensory signaling through the neural network (PVC and AVB locomotion command neurons) to the VB and DB motor neurons. The latter excite the body wall muscles inducing forward crawling (WHITE *et al.* 1986). The activity of these interneurons establishes the direction of locomotion (CHALFIE *et al.* 1985; ZHENG *et al.* 1999), whereas the AIB interneurons rather regulate the duration of forward locomotion. Ablation of AIB interneurons reduced short-duration forward movements, whereas the forward movement duration was extended in those worms (PIRRI and ALKEMA 2012; WAKABAYASHI *et al.* 2004). It is tempting to speculate that the increased locomotor activity and the enhanced locomotion behavior of *twk-7(null)* and $G\alpha_s$-PKA*(gf)* mutants might by a certain degree mimic the effect of sensory stimulation influencing the key parameters - velocity/frequency, amplitude, direction and persistence - in a manner typical for stimulated locomotion (CALHOUN *et al.* 2014; CALHOUN *et al.* 2015; FUJIWARA *et al.* 2002; GLORIA-SORIA and AZEVEDO 2008; GRAY *et al.* 2005; PIRRI and ALKEMA 2012; SHARPEE *et al.* 2014). Hence, since PKA is an established sensor of internal and external cues (CENTONZE *et al.* 2001; GOTO *et al.* 2015; VALJENT *et al.* 2005; YANG *et al.* 2014), we suggest that the $G\alpha_s$-PKA-TWK-7 pathway is a prime candidate to function as a mediator of adaptive locomotion behavior.

In conclusion, we presented convincing evidence for an epistatic interaction between the $G\alpha_s$-PKA pathway and TWK-7 which most probably share a common pathway being involved in the modulation of both locomotor activity and locomotion behavior during forward crawling that may mimic an adaptive response to specific environmental cues. Thus, we uncover a simple mechanism where a complex locomotion behavior might be modulated at the level of GABAergic motor neurons by the activity of the $G\alpha_s$-PKA pathway acting epistatically through the leak K^+ channel TWK-7.

4. Materials and Methods

4.1 Strains and culturing

All *C. elegans* strains were grown at 20°C on nematode growth media (NGM) agar plates seeded with OP50 *E. coli* as a food source (BRENNER 1974). Transgenic strains were generated by biolistic bombardment (WILM *et al.* 1999). The following strains were obtained from the *Caenorhabditis* Genetics Center (USA): Bristol N2 (used as wild-type), CB1112 *cat-2(e1112)II,* RB1239 *twk-30(ok1304)I* 1000bp deletion, *twk-40(tm6834)III* 473 bp deletion„ VC40352 *twk-43(gk590127)V* substitution L^{232}Ochre, VC40313 *twk-46(gk568572)V* substitution $G^{125}E$; *otEx4803* (expressing DsRed under a 3000 bp *twk-7* promoter) (KRATSIOS *et al.* 2012), LY120 *twk-7(nf120)III*, VC40681 *twk-7(gk760044)III*, RB1239 *twk-30(ok1304)I,* CB403 *unc-29(e403)I*, MT2426 *goa-1(n1134)I, twk-7(nf120)III*, *kin-2(ce179)I*, *pde4(kg1034)*, *gsa-1(ce94)I*, *egl-30(ad805)I*, *egl-8(e2917)V* and *dgk-1(nu62)X*. The strain MT1908 *nDf21/dpy-19(e1259),unc-32(e189)III* was used for genetic complementation studies. The strain used for cell specific expression pattern was LX929 *unc-17p::*GFP*(vsIs48).* For co-localization studies we used the thermosensitive strain GE24 *pha-1(e2123)III* transformed with the plasmid of interest and the rescuing plasmid pBX as co-marker (GRANATO *et al.* 1994). Double mutants were generated using standard genetic methods without additional marker mutations. Homozygosity of alleles in each double mutant was confirmed by PCR in case of deletion mutations, by restriction length polymorphism analysis in case of appropriate SNP mutations or, in all other cases, by sequencing of amplified genomic DNA.

4.2 Molecular biology and transfection of *C. elegans*

Transgenic strains were generated by biolistic bombardment following the protocol of (WILM *et al.* 1999). For rescue experiments the *myo-2p*::GFP::pPD118.33 plasmid was used as co-marker. Oligonucleotides used for amplification of the following constructs are listed in **Table S2.**

4.3 Genetic constructs

***twk-7p::TWK-7::mCherry::let-858(3'UTR)*:**
This rescue construct was generated by cloning a 12.1 kb genomic sequence including 3.0 kb upstream of the translational start site into the *p*PD118.33DD-*mCherry* vector.

twk-7p::TWK-7(G^{282}C)::mCherry::let-858(3'UTR) and ***twk-7p::TWK-7(T^{279}K)::mCherry::let-858(3'UTR)*:**
A 3.5 kb fragment was cut off of the *twk-7p*::TWK-7::mCherry construct by using *Pst*I. After gel purification the isolated fragment was further digested by *Bgl*II resulting in a 2.4 kb product of interest for subcloning into the vector pL4440. Site-directed mutagenesis was carried out by employing this construct and the complementary primer pairs corresponding to the sequences 5'-AACCGTCGTCACTACCATCGGATACGGTAATCCAGTTCCAG-3 (underlined nucleotide sequence was changed to TGT) and 5'-CTTTGCCGTAACCGTC GTCACTACCA-TCGGATACGGTAATC-3' (underlined triplet was changed into AAG) in order to obtain a G^{282}C and T^{279}K exchange in the TWK-7 protein sequence, respectively The mutated fragments were verified by sequencing, before cloning back into the *twk-7p*::TWK-7 ::mCherry construct via *Swa*I and *Bgl*II.

unc-17p(4.2kb)::TWK-7::mCherry::let-858(3'UTR), unc-17(1kb)p::TWK-7::mCherry::let-858(3'UTR), and ***unc-17(1kb)p::TWK-7(G^{282}C)::mCherry::let-858(3'UTR)*:**
The *unc-17p(4.2kb)* construct was generated by cloning the cholinergic neuron specific 4.2 kb promoter region of *unc-17* (restriction sites used: *Apa*I and *Nde*I) in front of the *twk-7* gene of 9142 bp (starting with translational start site) that is fused to mCherry reporter in the pBluescript vector. In addition, we replaced the 4.2 kb *unc-17* promoter sequence by a 1 kb *unc-17* promoter fragment that has been shown to drive gene expression solely in cholinergic motor neurons (KRATSIOS *et al.* 2012). For the dominant negative TWK-7 construct, a 2.4 kb fragment containing the G282C exchange was excised from *twk-7p::*TWK-7(G^{282}C)::mCherry vector by *Bgl*II and *Sac*II and introduced into the *unc-17(1kb)p::TWK-7::mCherry::let-858(3'UTR)* construct.

unc-4p::TWK-7::mCherry::let-858(3'UTR), unc-4p::TWK-7(G^{282}C)::mCherry::let-858(3'UTR), acr-5p::TWK-7::mCherry::let-858(3'UTR), acr-5p::TWK-7(G^{282}C)::mCherry ::let-858(3'UTR), unc47p::TWK-7::mCherry::let-858(3'UTR), and ***unc-47p:: TWK-7(G^{282}C)::mCherry::let-858(3'UTR)*:**
These constructs were produced by ligation of the cholinergic neuron specific promoter regions of *unc-4* (4.2 kb genomic DNA, restriction sites: *Apa*I and *Nde*I) and *acr-5* (4.3 kb genomic

DNA, restriction sites: *Apa*I and *Ase*I) and the GABAergic neuron specific promoter region of *unc-47* (2.9 kb genomic DNA, restriction sites: *Apa*I and *Nde*I) in front of the *twk-7* and respectively *twk-7($G^{282}C$)* gene of 9142 bp (starting with translational start site) that is fused to *mCherry* reporter in the *p*Bluescript vector.

The ***unc47p::TWK-7::mCherry::let-858(3'UTR)*** construct was engineered by ligation of the GABAergic neuron specific promoter regions of *unc-47* (2.9 kb genomic DNA, restriction sites: *Apa*I and *Nde*I) in front of the *twk-7* gene of 9142 bp (starting with translational start site) that is fused to *mCherry* reporter in the *p*Bluescript vector. The dominant negative kin-2 construct ***unc-47p::kin-2($G^{310}D$)*** construct was kindly provided by Derek Sieburth (Cell & Neurobiology Zilkha Neurogenetic Institute, Keck School of Medicine of USC) (WANG *et al.* 2013; WANG and SIEBURTH 2013). This allele was tested by sequencing of the corresponding *c*-DNA.

4.4 Locomotion assays and analysis

To quantify the number of body bends of swimming worms, 5 nematodes were transferred with a worm-picker (platinum wire) from standard NGM plates onto empty NGM plates to clean worms from bacteria. After approximately 1 min worms were placed in a 50 µl droplet of M9 buffer onto a diagnostic slide (3 wells, 10 mm diameter; Menzel). The worms were immediately filmed for 1 min with a VRmgic C-9+/BW PRO IR-CUT camera (VRmagic, Germany) attached to a Zeiss Stemi 2000-C microscope (Carl Zeiss AG, Germany). ImageJ wrMTrck wormtracker plugin according to the protocol described in (http://www.phage.dk /plugins/download/wrMTrck.pdf) used *.mov*-files to quantify the body bending swimming frequency. One body bend corresponds to the movement of the head region thrashing from one side to the other and back to the starting position. For the locomotion analysis on NGM agar plates we followed the protocol of (MILLER *et al.* 1999) with minor modifications. The assay was set up by placing 500 late L3 or early L4 stage larva on locomotion assay plates spread with a thin lawn of OP50 bacteria (100 µl of an OP50 overnight culture per plate, incubated for 20 h at 37°C). Worm plates were incubated at 20°C for 24 h, before the locomotion of young adult animals was filmed three times for 1 min with the camera setup described above. Spontaneous body bending crawling frequency was assessed by visual inspection of worms that were captured for at least 5 seconds. One body bend corresponds to the movement of the tip of the tail from one side to the other. Speed and forward locomotion efficiency (straightness value) were analyzed by using *ImageJ wrMTrck* wormtracker plugin (PEDERSEN 2011). The forward locomotion efficiency was calculated from the ratio of distance to track length, whereby the

distance represents the straight line from start to end coordinates of each recorded animal. In addition, a more detailed analysis we split locomotion behavior into forward, backward and resting time periods. The latter includes periods where worms move less than one body bend in forward or backward direction. Body bending crawling frequencies of single worms were separately assessed for forward and backward locomotion periods. Furthermore, we determined the relative time the worms spent on resting and forward and backward locomotion.

Basal slowing response assays were carried out as described by (SAWIN *et al.* 2000). Briefly, staged young adult animals were transferred to NGM plates with or without OP50 food bacteria. 2 min. after transfer, their locomotion rates were quantified by counting the number of body bends completed in four sequential 20 s intervals.

Stimulated forward locomotion assays were done as described in (GAGLIA and KENYON 2009). Staged young adult animals were transferred with a worm-picker from standard NGM plates to NGM assay plates spread with a thin lawn of OP50 food bacteria. Movies were taken immediately after transfer and every 30 min for 2 h. Body bending crawling frequency was assessed by visual inspection of the movies. Speed and forward locomotion efficiency was analyzed by using ImageJ wrMTrck wormtracker plugin.

4.5 Long-term tracking assay and analysis

NGM plates seeded with *E. coli* OP50 and incubated over night at 37°C. In order to assess the long term locomotion behavior, single well fed young adult animals were transferred into a 10 µl M9 drop on NGM plates and incubated for 16 h at 20 °C. For track assessment, worm traces were visualized on the backside of each NGM plate using an pencil marker and then captured as .jpeg file with an VRmgic C-9+/BW PRO IR-CUT camera (VRmagic, Germany) attached to a Zeiss Stemi 2000-C microscope (Carl Zeiss AG, Germany). Recorded tracks were finally ranked by visual inspection counting the squares crossed by each worm.

4.6 Body curvature analyses

Single swimming or crawling worms were filmed for 10 s Subsequently, their bodies were skeletonized and the resulting spine was divided into ten segments by using *MultiWormTracker*

(version 1.3.0-r1035) software (SWIERCZEK *et al.* 2011). The alteration of angles between adjacent segment pairs were calculated over time. Resulting values were transferred to MatLab and processed using the contour plot function.

4.7 Imaging of reporter strains

Transgenic animals were anesthetized and mounted in 5 mM levamisole, 5 mM aldicarb on a 2% agarose pad. Laser-scanning confocal fluorescence microscopy was carried out using a Zeiss Axio Imager Z2 upright microscope equipped with a Zeiss LSM 700 scanning confocal imaging system. Image acquisition and and processing was performed by employing Zeiss ZEN software.

4.8 Measurement of wave parameters

Movies recorded as previously described were opened using the *ImageJ* software. Calibration was adjusted for a resolution of 640x480 pixels at 64 pixels/mm. Worm lengths, wave lengths and amplitudes of sinusoidal ondulation have been measured using the scaled fragmented line tool along the spines/skeletons of three worms from each movie for a period of five body bends per worm **(Fig. S.14)**.

4.9 Calculation of the slip values for locomotion efficiency

Locomotion efficiency was introduced as the amount of slip (S) by *Gray and Lissman (1964)* for the locomotion of nematodes. Slip values were calculated from the ratio between velocity (V_λ) of the ondulating wave propagated over the worm spine and the velocity (V_x) of the moving worm.

$S = \left(1 - \frac{V_\lambda}{V_x}\right) \times 100$; where $V_\lambda = f \times \lambda$

f bending frequency

λ wave length

4.10 Pharmacological assays

Aldicarb and levamisole sensitivity assays were performed as blinded experiments (MAHONEY *et al.* 2006; SCHADE *et al.* 2005). Briefly, 25-30 synchronized young adult worms (age: 3 days) were transferred to the center of a 60 mm NGM plate (spot 5 µl bacteria) containing 1 mM aldicarb or 0.5 mM levamisole and the percentage of paralyzed animals was monitored over time. Locomotion was assessed by prodding animals with a platinum wire every 15 minutes following exposure to drug. Worms that failed to response to this stimulus were classified as paralyzed.

4.11 Prediction of PKA-phosphorylation sites

Protein kinase A (cAMP-dependent kinase, PKA) is a serine/threonine kinase with approximately 150 known substrate proteins. About 20 conserved sequence positions flanking the phosphorylated residue on both sides have been identified. The *pkaPS* online tool available at http://mendel.imp.univie.ac.at/sat/pkaPS is based on this refined recognition motif (NEUBERGER *et al.* 2007). For recognition of phosphorylation sites along the amino acid sequence of TWK-7, we translated the protein coding DNA regions using the *SnapGene Viewer* tool (www.snapgene.com/) into the corresponding amino acid sequences and performed the prediction with *pkaPS* adjusted for scores >0.

5. References

ALLER, M. I., E. L. VEALE, A. M. LINDEN, C. SANDU, M. SCHWANINGER *et al.*, 2005 Modifying the subunit composition of TASK channels alters the modulation of a leak conductance in cerebellar granule neurons. J Neurosci **25:** 11455-11467.

BAKHSHISHAYAN, S., A. ENOMOTO, T. TSUJI, S. TANAKA, T. YAMANISHI *et al.*, 2013 Protein kinase A regulates the long-term potentiation of intrinsic excitability in neonatal trigeminal motoneurons. Brain Res **1541:** 1-8.

BARYSHNIKOVA, A., M. COSTANZO, C. L. MYERS, B. ANDREWS and C. BOONE, 2013 Genetic interaction networks: toward an understanding of heritability. Annu Rev Genomics Hum Genet **14:** 111-133.

BEN AROUS, J., S. LAFFONT and D. CHATENAY, 2009 Molecular and sensory basis of a food related two-state behavior in C. elegans. PLoS One **4:** e7584.

BENDESKY, A., M. TSUNOZAKI, M. V. ROCKMAN, L. KRUGLYAK and C. I. BARGMANN, 2011 Catecholamine receptor polymorphisms affect decision-making in C. elegans. Nature **472:** 313-318.

BHATTACHARYA, R., D. TOUROUTINE, B. BARBAGALLO, J. CLIMER, C. M. LAMBERT *et al.*, 2014 A Conserved Dopamine-Cholecystokinin Signaling Pathway Shapes Context-Dependent Caenorhabditis elegans Behavior. PLoS Genet **10**.

BIDAYE, S. S., C. MACHACEK, Y. WU and B. J. DICKSON, 2014 Neuronal control of Drosophila walking direction. Science **344:** 97-101.

BOULIN, T., M. GIELEN, J. E. RICHMOND, D. C. WILLIAMS, P. PAOLETTI *et al.*, 2008 Eight genes are required for functional reconstitution of the Caenorhabditis elegans levamisole-sensitive acetylcholine receptor. Proc Natl Acad Sci U S A **105:** 18590-18595.

BOYLE, J. H., S. BERRI and N. COHEN, 2012 Gait Modulation in C. elegans: An Integrated Neuromechanical Model. Front Comput Neurosci **6:** 10.

BRENNER, S., 1974 The genetics of Caenorhabditis elegans. Genetics **77:** 71-94.

BRUNDAGE, L., L. AVERY, A. KATZ, U. J. KIM, J. E. MENDEL *et al.*, 1996 Mutations in a C. elegans Gqalpha gene disrupt movement, egg laying, and viability. Neuron **16:** 999-1009.

BRYDEN, J., and N. COHEN, 2008 Neural control of Caenorhabditis elegans forward locomotion: the role of sensory feedback. Biol Cybern **98:** 339-351.

BUCKINGHAM, S. D., J. F. KIDD, R. J. LAW, C. J. FRANKS and D. B. SATTELLE, 2005 Structure and function of two-pore-domain K+ channels: contributions from genetic model organisms. Trends Pharmacol Sci **26:** 361-367.

BURDOHAN, J. A., and C. M. COMER, 1996 Cellular organization of an antennal mechanosensory pathway in the cockroach, Periplaneta americana. J Neurosci **16:** 5830-5843.

CALHOUN, A. J., S. H. CHALASANI and T. O. SHARPEE, 2014 Maximally informative foraging by Caenorhabditis elegans. Elife **3**.

CALHOUN, A. J., A. TONG, N. POKALA, J. A. FITZPATRICK, T. O. SHARPEE *et al.*, 2015 Neural Mechanisms for Evaluating Environmental Variability in Caenorhabditis elegans. Neuron **86:** 428-441.

CENTONZE, D., B. PICCONI, P. GUBELLINI, G. BERNARDI and P. CALABRESI, 2001 Dopaminergic control of synaptic plasticity in the dorsal striatum. Eur J Neurosci **13:** 1071-1077.

CHALFIE, M., J. E. SULSTON, J. G. WHITE, E. SOUTHGATE, J. N. THOMSON *et al.*, 1985 The neural circuit for touch sensitivity in Caenorhabditis elegans. J Neurosci **5:** 956-964.

CHARLIE, N. K., A. M. THOMURE, M. A. SCHADE and K. G. MILLER, 2006 The dunce cAMP phosphodiesterase PDE-4 negatively regulates G alpha(s)-dependent and G alpha(s)-independent cAMP pools in the Caenorhabditis elegans synaptic signaling network. Genetics **173:** 111-130.

CHEUNG, U., H. L. ATWOOD and R. S. ZUCKER, 2006 Presynaptic effectors contributing to cAMP-induced synaptic potentiation in Drosophila. J Neurobiol **66:** 273-280.

CLARK, D. A., C. V. GABEL, T. M. LEE and A. D. SAMUEL, 2007 Short-term adaptation and temporal processing in the cryophilic response of Caenorhabditis elegans. J Neurophysiol **97:** 1903-1910.

COSTANZO, M., A. BARYSHNIKOVA, J. BELLAY, Y. KIM, E. D. SPEAR *et al.*, 2010 The genetic landscape of a cell. Science **327:** 425-431.

CZIRJAK, G., and P. ENYEDI, 2010 TRESK background K(+) channel is inhibited by phosphorylation via two distinct pathways. Journal of Biological Chemistry **285:** 14549-14557.

DE BONO, M., and C. I. BARGMANN, 1998 Natural variation in a neuropeptide Y receptor homolog modifies social behavior and food response in C. elegans. Cell **94:** 679-689.

DE LA CRUZ, I. P., J. Z. LEVIN, C. CUMMINS, P. ANDERSON and H. R. HORVITZ, 2003 sup-9, sup-10, and unc-93 may encode components of a two-pore K+ channel that coordinates muscle contraction in Caenorhabditis elegans. J Neurosci **23:** 9133-9145.

DE LA CRUZ, I. P., L. MA and H. R. HORVITZ, 2014 The Caenorhabditis elegans iodotyrosine deiodinase ortholog SUP-18 functions through a conserved channel SC-box to regulate the muscle two-pore domain potassium channel SUP-9. PLoS Genet **10:** e1004175.

DECHER, N., K. WEMHONER, S. RINNE, M. F. NETTER, M. ZUZARTE *et al.*, 2011 Knock-out of the potassium channel TASK-1 leads to a prolonged QT interval and a disturbed QRS complex. Cell Physiol Biochem **28:** 77-86.

DONNER, B. C., M. SCHULLENBERG, N. GEDULDIG, A. HUNING, J. MERSMANN *et al.*, 2011 Functional role of TASK-1 in the heart: studies in TASK-1-deficient mice show

prolonged cardiac repolarization and reduced heart rate variability. Basic Res Cardiol **106:** 75-87.

ENYEDI, P., and G. CZIRJAK, 2010 Molecular background of leak K+ currents: two-pore domain potassium channels. Physiol Rev **90:** 559-605.

FANG-YEN, C., M. WYART, J. XIE, R. KAWAI, T. KODGER *et al.*, 2010 Biomechanical analysis of gait adaptation in the nematode Caenorhabditis elegans. Proc Natl Acad Sci U S A **107:** 20323-20328.

FELIX, M. A., and C. BRAENDLE, 2010 The natural history of Caenorhabditis elegans. Curr Biol **20:** R965-969.

FLEMING, J. T., M. D. SQUIRE, T. M. BARNES, C. TORNOE, K. MATSUDA *et al.*, 1997 Caenorhabditis elegans levamisole resistance genes lev-1, unc-29, and unc-38 encode functional nicotinic acetylcholine receptor subunits. J Neurosci **17:** 5843-5857.

FUJIWARA, M., P. SENGUPTA and S. L. MCINTIRE, 2002 Regulation of body size and behavioral state of C. elegans by sensory perception and the EGL-4 cGMP-dependent protein kinase. Neuron **36:** 1091-1102.

GAGLIA, M. M., and C. KENYON, 2009 Stimulation of movement in a quiescent, hibernation-like form of Caenorhabditis elegans by dopamine signaling. J Neurosci **29:** 7302-7314.

GJORGJIEVA J, B. D., HASPEL G, 2014 Neurobiology of Caenorhabditis elegans Locomotion: where do we stand? Bioscience **64:** 476-486.

GLORIA-SORIA, A., and R. B. AZEVEDO, 2008 npr-1 Regulates foraging and dispersal strategies in Caenorhabditis elegans. Curr Biol **18:** 1694-1699.

GOTO, A., I. NAKAHARA, T. YAMAGUCHI, Y. KAMIOKA, K. SUMIYAMA *et al.*, 2015 Circuit-dependent striatal PKA and ERK signaling underlies rapid behavioral shift in mating reaction of male mice. Proc Natl Acad Sci U S A **112:** 6718-6723.

GRANATO, M., H. SCHNABEL and R. SCHNABEL, 1994 pha-1, a selectable marker for gene transfer in C. elegans. Nucleic Acids Res **22:** 1762-1763.

GRAY, J., and H. W. LISSMANN, 1964 The Locomotion of Nematodes. J Exp Biol **41:** 135-154.

GRAY, J. M., J. J. HILL and C. I. BARGMANN, 2005 A circuit for navigation in Caenorhabditis elegans. Proc Natl Acad Sci U S A **102:** 3184-3191.

HELL, J. W., 2010 Beta-adrenergic regulation of the L-type Ca2+ channel Ca(V)1.2 by PKA rekindles excitement. Sci Signal **3:** pe33.

HU, S., T. PAWSON and R. M. STEVEN, 2011 UNC-73/trio RhoGEF-2 activity modulates Caenorhabditis elegans motility through changes in neurotransmitter signaling upstream of the GSA-1/Galphas pathway. Genetics **189:** 137-151.

HUANG, K. M., P. COSMAN and W. R. SCHAFER, 2008 Automated detection and analysis of foraging behavior in Caenorhabditis elegans. J Neurosci Methods **171:** 153-164.

KAWANO, T., M. D. PO, S. GAO, G. LEUNG, W. S. RYU *et al.*, 2011 An imbalancing act: gap junctions reduce the backward motor circuit activity to bias C. elegans for forward locomotion. Neuron **72:** 572-586.

KIM, S., J. A. GOVINDAN, Z. J. TU and D. GREENSTEIN, 2012 SACY-1 DEAD-Box helicase links the somatic control of oocyte meiotic maturation to the sperm-to-oocyte switch and gamete maintenance in Caenorhabditis elegans. Genetics **192:** 905-928.

KIM, S., C. SPIKE and D. GREENSTEIN, 2013 Control of oocyte growth and meiotic maturation in Caenorhabditis elegans. Adv Exp Med Biol **757:** 277-320.

KOLLEWE, A., A. Y. LAU, A. SULLIVAN, B. ROUX and S. A. GOLDSTEIN, 2009 A structural model for K2P potassium channels based on 23 pairs of interacting sites and continuum electrostatics. J Gen Physiol **134:** 53-68.

KRATSIOS, P., A. STOLFI, M. LEVINE and O. HOBERT, 2012 Coordinated regulation of cholinergic motor neuron traits through a conserved terminal selector gene. Nat Neurosci **15:** 205-214.

KUNKEL, M. T., D. B. JOHNSTONE, J. H. THOMAS and L. SALKOFF, 2000 Mutants of a temperature-sensitive two-P domain potassium channel. J Neurosci **20:** 7517-7524.

KUROMI, H., and Y. KIDOKORO, 2005 Exocytosis and endocytosis of synaptic vesicles and functional roles of vesicle pools: lessons from the Drosophila neuromuscular junction. Neuroscientist **11:** 138-147.

LACKNER, M. R., S. J. NURRISH and J. M. KAPLAN, 1999 Facilitation of synaptic transmission by EGL-30 Gqalpha and EGL-8 PLCbeta: DAG binding to UNC-13 is required to stimulate acetylcholine release. Neuron **24:** 335-346.

LALEVEE, N., B. MONIER, S. SENATORE, L. PERRIN and M. SEMERIVA, 2006 Control of cardiac rhythm by ORK1, a Drosophila two-pore domain potassium channel. Curr Biol **16:** 1502-1508.

LAZARENKO, R. M., S. C. WILLCOX, S. SHU, A. P. BERG, V. JEVTOVIC-TODOROVIC *et al.*, 2010 Motoneuronal TASK channels contribute to immobilizing effects of inhalational general anesthetics. J Neurosci **30:** 7691-7704.

LEE, J. H., J. KONG, J. Y. JANG, J. S. HAN, Y. JI *et al.*, 2014 Lipid droplet protein LID-1 mediates ATGL-1-dependent lipolysis during fasting in Caenorhabditis elegans. Mol Cell Biol **34:** 4165-4176.

LESAGE, F., C. TERRENOIRE, G. ROMEY and M. LAZDUNSKI, 2000 Human TREK2, a 2P domain mechano-sensitive K+ channel with multiple regulations by polyunsaturated fatty acids, lysophospholipids, and Gs, Gi, and Gq protein-coupled receptors. Journal of Biological Chemistry **275:** 28398-28405.

LEWIS, J. A., C. H. WU, H. BERG and J. H. LEVINE, 1980 The genetics of levamisole resistance in the nematode Caenorhabditis elegans. Genetics **95:** 905-928.

LUDWAR, B., S. WESTMARK, A. BUSCHGES and J. SCHMIDT, 2005 Modulation of membrane potential in mesothoracic moto- and interneurons during stick insect front-leg walking. J Neurophysiol **94:** 2772-2784.

LUERSEN, K., U. FAUST, D. C. GOTTSCHLING and F. DORING, 2014 Gait-specific adaptation of locomotor activity in response to dietary restriction in Caenorhabditis elegans. J Exp Biol **217:** 2480-2488.

LUO, L., C. V. GABEL, H. I. HA, Y. ZHANG and A. D. SAMUEL, 2008 Olfactory behavior of swimming C. elegans analyzed by measuring motile responses to temporal variations of odorants. J Neurophysiol **99:** 2617-2625.

MAHONEY, T. R., S. LUO and M. L. NONET, 2006 Analysis of synaptic transmission in Caenorhabditis elegans using an aldicarb-sensitivity assay. Nat Protoc **1:** 1772-1777.

MAJERCAK, J., D. KALDERON and I. EDERY, 1997 Drosophila melanogaster deficient in protein kinase A manifests behavior-specific arrhythmia but normal clock function. Mol Cell Biol **17:** 5915-5922.

MAJMUDAR, T., E. E. KEAVENY, J. ZHANG and M. J. SHELLEY, 2012 Experiments and theory of undulatory locomotion in a simple structured medium. J R Soc Interface **9:** 1809-1823.

MARDER, E., and R. L. CALABRESE, 1996 Principles of rhythmic motor pattern generation. Physiol Rev **76:** 687-717.

MCINTIRE, S. L., E. JORGENSEN and H. R. HORVITZ, 1993a Genes required for GABA function in Caenorhabditis elegans. Nature **364:** 334-337.

MCINTIRE, S. L., E. JORGENSEN, J. KAPLAN and H. R. HORVITZ, 1993b The GABAergic nervous system of Caenorhabditis elegans. Nature **364:** 337-341.

MILLER, K. G., M. D. EMERSON and J. B. RAND, 1999 Goalpha and diacylglycerol kinase negatively regulate the Gqalpha pathway in C. elegans. Neuron **24:** 323-333.

NAGY, S., Y. C. HUANG, M. J. ALKEMA and D. BIRON, 2015 Caenorhabditis elegans exhibit a coupling between the defecation motor program and directed locomotion. Sci Rep **5:** 17174.

NEUBERGER, G., G. SCHNEIDER and F. EISENHABER, 2007 pkaPS: prediction of protein kinase A phosphorylation sites with the simplified kinase-substrate binding model. Biol Direct **2:** 1.

NGUYEN, M., A. ALFONSO, C. D. JOHNSON and J. B. RAND, 1995 Caenorhabditis elegans mutants resistant to inhibitors of acetylcholinesterase. Genetics **140:** 527-535.

NGUYEN, P. V., and N. H. WOO, 2003 Regulation of hippocampal synaptic plasticity by cyclic AMP-dependent protein kinases. Prog Neurobiol **71:** 401-437.

NURRISH, S., L. SEGALAT and J. M. KAPLAN, 1999 Serotonin inhibition of synaptic transmission: Galpha(0) decreases the abundance of UNC-13 at release sites. Neuron **24:** 231-242.

OLSCHEWSKI, A., Y. LI, B. TANG, J. HANZE, B. EUL *et al.*, 2006 Impact of TASK-1 in human pulmonary artery smooth muscle cells. Circ Res **98:** 1072-1080.

OPPERMAN, C. H., and S. CHANG, 1991 Effects of Aldicarb and Fenamiphos on Acetycholinesterase and Motility of Caenorhabditis elegans. J Nematol **23:** 20-27.

PARK, S., H. HWANG, S. W. NAM, F. MARTINEZ, R. H. AUSTIN *et al.*, 2008 Enhanced Caenorhabditis elegans locomotion in a structured microfluidic environment. PLoS One **3:** e2550.

PARK, S. K., S. A. SEDORE, C. CRONMILLER and J. HIRSH, 2000 Type II cAMP-dependent protein kinase-deficient Drosophila are viable but show developmental, circadian, and drug response phenotypes. Journal of Biological Chemistry **275:** 20588-20596.

PATEL, A. J., E. HONORE, F. MAINGRET, F. LESAGE, M. FINK *et al.*, 1998 A mammalian two pore domain mechano-gated S-like K+ channel. EMBO J **17:** 4283-4290.

PEDERSEN, J. S., 2011 *C. elegans* motility analysis in ImageJ - A practical approach. 1-15.

PERRIER, J. F., A. ALABURDA and J. HOUNSGAARD, 2003 5-HT1A receptors increase excitability of spinal motoneurons by inhibiting a TASK-1-like K+ current in the adult turtle. J Physiol **548:** 485-492.

PETERSEN, C., P. DIRKSEN and H. SCHULENBURG, 2015 Why we need more ecology for genetic models such as C. elegans. Trends Genet.

PIERCE-SHIMOMURA, J. T., B. L. CHEN, J. J. MUN, R. HO, R. SARKIS *et al.*, 2008 Genetic analysis of crawling and swimming locomotory patterns in C. elegans. Proc Natl Acad Sci U S A **105:** 20982-20987.

PIRRI, J. K., and M. J. ALKEMA, 2012 The neuroethology of C. elegans escape. Curr Opin Neurobiol **22:** 187-193.

RENIGUNTA, V., G. SCHLICHTHORL and J. DAUT, 2015 Much more than a leak: structure and function of K-2P-channels. Pflugers Archiv-European Journal of Physiology **467:** 867-894.

REYNOLDS, N. K., M. A. SCHADE and K. G. MILLER, 2005 Convergent, RIC-8-dependent Galpha signaling pathways in the Caenorhabditis elegans synaptic signaling network. Genetics **169:** 651-670.

SALKOFF, L., A. BUTLER, G. FAWCETT, M. KUNKEL, C. MCARDLE *et al.*, 2001 Evolution tunes the excitability of individual neurons. Neuroscience **103:** 853-859.

SAWIN, E. R., R. RANGANATHAN and H. R. HORVITZ, 2000 C. elegans locomotory rate is modulated by the environment through a dopaminergic pathway and by experience through a serotonergic pathway. Neuron **26:** 619-631.

SCHADE, M. A., N. K. REYNOLDS, C. M. DOLLINS and K. G. MILLER, 2005 Mutations that rescue the paralysis of Caenorhabditis elegans ric-8 (synembryn) mutants activate the G alpha(s) pathway and define a third major branch of the synaptic signaling network. Genetics **169:** 631-649.

SCHMIDT, C., F. WIEDMANN, P. A. SCHWEIZER, R. BECKER, H. A. KATUS *et al.*, 2012 Novel electrophysiological properties of dronedarone: inhibition of human cardiac two-pore-

domain potassium (K2P) channels. Naunyn Schmiedebergs Arch Pharmacol **385:** 1003-1016.

SCHONEICH, S., K. SCHILDBERGER and P. A. STEVENSON, 2011 Neuronal organization of a fast-mediating cephalothoracic pathway for antennal-tactile information in the cricket (Gryllus bimaculatus DeGeer). J Comp Neurol **519:** 1677-1690.

SCHREIBER, M. A., J. T. PIERCE-SHIMOMURA, S. CHAN, D. PARRY and S. L. MCINTIRE, 2010 Manipulation of behavioral decline in Caenorhabditis elegans with the Rag GTPase raga-1. PLoS Genet **6:** e1000972.

SENGUPTA, P., and A. D. SAMUEL, 2009 Caenorhabditis elegans: a model system for systems neuroscience. Curr Opin Neurobiol **19:** 637-643.

SHARPEE, T. O., A. J. CALHOUN and S. H. CHALASANI, 2014 Information theory of adaptation in neurons, behavior, and mood. Curr Opin Neurobiol **25:** 47-53.

SHTONDA, B. B., and L. AVERY, 2006 Dietary choice behavior in Caenorhabditis elegans. J Exp Biol **209:** 89-102.

SIEBURTH, D., J. M. MADISON and J. M. KAPLAN, 2007 PKC-1 regulates secretion of neuropeptides. Nat Neurosci **10:** 49-57.

ST ONGE, R. P., R. MANI, J. OH, M. PROCTOR, E. FUNG *et al.*, 2007 Systematic pathway analysis using high-resolution fitness profiling of combinatorial gene deletions. Nature Genetics **39:** 199-206.

SUZUKI, K., A. D. GRINNELL and Y. KIDOKORO, 2002 Hypertonicity-induced transmitter release at Drosophila neuromuscular junctions is partly mediated by integrins and cAMP/protein kinase A. J Physiol **538:** 103-119.

SWIERCZEK, N. A., A. C. GILES, C. H. RANKIN and R. A. KERR, 2011 High-throughput behavioral analysis in C. elegans. Nat Methods **8:** 592-598.

TERRENOIRE, C., I. LAURITZEN, F. LESAGE, G. ROMEY and M. LAZDUNSKI, 2001 A TREK-1-like potassium channel in atrial cells inhibited by beta-adrenergic stimulation and activated by volatile anesthetics. Circ Res **89:** 336-342.

TRUDEAU, L. E., D. G. EMERY and P. G. HAYDON, 1996 Direct modulation of the secretory machinery underlies PKA-dependent synaptic facilitation in hippocampal neurons. Neuron **17:** 789-797.

VALJENT, E., V. PASCOLI, P. SVENNINGSSON, S. PAUL, H. ENSLEN *et al.*, 2005 Regulation of a protein phosphatase cascade allows convergent dopamine and glutamate signals to activate ERK in the striatum. Proc Natl Acad Sci U S A **102:** 491-496.

WAKABAYASHI, T., I. KITAGAWA and R. SHINGAI, 2004 Neurons regulating the duration of forward locomotion in Caenorhabditis elegans. Neurosci Res **50:** 103-111.

WANG, H., K. GIRSKIS, T. JANSSEN, J. P. CHAN, K. DASGUPTA *et al.*, 2013 Neuropeptide Secreted from a Pacemaker Activates Neurons to Control a Rhythmic Behavior. Current Biology **23:** 746-754.

WANG, H., and D. SIEBURTH, 2013 PKA controls calcium influx into motor neurons during a rhythmic behavior. PLoS Genet **9:** e1003831.

WEN, Q., M. D. PO, E. HULME, S. CHEN, X. LIU *et al.*, 2012 Proprioceptive coupling within motor neurons drives C. elegans forward locomotion. Neuron **76:** 750-761.

WHITE, J. G., E. SOUTHGATE, J. N. THOMSON and S. BRENNER, 1976 The structure of the ventral nerve cord of Caenorhabditis elegans. Philos Trans R Soc Lond B Biol Sci **275:** 327-348.

WHITE, J. G., E. SOUTHGATE, J. N. THOMSON and S. BRENNER, 1986 The structure of the nervous system of the nematode Caenorhabditis elegans. Philos Trans R Soc Lond B Biol Sci **314:** 1-340.

WILM, T., P. DEMEL, H. U. KOOP, H. SCHNABEL and R. SCHNABEL, 1999 Ballistic transformation of Caenorhabditis elegans. Gene **229:** 31-35.

YANG, L., M. L. GILBERT, R. ZHENG and G. S. MCKNIGHT, 2014 Selective expression of a dominant-negative type Ialpha PKA regulatory subunit in striatal medium spiny neurons impairs gene expression and leads to reduced feeding and locomotor activity. J Neurosci **34:** 4896-4904.

YANIK, M. F., H. CINAR, H. N. CINAR, A. D. CHISHOLM, Y. JIN *et al.*, 2004 Neurosurgery: functional regeneration after laser axotomy. Nature **432:** 822.

YU, H., B. ALEMAN-MEZA, S. GHARIB, M. K. LABOCHA, C. J. CRONIN *et al.*, 2013 Systematic profiling of Caenorhabditis elegans locomotive behaviors reveals additional components in G-protein Galphaq signaling. Proc Natl Acad Sci U S A **110:** 11940-11945.

ZHENG, R. M., L. H. YANG, M. A. SIKORSKI, L. C. ENNS, T. A. CZYZYK *et al.*, 2013 Deficiency of the RII beta subunit of PKA affects locomotor activity and energy homeostasis in distinct neuronal populations. Proc Natl Acad Sci U S A **110:** E1631-E1640.

ZHENG, Y., P. J. BROCKIE, J. E. MELLEM, D. M. MADSEN and A. V. MARICQ, 1999 Neuronal control of locomotion in C-elegans is modified by a dominant mutation in the GLR-1 ionotropic glutamate receptor. Neuron **24:** 347-361.

ZHOU, K. M., Y. M. DONG, Q. GE, D. ZHU, W. ZHOU *et al.*, 2007 PKA activation bypasses the requirement for UNC-31 in the docking of dense core vesicles from C. elegans neurons. Neuron **56:** 657-669.

6. Supporting Information

6.1 Figures

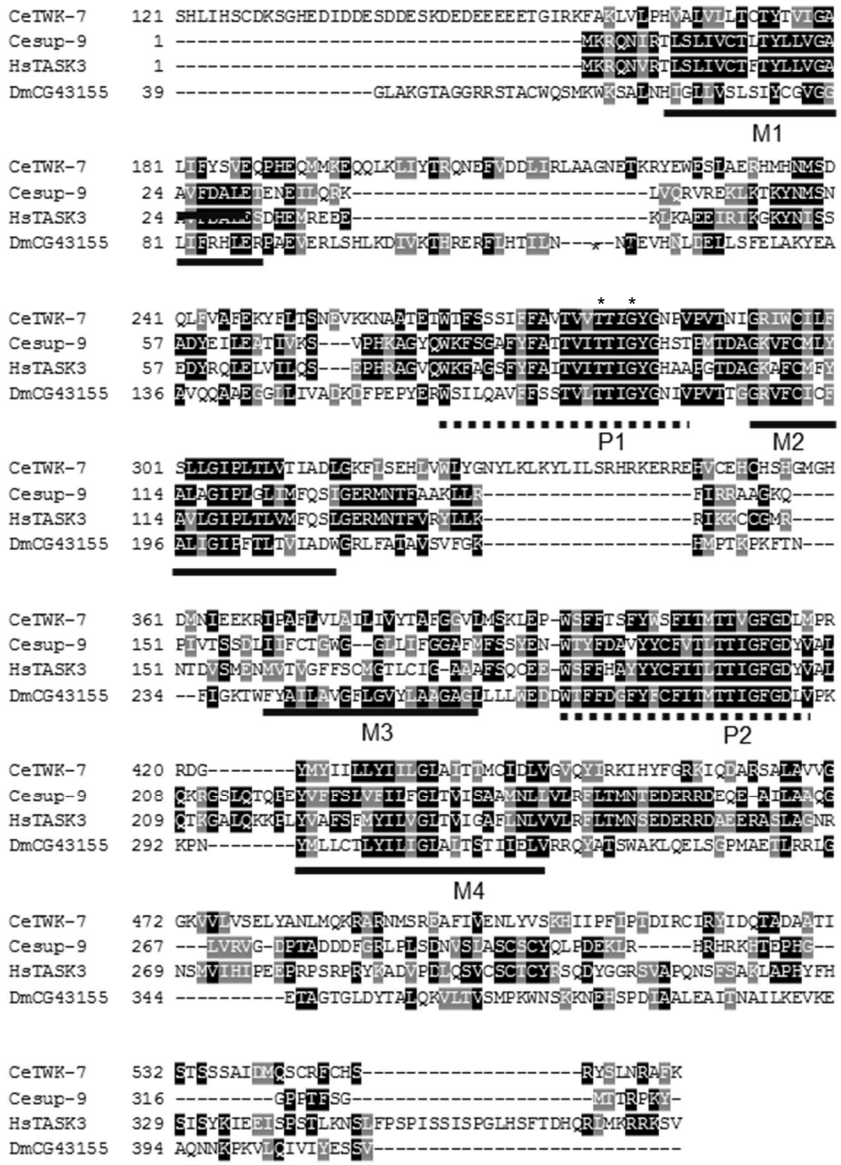

Figure S 1: Amino acid sequence analysis of *C. elegans* TWK-7.

The gene *twk-7* encodes a predicted protein of 557 amino acid residues with only moderate sequence similarity (20-25%) to other K_2P channels, such as *C. elegans* SUP-9/TWK-38, mammalian TASK3 and the predicted *Drosophila melanogaster* K_2P channel CG43155. Similarity is restricted mainly to the two pore domains P1 and P2 including the K^+ channel specific ion selectivity filter and the transmembrane domains M1, M2, and M4. The crucial amino acid residues T^{279} and G^{282} within the selectivity filter are indicated by asterisks. Note that the TWK-7 sequence in the alignment starts at position 121. Owing to an unusually extended N-terminus of approximately 160 amino acid residues, the deduced TWK-7 polypeptide with a predicted molecular mass of 64.2 kDa is considerably larger than mammalian K_2P channels or *C. elegans* SUP-9/TWK-38 with deduced molecular masses of about 42 and 37 kDa, respectively.

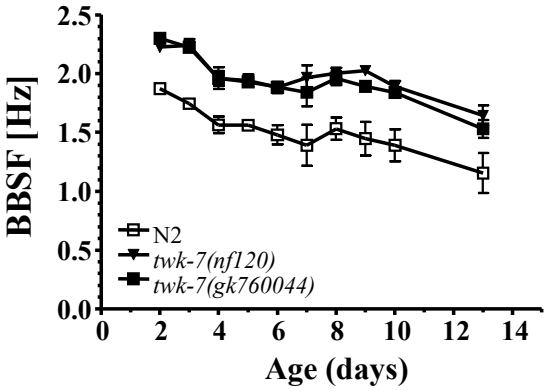

Figure S 2: Analysis of age-dependent swimming activity.

In order to explore the persistence of BBSF, the swimming activity of wild-type animals and *twk-7(nf120)* mutants were determined at different ages. The bars represent the means (± SD) of N ≥4 independent experiments involving n ≥40 animals.

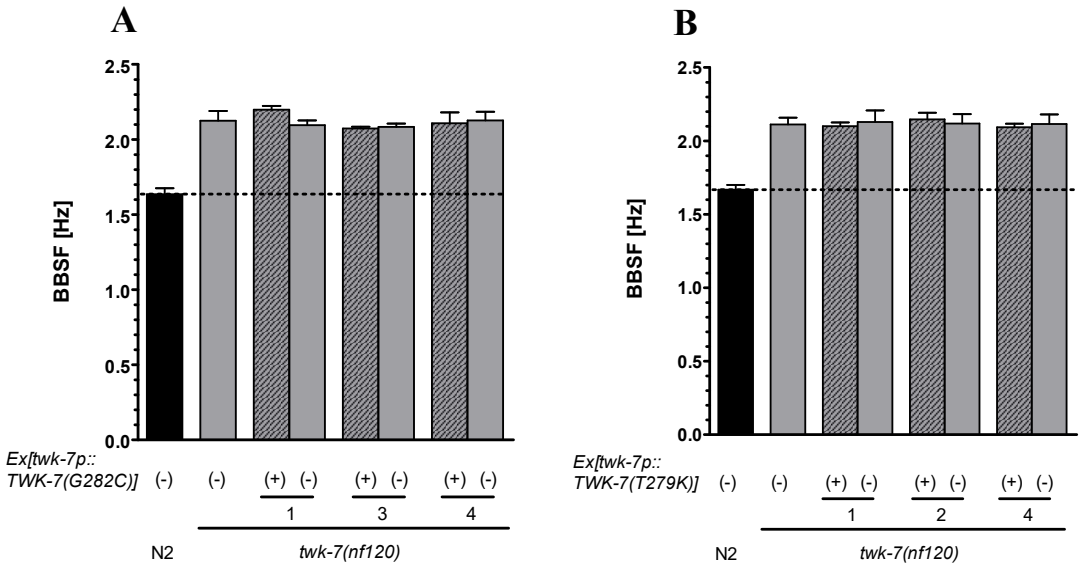

Figure S 3: Expression of TWK-7 selectivity filter mutations $G^{282}C$ and $T^{279}K$ did not affect the swimming activity of *twk-7(nf120)* mutant worms.

The body bending swimming frequencies (BBSF) of three independent transgenic lines (+) expressing **(A)** the TWK-7($G^{282}C$) and **(B)** the TWK-7($T^{279}K$) channel mutant were compared with those of their non-transgenic siblings, N2 and *twk-7(nf120)* worms. Each bar represents the mean (± SD) of three independent experiments involving n = 30 animals. Dotted lines indicate the wild-type levels.

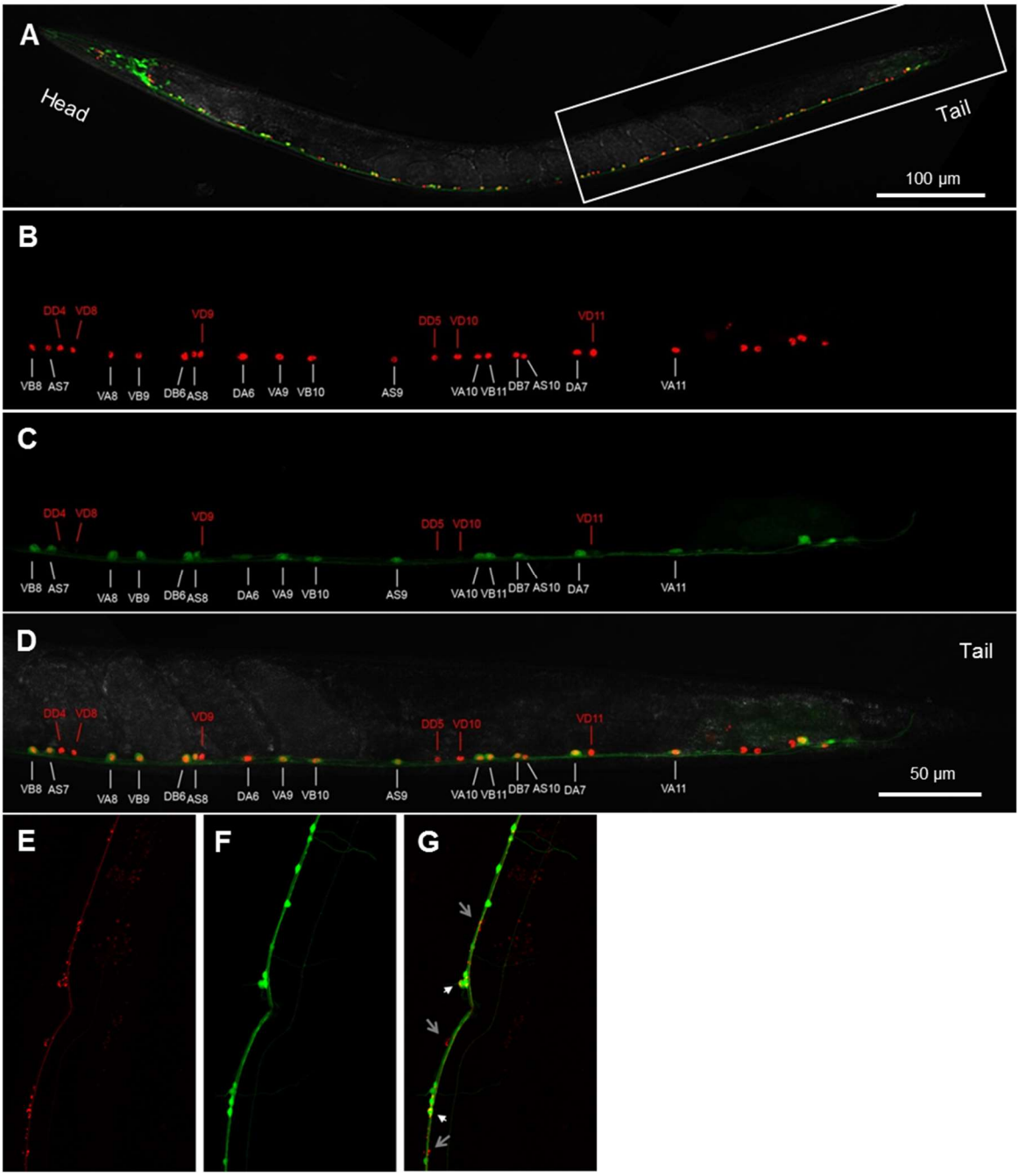

Figure S 4: The Expression pattern of *C. elegans* TWK-7.
(A-D) Laser scanning microscopy analysis of worms expressing the reporter proteins GFP and DsRed under the control of the cholinergic neuron specific *unc-17(4.2kb)* and the *twk-7(3.0kb)* promoter, respectively. The box in (A) marks the posterior part of the body shown in more detail in **(B-D)**, where A-, B-, AS- and D-type motor neurons of the posterior ventral nerve cord are labeled according to their numbering (Altun, Z.F. and Hall, D.H. 2011. Nervous system, general description in *Worm Atlas (doi:10.3908/wormatlas.1.18).* **(E-G)** Laser scanning microscopy analysis of worms expressing GFP and a TWK-7::mCherry fusion protein under the control of the *unc-17(4.2kb)* and *twk-7(3.0kb)* promoter, respectively. Small white arrows indicate exemplarily motor neurons that contain cytosolic GFP and punctuated and membrane-bound expression of mCherry. Gray arrows point to D-type neurons that express solely mCherry.

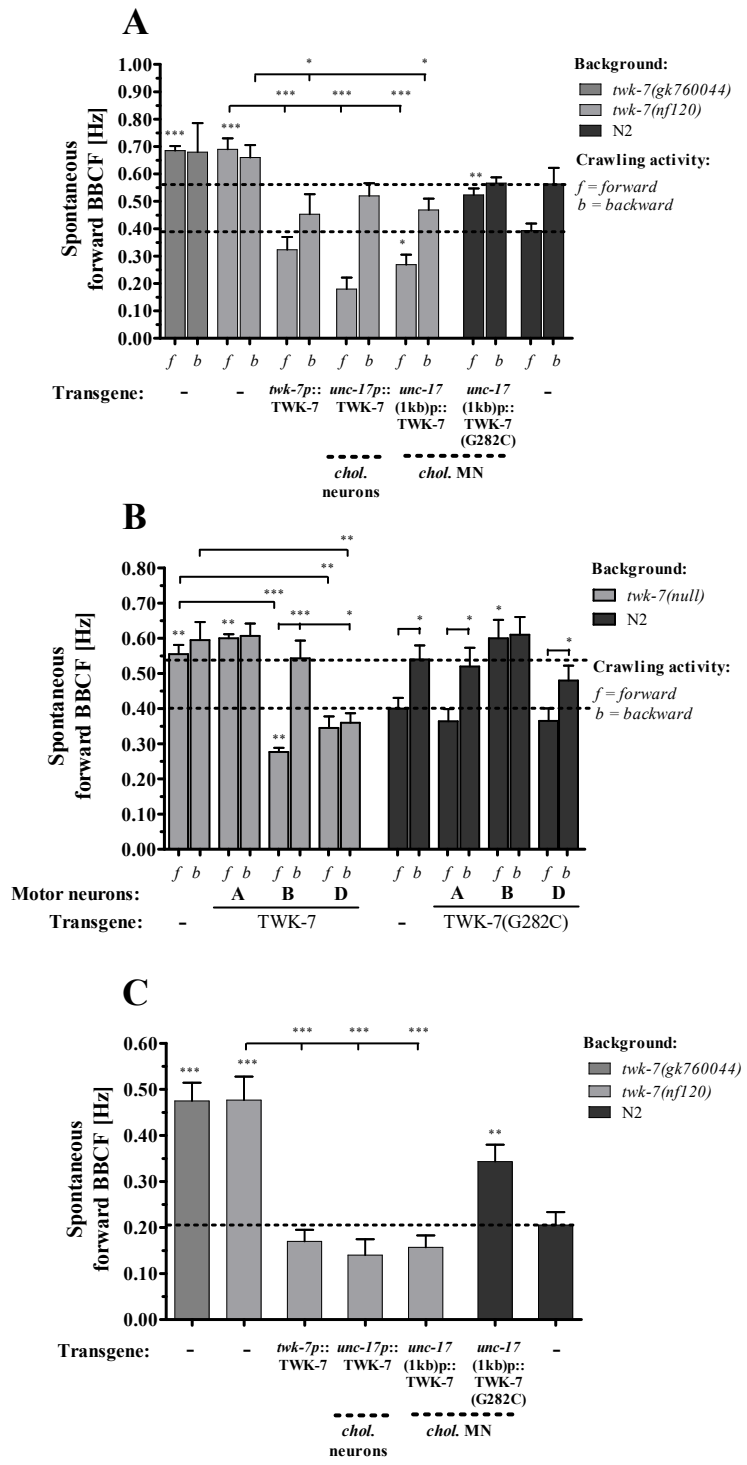

Figure S 5: Body bending frequencies during forward and backward crawling periods.
L4 worms were transferred to fresh NGM assay plates and after 24 h at 20°C their spontaneous body bending frequencies were determined for wild type, the *twk-7(null)* alleles and worms expressing wild-type TWK-7 or dominant negative TWK-7 in **(A)** the TWK-7 specific neurons, cholinergic motor neurons and in **(B)** the motor neuron subtypes A-, B-, and D-. Periods of forward *(f)* and backward *(b)* crawling were assessed separately. Resting periods were not considered. The **(C)** BBCF of basal spontaneous crawling (backward movement and resting periods included) for the worms presented in (A) and (B). Columns represent the means ± SEM of at least three independent experiments with n ≥ 30 animals (Students t-test, * $p < 0.05$, ** $p < 0.01$ and *** $p < 0.001$). Dotted lines indicate the wild-type levels.

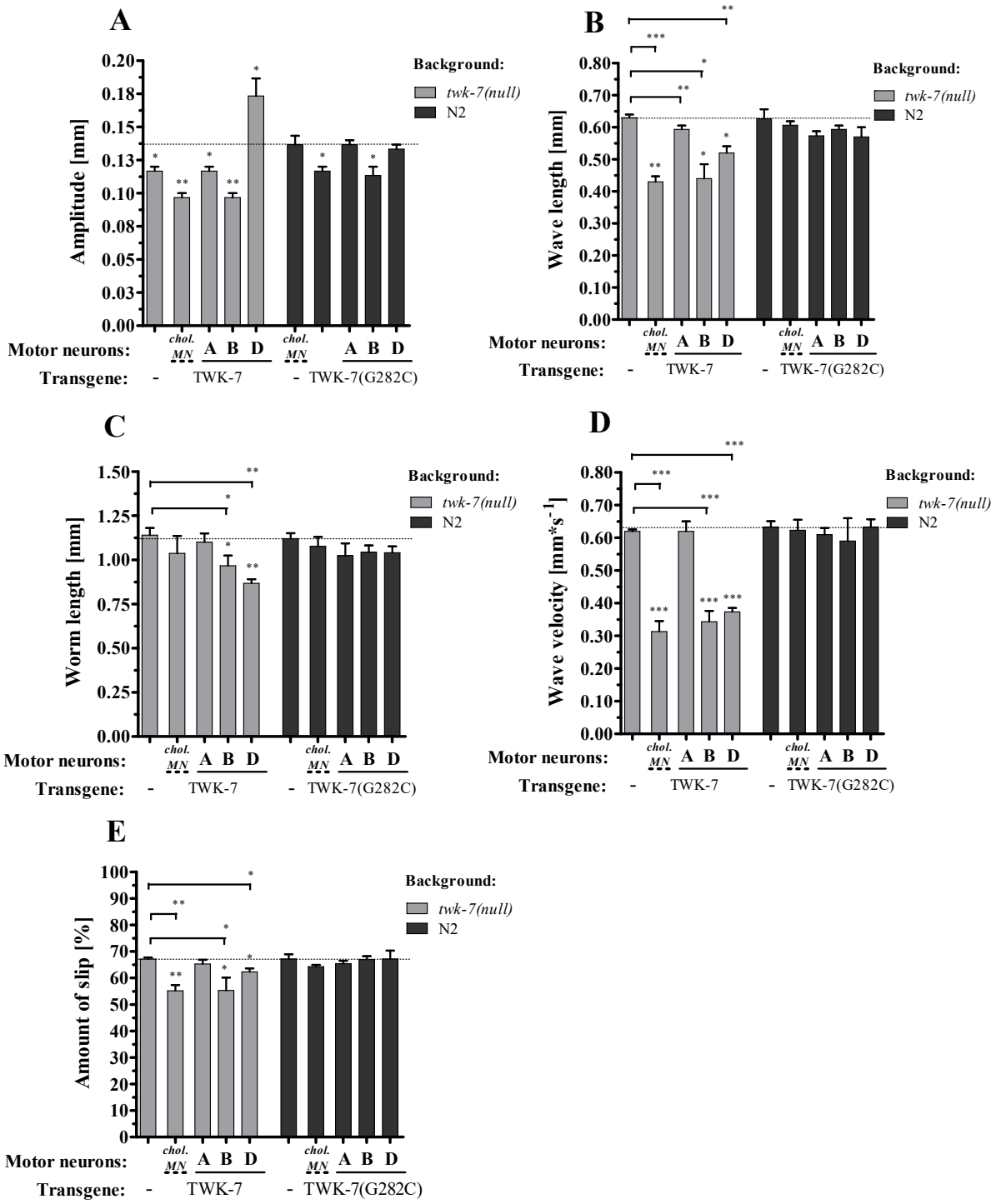

Figure S 6: The wave parameters (absolute values), worm lengths and locomotor efficiencies during spontaneous crawling.

The absolute values of the **(A)** wave amplitudes, **(B)** wave lengths and **(C)** worms lengths measured with *ImageJ* are depicted. The **(D)** wave velocity is calculated as the product between the bending frequency and the wave length of the respective worm. The **(E)** amount of slip represents the locomotor inefficiency as described by (GRAY and LISSMANN 1964). Columns represent the means ± SEM of at least three independent experiments with n ≥ 30 animals (Students t-test, * $p < 0.05$, ** $p < 0.01$ and *** $p < 0.001$). Dotted lines indicate the wild-type levels.

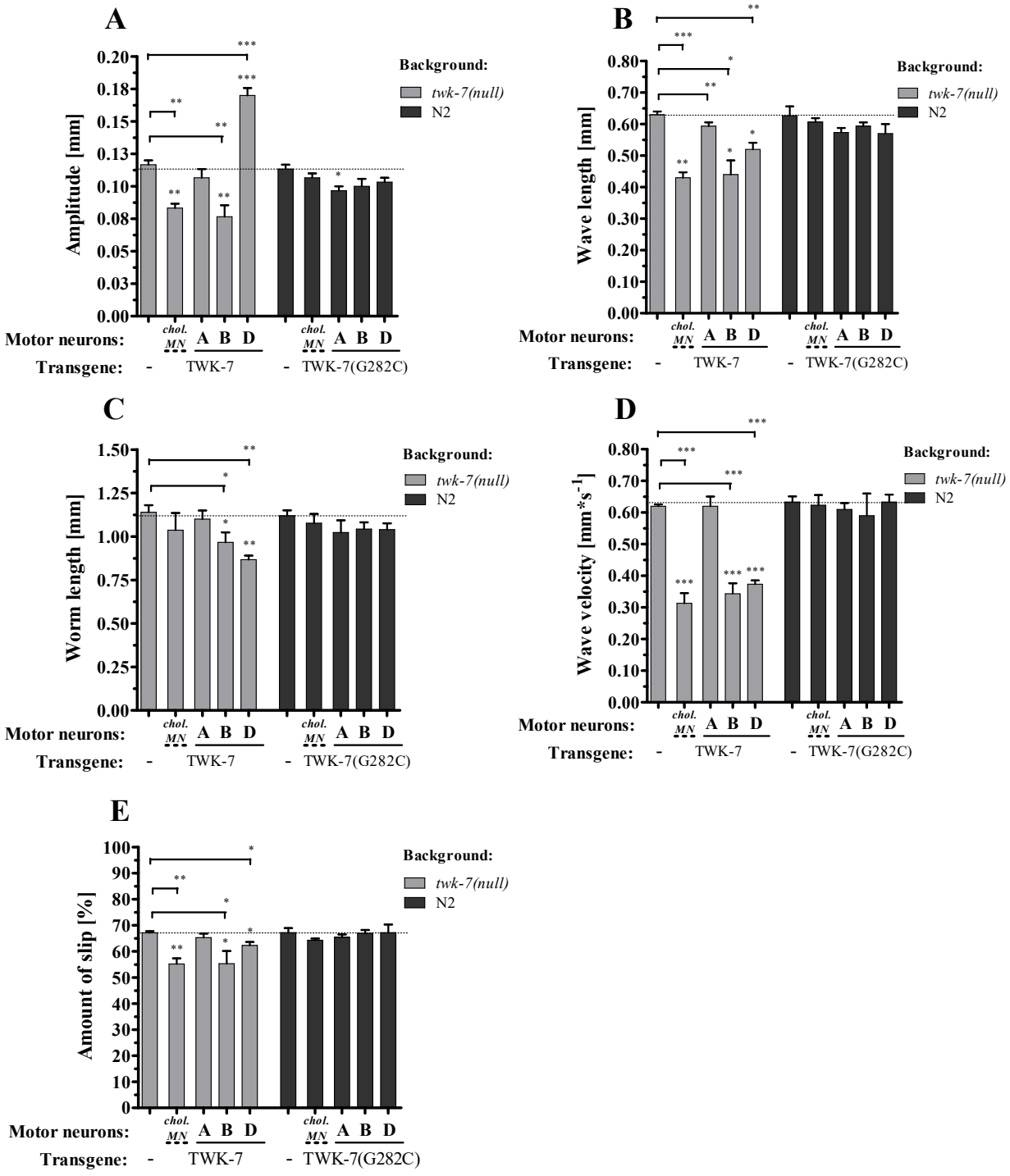

Figure S 7: The wave parameters (absolute values), worm lengths and locomotor efficiencies during stimulated crawling.

The absolute values of the **(A)** wave amplitudes, **(B)** wave lengths and **(C)** worms lengths analyzed with *ImageJ* are depicted. The **(D)** wave velocity is given by the product of the bending frequency and the wave length of the respective worm. The **(E)** amount of slip reflects the locomotor inefficiency as described by (GRAY and LISSMANN 1964). Columns represent the means ± SEM of at least three independent experiments with $n \geq 30$ animals (Students t-test, * $p < 0.05$, ** $p < 0.01$ and *** $p < 0.001$). Dotted lines indicate the wild-type levels.

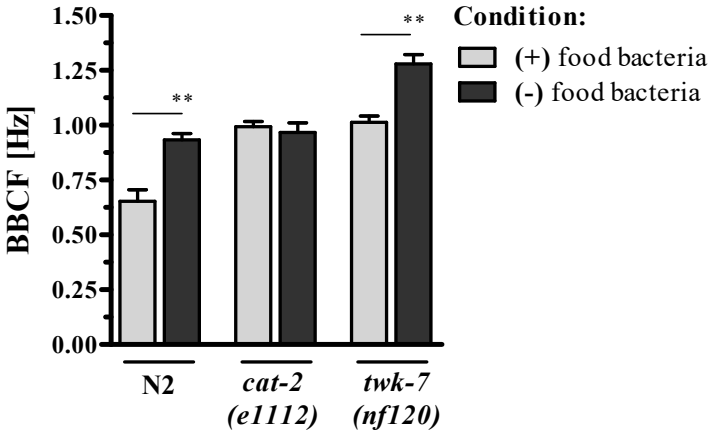

Figure S 8: Analysis of the food induced basal slowing response.

The body bending crawling rates of staged young adult animals (age 72 h) were quantified off and on food. N2 worms slowed their locomotion rate from 0.93 Hz to 0.65 Hz when reaching a bacterial lawn (basal slowing response), while the dopamine deficient *cat-2(e1112)* animals remained at the same level (approximately 1 Hz). This is consistent with previous studies (SAWIN *et al.* 2000) and confirms that the basal slowing response is a dopamine-dependent mechanism. *twk-7(nf120)* animals crawled with higher body bending frequencies than wild-type and *cat-2* deficient worms in the absence of food. However, they reduced their locomotion rates from about 1.3 Hz to a value of approximately 1 Hz when they encounter a bacterial food source. This reduction by 0.3 Hz is similar to that observed for wild-type worms (see above) indicating that *twk-7* is not involved in the process of food induced basal slowing. For a more detailed description of the assay see Suppl. Material and Methods. Columns represent the means (± SEM) of three independent experiments with n = 30 animals (Students t-test, ** $p < 0.01$).

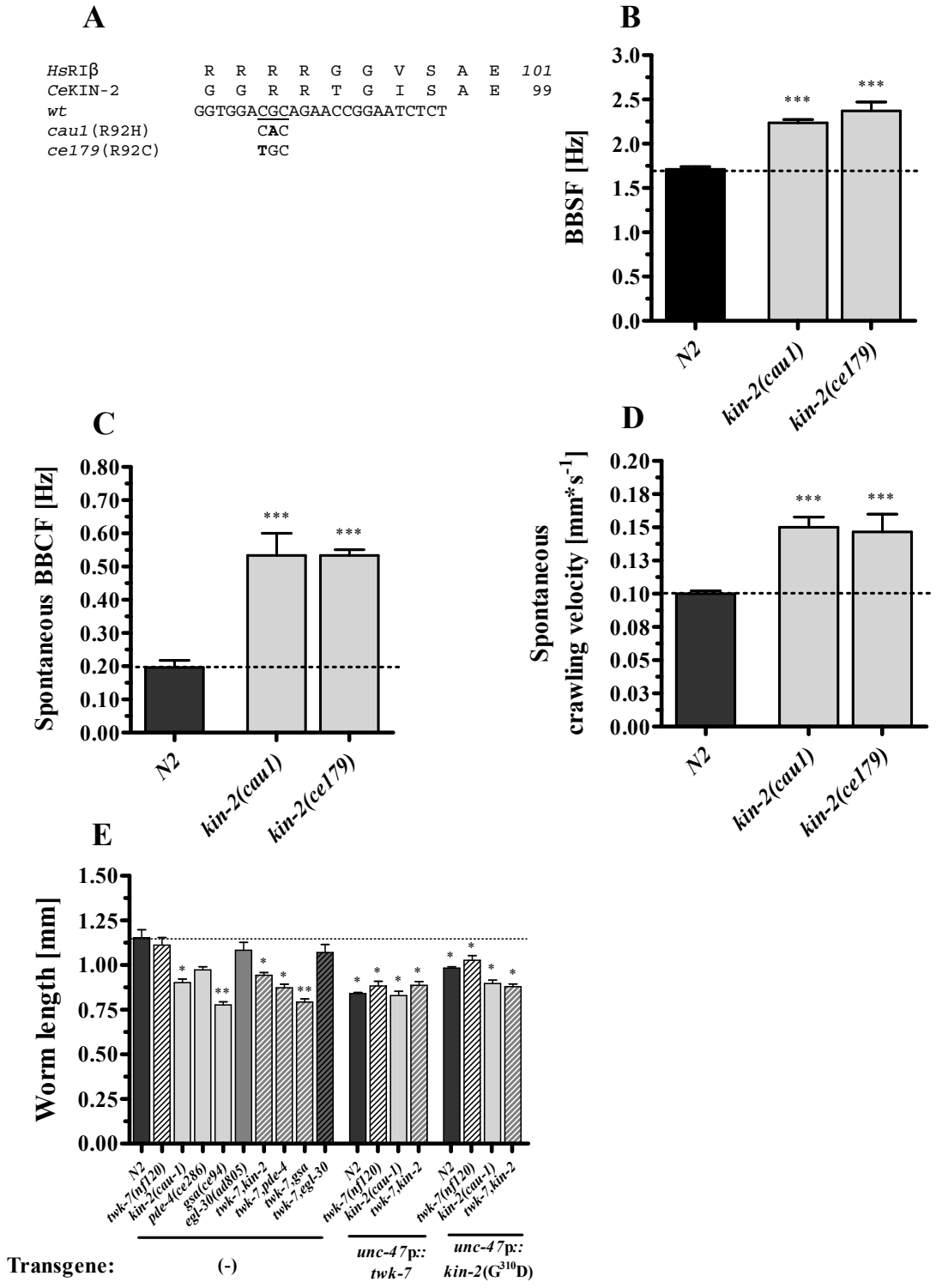

Figure S 9: The characteristics of the screened reduction-of-function KIN-2 worms.

The **(A)** inhibitory pseudo-substrate domains of the regulatory subunit of PKA/KIN-1 (RIβ/KIN-2) from human and *C. elegans* are aligned. The nucleotide exchanges that result in the $R^{92}H$ and $R^{92}C$ substitution in the *cau1* and *ce179* allele, respectively, are shown. The reduction-of-function allele *kin-2(cau-1)* found in the genetic screen revealed significantly increased **(B)** swimming frequencies, **(C)** crawling frequencies and **(D)** velocities compared to wild-type animals. The **(E)** Body lengths of non-transgenic and transgenic animals are depicted. Dotted lines indicate the wild-type level. All values represent the means (± SEM) of at least N ≥ 3 independent experiments involving n ≥30 never starved animals. *p < 0.05; **p < 0.01; ***p < 0.001 (Student's t-test).

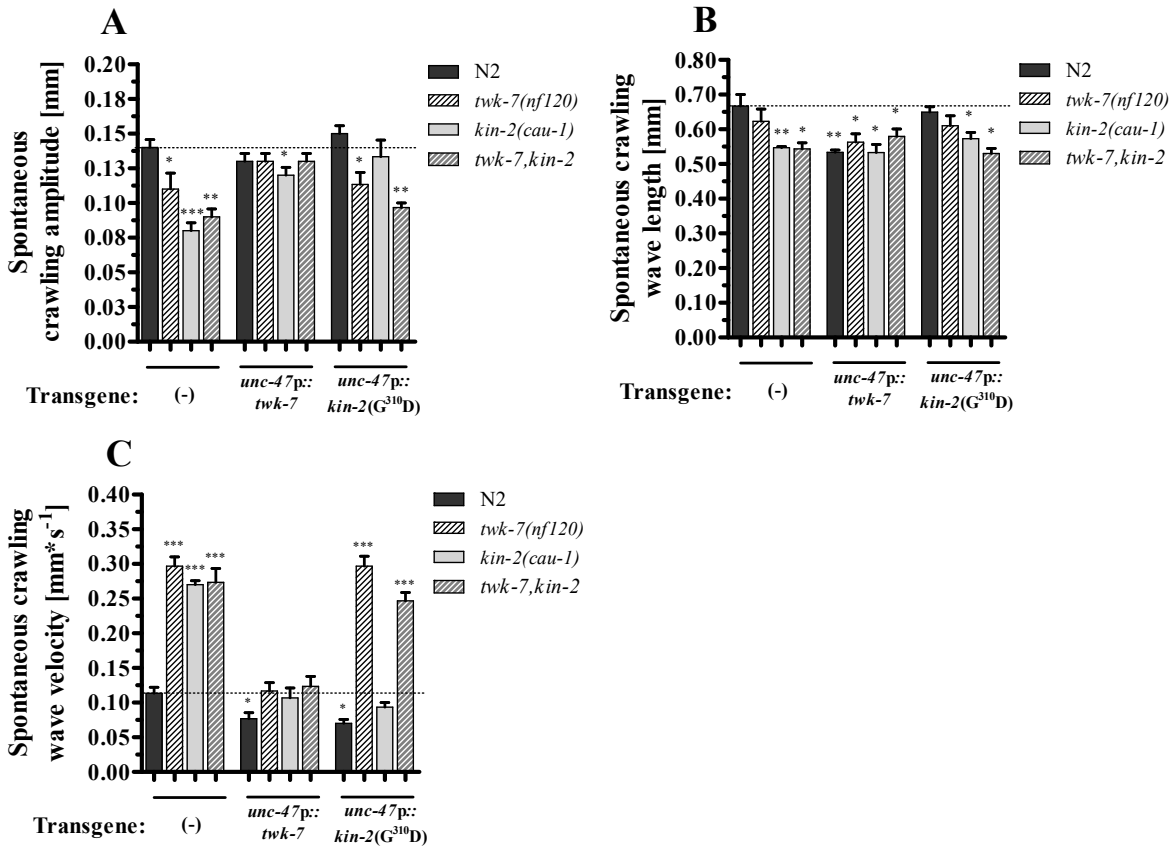

Figure S 10: The absolute values of amplitude, wave length, and wave velocity during spontaneous crawling.

The **(A)** amplitudes and **(B)** wave lengths are to be understood as related the respective body lengths. The **(C)** velocities of the wave propagated along the body were calculated as the product between the BBCF and the corresponding absolute wave lengths. During spontaneous crawling the wave velocities are significantly elevated in the non-transgenic *twk-7(null)*, *kin-2(cau-1)* and the *twk-7,kin-2* double mutants due to their increased crawling activity when compared with the wild-type worms (see Fig. 14B; 17A). In contrast, transgenic animals overexpressing wild-type *twk-7* or dominant negative *kin-2(G^{310}D)* exhibit diminished wave velocities, except the *twk-7(null) and twk-7,kin-2* mutants carrying *kin-2(G^{310}D).* Dotted lines indicate the wild-type level. All values represent the means (± SEM) of at least N ≥3 independent experiments involving n ≥30 never starved animals. *p < 0.05; **p < 0.01; ***p < 0.001 (Student's t-test).

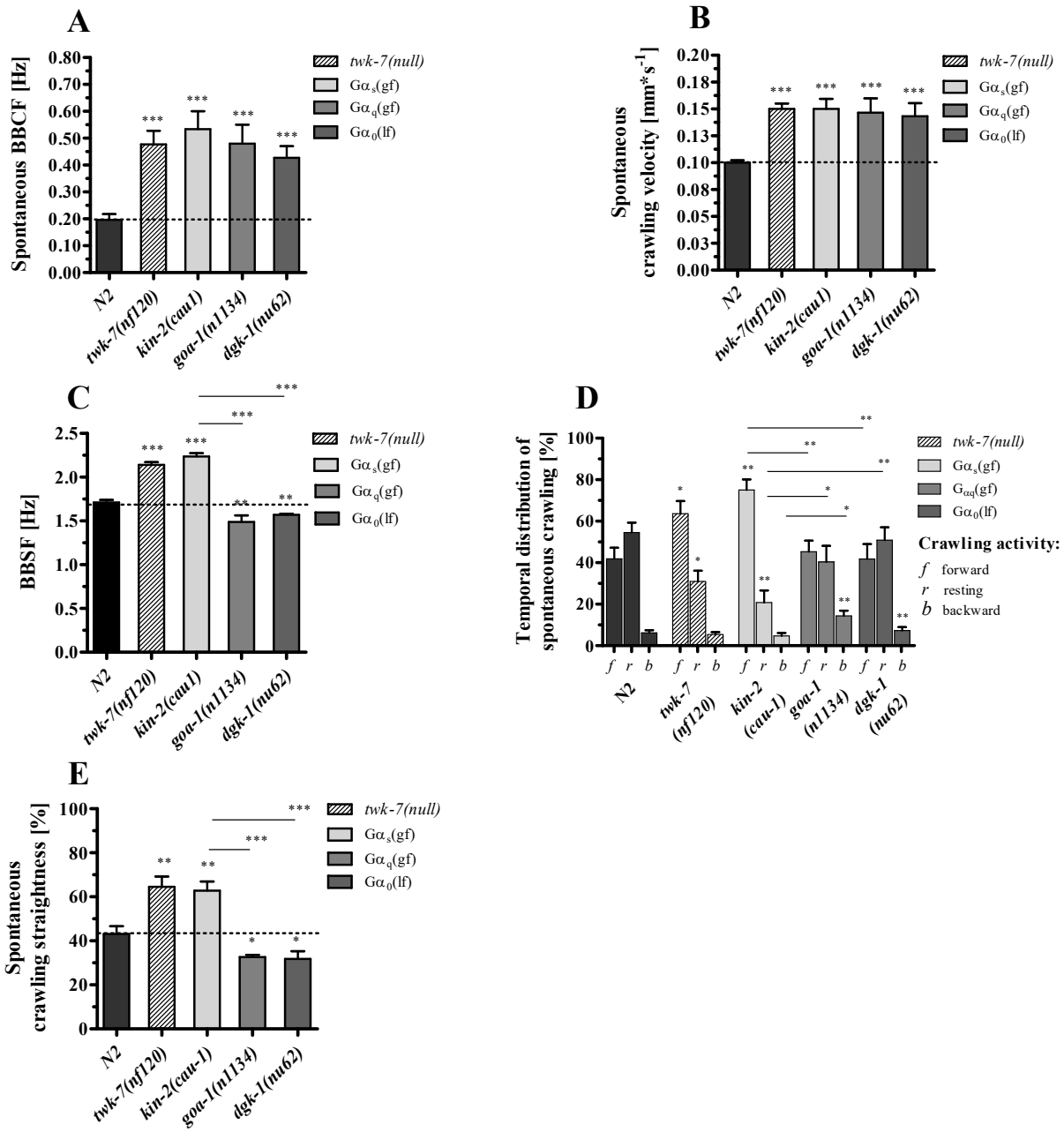

Figure S 11: The activities and behaviors of *twk-7(null)* and *kin-2(cau-1)* compared to hyperactive $G\alpha_{q/0}$ mutant worms.

The hyperactive $G\alpha_{q/0}$ mutants *goa-1(n1134)* and *dgk-1(nu62)* exhibited similarily increased **(A)** BBCF and **(B)** crawling but decreased **(C)** BBSF than compared with the *kin-2(cau-1)* and *twk-7(null)* animals. The BBSF of $G\alpha_{q/0}$ mutants were even lower when compared to the wild-type animals. These hyperactive strains presented **(D)** extended resting periods, increased backward movements and **(E)** lower straightness rates during spontaneous crawling. Dotted lines indicate the wild-type level. All values represent the means (± SEM) of at least N ≥3 independent experiments involving n ≥30 never starved animals. *p < 0.05; **p < 0.01; ***p < 0.001 (Student's t-test).

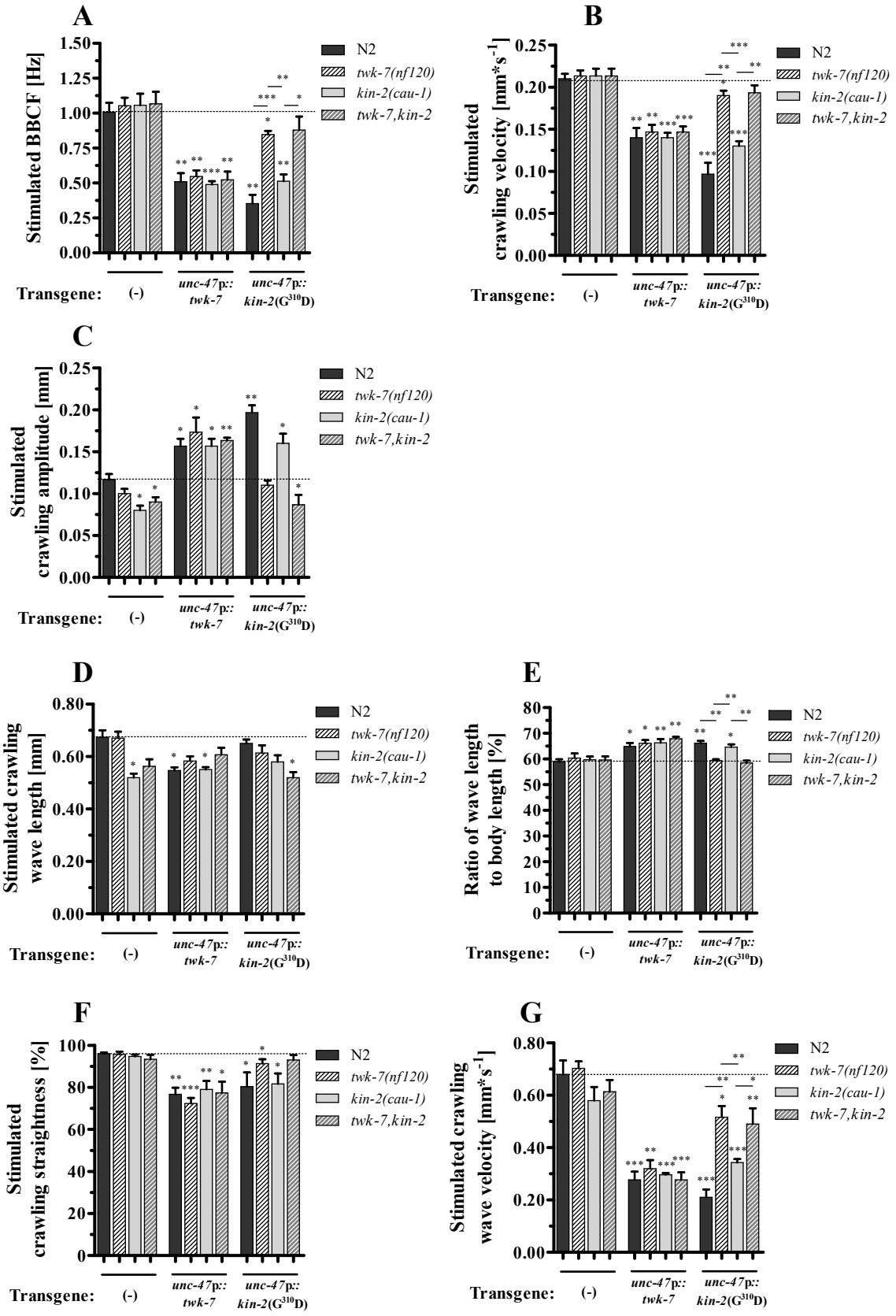

Figure S 12: The stimulated locomotion activities and behaviors of *twk-7(null)* and *kin-2(cau-1)* transgenes with suppressed GABAergic signaling.

After stimulation, wild-types, single and double mutants raised their activities reaching similar elevated levels when compared to the spontaneous condition (Fig. 19A, B). Stimulated transgenic worms presented strikingly suppressed **(A)** bending frequencies and **(B)** velocities showing extremely high **(C)** bending amplitudes (here, the absolute values), **(D)** elevated wave

lengths (here, absolute values) and **(E)** wave length to body length ratios in comparison to the non-transgenic animals. The **(F)** straightness rates and **(G)** wave velocities are also diminished compared with the non-transgenic animals. Decisively, the *twk-7(null)* and *twk-7,kin-2* transgenes overexpressing the dominant negative *kin-2(G^{310}D)* allel are not significantly affected **(A-G)**. Dotted lines indicate the wild-type level. All values represent the means (± SEM) of at least N ≥3 independent experiments involving n ≥30 never starved animals. *p < 0.05; **p < 0.01; ***p < 0.001 (Student's t-test).

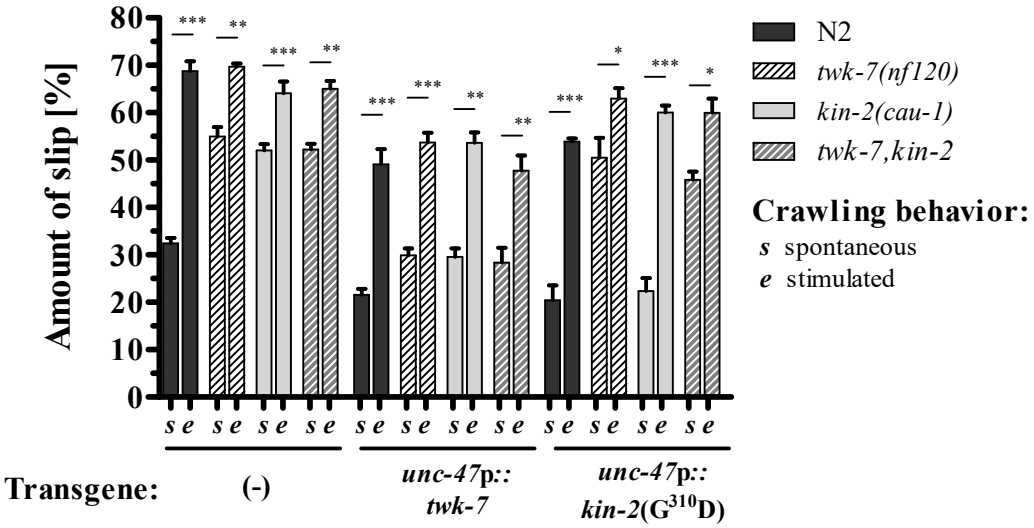

Figure S 13: The locomotion inefficiency represented by the amount of slip.
The slip values of wild-type, mutants and transgenic animals during spontaneous ***(s)*** and stimulated (escape-like) ***(e)*** crawling activity on *E.coli* (OP50) lawn are depicted (see Materials and Methods for calculation formula). Interestingly, the slip values raise by increasing the locomotor activity (compare with Fig. 3A, B and 4A, B) when worms crawl on the same surface (here, OP50 lawn). All values represent the means (± SEM) of at least N ≥ 3 independent experiments involving n ≥30 never starved animals. *p < 0.05; **p < 0.01; ***p < 0.001 (Student's t-test).

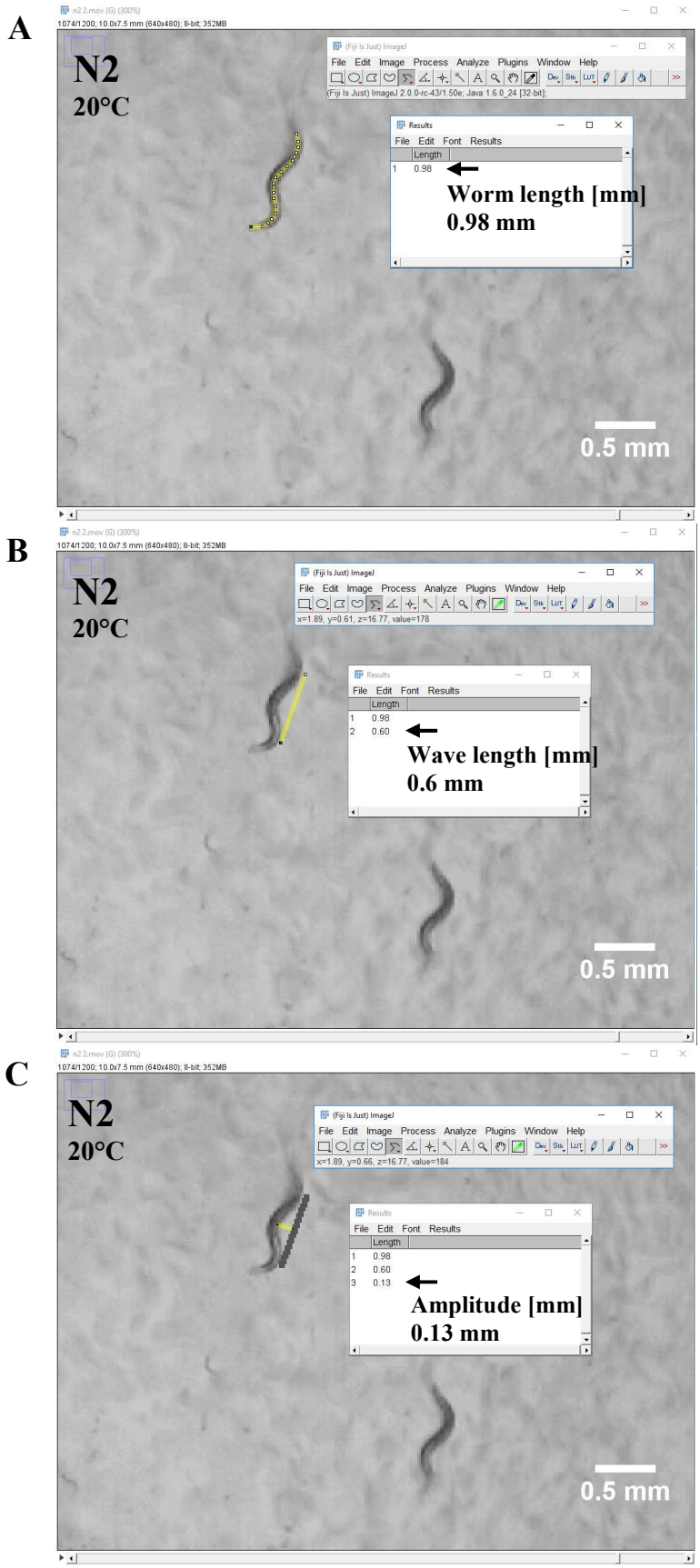

Figure S 14: Method of measurement for body lengths and shape parameters.

The **(A)** body lengths, (B) amplitudes and **(C)** wave lengths were measured on calibrated and scaled images using the „segmented line" tool of the *ImageJ* software. Pictures were captured from recorded movies with a resolution of 640x480px were 1mm = 64px (see Materials and Methods section).

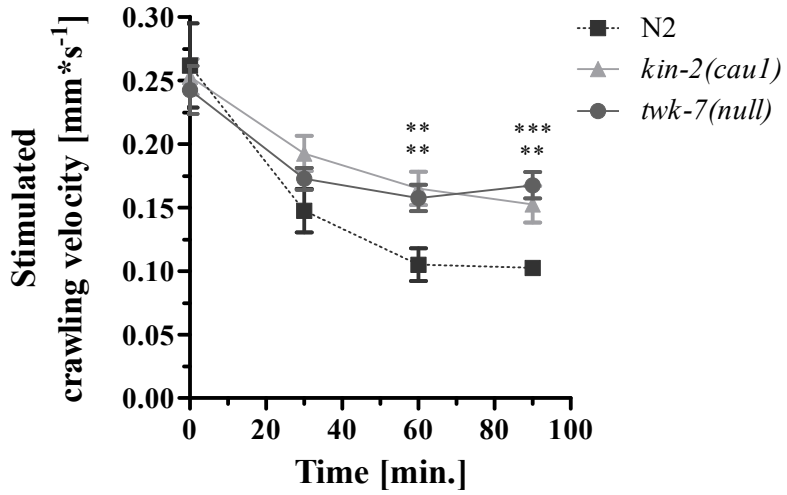

Figure S 15: Persistence of the stimulated crawling velocities.

The crawling velocities of young adult N2, *twk-7(nf120)* and *kin-2(cau-1)* (age 72 h) were monitored over time after stimulation by transfer to fresh NGM agar plates. Each data point represents the mean ± SD of four independent determinations with n = 40 animals. The velocities of the stimulated worms declined within the first 30 min and reached a plateau after 60 min with values similar to the spontaneous crawling velocities. Starting with similar stimulated crawling velocities, significant differences between the strains became apparent after 30 min. (Students t-test, * $p < 0.05$, ** $p < 0.01$ and *** $p < 0.001$).

6.2 Tables

Table S 1: The amino acid sequence of TWK-7 includes PKA-specific phosphorylation sites.

A prediction of PKA-phosphorylation sites was performed with the *pkaPS* tool adjusted for scores >0 (see Materials and Methods). Five PKA-specific phosphorylation sites were found along the amino acid sequence of TWK-7 at the positions 2, 13, 81, 444 and 502 of those the amino acids at 81 and 444 were predicted to be highly specific.

pkaPS prediction results

Results

Description	Position	Score	Sequence	Profile	T_1	T_2	T_3	T_4	T_5	T_6	T_7	T_8	T_9	T_{10}	T_{11}	T_{12}	T_{13}	T_{14}
t7	2	0.28	*MTSSSRGYQRVDSSGDGGSLLMEEE	0.31					-0.02	-0.01								
	13	0.31	*MTSSSRGYQRVDSSGDGGSLLMEEEGDNPHEALLHR	0.53		-0.02	-0.02		-0.02	-0.01		-0.01			-0.12			
	81	0.96	MDDRVTEIPEGFHRRQRRSGHEDIDDESDDESKDEDEEEEET	1.11		-0.01			-0.04	-0.05	-0.03		-0.02					
	444	0.68	VLVSELYANLMQKRARNMSREAFIVENLYVSKHIIPFIPTDI	1.42		-0.01						-0.01	-0.01		-0.10	-0.09	-0.36	-0.15
	502	0.64	TSSSAIDMQSCRFCHSRYSLNRAFK*	0.96		-0.02	-0.02				-0.06	-0.01	-0.13		-0.01	-0.06		-0.01

Summary	
Submitted sequences:	1
Submitted S/T residues:	67
Number of predicted sites:	5

Table S 2: Sequences of oligonucleotides and restriction sites

Nucleotide sequence (restriction sites are underlined)	
twk7p(-3000)-S (ApaI)	GCGC GGGCCC ACAGCGATACCCAACCCCGTTC
twk-7(ORF)-AS (BamHI)	GCGC GGATCC TTTGAATGCACGATTGAGAGA
unc17p(-4127)-S (ApaI)	GCGC GGGCCC GTTTTTGGGATTTTTGCGGG
unc-17p-AS (NdeI)	GCGC CATATG CTCTCTCTCTCCCCCTGGAATATTTTAT
unc-17p(1kb)-AS (NdeI)	GCGC CATATG GAAGAAGCTTCCACCTCCTTCG
twk-7(ORF)-S (ApaI, NdeI)	GCGC GGGCCCGGGCATATGACTTCATCATCTCGTGG
twk-7(nf120)-S	TTCGTACTCATTTCCGGTCAGC (deletion)
twk-7(nf120)-AS	CCAAACAAGATGTTCAGATAGG
twk7(gk760037)-S	AAACGGCGAAACGGGACAAACC (*Bgl*II)
twk7(gk760037)-AS	TCTAGAATCTGAATTTCTGTGACGACG
twk-30(ok1304)-S	AGTTGGCAAATGATTCGGAG (deletion)
twk-30(ok1304)-AS	GTCGAATCGAAGATCAGGGA
twk-40(tm6834)-S	CGTAGACAACGTCACTCGCA (deletion)
twk-40(tm6834)-AS	GATCCTTTGGAGCATAAGCT
twk-43(gk590127)-S	CCTTAGATCCTTGAAACATCA (*Bsh*NI)
twk-43(gk590127)-AS	CCATTAATCTCTGTGTTTCTT
twk-46(gk568572)-S	CACTCACTATTTCCCAAGACA (*Bse*GI)
twk-46(gk568572)-AS	CGAATTTATGCTTTGCGAATC
unc-4p-S (*Apa*I)	GC GGGCCC GCTTCCCCAAATTGGAACAG
unc-4p-AS (*Ase*I)	GC ATTAAT TTTCACTTTTTGGAAGAAGAAGATCC
acr-5p-S (*Apa*I)	GC GGGCCC CATTTGTTGAAAAAACGTACGG
acr-5p-AS (*Ase*I)	GC ATTAAT GCTGAAAATTGTTTTTAAAGC
unc-47p-S (*Apa*I)	GC GGGCCC AATGGGAGAATAAATGGGACGG
unc-47p-AS (*Nde*I)	GC CATATG CTGTAATGAAATAAATGTGACGCTGTCG
kin-2(ORF)-S	ATGTCGGGTGGAAACGAAGAG
kin-2(ORF)-AS	GGGAACATGGCATCGTACATGG (*cau-1*; $C^{245}T$; *Cse*I)

6.3 Movie Files

Movie M1: Spontaneous crawling N2 worms on NGM agar present normal locomotion rates under *ad libitum* feeding at 20°C.

Movie M2: Spontaneous crawling *twk-7(nf120)* worms on NGM agar present elevated locomotion rates under *ad libitum* feeding at 20°C.

Movie M3: N2 wild type worms exhibit normal locomotion rates during swimming in M9 buffer at 20°C.

Movie M4: *twk-7(nf120)* mutants show increased locomotor activity during swimming in M9 buffer at 20°C.

Movie M5: The elevated locomotion rate of spontaneous crawling *twk-7(nf120)* mutants is rescued to a normal level by the expression of the rescue construct *cauEx[twk-7p*::TWK-7*]* crawling.

Movie M6: N2 animals exhibit fast and straightforward locomotion after transfer on new NGM agar plates seeded with *E. coli* OP50 at 20°C. Worms were recorded immediately after stimulation by transfer to a new NGM agar plate using a platinum wire.

Movie M7: The *twk-7(nf120)* mutant worms phenocopy the fast and straightforward locomotion mode of wild-types after transfer on new NGM agar plates seeded with *E. coli* OP50 at 20°C. Worms were recorded immediately after stimulation by transfer to a new NGM agar plate using a platinum wire.

Movie M8: The *twk-7(nf120)* mutants expressing the rescue construct *cauEx[twk-7p*::TWK-7*]* exhibit decreased locomotion rates after stimulation by transfer on new NGM agar plates seeded with *E. coli* OP50 at 20°C. Worms were recorded immediately after stimulation by transfer to a new NGM agar plate using a platinum wire.

Movie M9. Stimulated *kin-2(cau-1)* mutants recorded for 20 s at 20°C under *ad libitum* feeding condition.

Movie M10. Stimulated *twk-7(null)* mutant worms with altered locomotion parameters overexpressing wild-type *twk-7* in the GABAergic motor neurons recorded for 20 s at 20°C under *ad libitum* feeding condition.

Movie M11. Stimulated *kin-2(cau-1)* mutant worms with altered locomotion parameters overexpressing wild-type *twk-7* in the GABAergic motor neurons recorded for 20 s at 20°C under *ad libitum* feeding condition. The phenotype shows high similarity with the *twk-7(null)* transgenes in movie **M10**.

Movie M12. Stimulated *kin-2(cau-1)* mutant worms overexpressing the dominant negative *kin-2* allele in the GABAergic motor neurons recorded for 20 s at 20°C under *ad libitum* feeding condition. These transgenes exhibit slowed activity and increased bending amplitudes when compared with the corresponding non-transgenes (compare with M3).

Movie M13. Stimulated *twk-7(null)* mutant worms overexpressing the dominant negative *kin-2* allele in the GABAergic motor neurons recorded for 20 s at 20°C under *ad libitum* feeding condition. The phenotype induced by kin-2($G^{310}D$) is rescued in the *twk-7(null)* genetic background (compare with **M5**) indicating the PKA/KIN-1 and TWK-7 share a common pathway.

Abbreviations

µl	Microliters
bp	Base pairs
BBSF	Body bending swimming frequency
BBCF	Body bending crawling frequency
Ca	Calcium
cAMP	Cyclic adenosine mono phosphate
cDNA	Complementary DNA
chol.	Cholinergic
DAG	Diacylglycerol
$G\alpha_{s,q,0}$	Heterotrimeric G protein subunits s, q, and 0
GFP	Green fluorescent protein
h	Hours
Hz	Hertz
kDa	kilodalton
min	Minutes
mm	Millimeters
mM	Millimol
MN	Motor neurons
PKA	Protein Kinase A
px	Pixel
s	Seconds

Danksagung

Es war ein außerordentlicher Weg…

Ich bedanke mich sehr bei meinem Doktorvater Prof. Dr. Frank Döring, der mich für die Forschung noch mehr begeistern konnte. Er hat vom ersten Augenblick an den „Wissenschaftler“ in mir erkannt und darüber hinaus all meine Persönlichkeiten (die positiven) gefördert.

Ein ganz besonderer Dank gilt Dr. Kai Lüersen, der mich über die Zeit meiner Promotion bedingungslos und enthusiastisch betreut und an meine Ideen geglaubt hat.

Mein größter Dank gilt meiner Lebensgefährtin Vanessa und ihren lieben Kindern Nikolas und Annelie, die immer an mich geglaubt und mich liebe-, verständnisvoll und unermüdlich in allen Lebenslagen unterstützt haben. Ich freue mich darauf in Zukunft wieder mehr Zeit mit ihnen verbringen zu können.

Curriculum vitae

PERSÖNLICHE DATEN

NAME:	DIETER-CHRISTIAN GOTTSCHLING
GEBURTSDATUM:	10.03.1973
GEBURTSORT:	IASI (RUMÄNIEN)
STAATSANGEHÖRIGKEIT:	DEUTSCH, RUMÄNISCH
FAMILIENSTAND:	LEDIG, KEINE KINDER

SCHULBILDUNG

Sept. 1980 bis Aug. 1985	deutschsprachige Grundschule in Sibiu (Rumänien)
Sept. 1985 bis Aug. 1988	Grundschule in Constanta (Rumänien)
Sept. 1988 bis Aug. 1990	mathematisches Gymnasium in Constanta
Nov. 1991 bis Aug. 1994	Graf Münster Gymnasium in Bayreuth
Sept.1994 bis Aug. 1997	Staatliche Fachoberschule Bayreuth ABSCHLUSS: Fachhochschulreife

GRUNDWEHRDIENST

Sept.1997 bis Juli 1998	FlaRak 34 in Rottenburg a.d. Laaber (Niederbayern)

BERUFSAUSBILDUNG

Sept.1998 bis Aug. 2001	Berufsfachschule für Diätassistenten in Bayreuth ABSCHLUSS: Staatlich geprüfter Diätassistent

FACHHOCHSCHUL-STUDIUM

Okt. 2001 bis Aug. 2007 (inkl. Praktika* und Diplomarbeit)	Fachhochschule Weihenstephan/Triesdorf ABSCHLUSS: Dipl. Ing. (FH) Ernährung und Versorgungsmanagement

DIPLOMARBEIT

Nov. 2006 bis Okt. 2007	„Optische und taktile Beurteilung gegarter Filets mit verschiedenen Fett- und Astaxanthingehalte gefütterter Bachforellen *(Salmo trutta forma fario)* und Seesaiblinge *(Salvelinus alpinus)*“ ORT: Lehranstalt für Fischerei des Regierungsbezirks Oberfranken in Aufseß (Bayern)

STUDIENBEGLEITENDE TÄTIGKEITEN

März 2004 bis Aug. 2005	Untersuchungen zum Fettgehalt und -zusammensetzung in einheimischen Speisefischen ORT: Lehranstalt für Fischerei des Regierungsbezirks Oberfranken in Aufseß (Bayern)
Apr. 2005 bis Aug. 2006	Bestimmung der Astaxanthingehalte in Salmoniden (Lachs-artige Speisefische); ORT: Lehranstalt für Fischerei des Regierungsbezirks Oberfranken in Aufseß
Dez. 2006 bis Juni 2007	Projektstudie zur Untersuchung der Grenzwerte für Koffein in handelsüblichen Erfrischungsgetränken mittels HPLC ORT: Chemielabor HTE1 der Fachhochschule Weihenstephan in Triesdorf

FREIWILLIGE PRAKTIKA

Sept. 2004 bis Feb. 2005	Langzeitstudie zur Bestimmung der Zusammenhänge zwischen Wachstumsraten, Sauerstoffsättigung, Temperatur und Mortalität bei Elsässer-Saiblingen nach definierter Fütterung ORT: Lehranstalt für Fischerei des Regierungsbezirks Oberfranken in Aufseß

Apr. 2006 bis Nov. 2007	Fisch-Monitoring zur Implementierung der EU Wasser-Rahmen-Richtlinie in Oberfranken (Bayern) ORT: Bezirksregierung von Oberfranken in Bayreuth

HOCHSCHUL-STUDIUM

Okt. 2009 – März. 2013	Christian-Albrechts-Universität zu Kiel ABSCHLUSS: MSc. Ökotrophologie

MASTERARBEIT

Apr. 2011 bis Mai. 2012	„Identification and characterisation of *Caenorhabditis elegans* mutants with altered body composition“ Auszeichnung: Helmut F. Ebersdobler-Preis 2012 ORT: Institut für Humanernährung und Lebensmittelkunde, Abteilung Molekulare Prävention

PROMOTION

März. 2013 bis Juli 2016	Institut für Humanernährung und Lebensmittelkunde, Abteilung Molekulare Prävention ABSCHLUSS: Promotion „The *C. elegans* potassium leak channel TWK-7 and the canonical $G\alpha_s$-Protein Kinase A pathway act epistatically in GABAergic motor neurons to affect locomotion behavior” DISPUTATION: 13.07.2016

PUBLIKATIONEN

Dez. 2004	Gottschling D.-C., Popp M., Taschner G., Schürer F., Klupp R.; *Zur Frage des Fettgehaltes bei teichwirtschaftlich genutzten Salmoniden*; Fachzeitschrift für Binnenfischerei 55 Jahrgang; Fischer & Teichwirt 12/04; Nürnberg; 931-933.
Feb. 2006	Gottschling D.-C., Popp M., Taschner G., Schürer F., Klupp R.; *Astaxanthingehalte in Salmoniden der LF Aufseß*; Fachzeitschrift für Binnenfischerei 57 Jahrgang; Fischer & Teichwirt 2/06; Nürnberg; 49-53.
Apr. 2014	Lüersen K, Faust U, Gottschling D-C, Döring F; *Gait-specific adaptation of locomotor activity in response to dietary restriction in Caenorhabditis elegans*; The Journal of Experimental Biology (2014) doi:10.1242/jeb.099382, 2480-2488.
März 2016	Lüersen K, Gottschling D-C, Döring F; *The C. elegans leak K^+ channel TWK-7 regulates specific locomotion behaviors in motor neurons*; GENETICS, under review.

Eidesstattliche Erklärungen

Hiermit erkläre ich, Dieter-Christian Gottschling, an Eides statt, dass ich die vorgelegte Dissertation mit dem Titel **„The *C. elegans* potassium leak channel TWK-7 and the canonical Gα_s-Protein Kinase A pathway act epistatically in GABAergic motor neurons to affect locomotion behavior“** selbständig und ohne unerlaubte Hilfe angefertigt habe und dass ich die Arbeit noch keinem anderen Fachbereich bzw. noch keiner anderen Fakultät vorgelegt habe.

Kiel, den

Hiermit erkläre ich, Dieter-Christian Gottschling, dass gegen mich nicht strafrechtlich ermittelt wird.

Kiel, den

Hiermit erkläre ich, Dieter-Christian Gottschling, dass diese Dissertationsarbeit nach den Regeln guter wissenschaftlicher Praxis (Standard wissenschaftlichen Arbeitens nach den Empfehlungen der DFG) verfasst wurde.

Kiel, den

Eidesstattliche Erklärung zur Abgabe einer elektronischen Dissertation zur Veröffentlichung durch die Universitätsbibliothek Kiel

1. Original
Die Doktorandin / der Doktorand versichert hiermit an Eides statt, dass die in der Universitätsbibliothek abgelieferte elektronische Dissertation mit dem vom Promotionsausschuss genehmigten Prüfungsexemplar übereinstimmt und formal den Bestimmungen der Promotionsordnung entspricht. Die Drucklegung der Dissertation wurde vom Promotionsausschuss genehmigt. Datenformate, Datenträger und die Metadaten
sowie die Anzahl der abzugebenden unentgeltlichen Exemplare in Papierform und elektronischer Form entsprechen den Vorgaben der Universitätsbibliothek Kiel und der jeweiligen Promotionsordnung.

2. Veröffentlichungsrecht
Die Doktorandin / der Doktorand gestattet der Universitätsbibliothek Kiel, Kopien der elektronischen Dissertation zu erstellen, und diese unter Verwendung der Metadaten auf ihren Servern für die Benutzung bereitzustellen, ggf. in andere Formate zu konvertieren und ihre bibliographischen Daten und ggf. das Abstract Datenbanken zugänglich zu machen. Die elektronische Dissertation wird archiviert und im Internet publiziert, solange dies technisch und mit vertretbarem Aufwand möglich ist.
Die Doktorandin / der Doktorand räumt somit der Universitätsbibliothek Kiel das einfache Nutzungsrecht ein, die elektronische Dissertation in Datennetzen öffentlich wiederzugeben und auf Einzelabruf zu übertragen. Der Lieferung der elektronischen Dissertation an die Deutsche Nationalbibliothek und ggf. an die fachlich zuständigen Sondersammelgebietsbibliotheken und der dortigen Speicherung zwecks Archivierung und Zurverfügungstellung nach geltendem Recht stimmt die Doktorandin / der Doktorand zu. Die Universitätsbibliothek Kiel stellt eine Bescheinigung über das Erbringen der Publikationspflicht aus.

3. Rechte Dritter
Die Doktorandin / der Doktorand versichert, dass mit der elektronischen Publikation der Dissertation keine Rechte Dritter verletzt werden und dass die Universitätsbibliothek von etwaigen Rechten Dritter freigestellt wird. Insbesondere gilt bei kumulierenden Dissertationen: Die Doktorandin / der Doktorand verpflichtet sich, für jeden in seiner kumulierenden Dissertation enthaltenen und bereits publizierten bzw. zur Publikation an anderer Stelle angenommenen Beitrag das Recht zur elektronischen Veröffentlichung auf den Servern der Universitätsbibliothek von den Verlagen schriftlich einzuholen und vorzulegen.

4. Datenschutz
Die Doktorandin / der Doktorand ist damit einverstanden, dass ihre / seine persönlichen Daten gemäß Promotionsordnung maschinell gespeichert und zusammen mit der Dissertation bereitgestellt werden. Sofern die abgelieferten Dateien ihren / seinen Lebenslauf enthalten, stimmt sie / er der Publikation des Lebenslaufs in der elektronischen Version der Dissertation zu.

5. Personalien
Name, Vorname: Gottschling, Dieter-Christian
Geburtsdatum, Geburtsort: 10.03.1073, Iaşi (Rumänien)
Straße, Nr.: Fliegender Holländer 35
PLZ: Ort: 24159 Kiel
Telefon: 0172 6389355
E-Mail: dcgottschling@googlemail.com

6. Angaben zur Dissertation

Titel: The *C. elegans* potassium leak channel TWK-7 and the canonical $G\alpha_s$-Protein Kinase A pathway act epistatically in GABAergic motor neurons to affect locomotion behavior

Fakultät: Agrar- und ernährungswissenschaftliche Fakultät

Gutachter: 1. Prof. Dr. Frank Döring, 2. Prof. Dr. Gerald Rimbach

Datum der mündlichen Prüfung: 13.07.2016

Datum des Hochladens der elektronischen Dissertation auf MACAU:

Kiel, den _____ _____